

Alma Mater Studiorum - Università di Bologna

DOTTORATO DI RICERCA IN
SCIENZA E CULTURA DEL BENESSERE E DEGLI STILI DI VITA

Ciclo 34

Settore Concorsuale: 06/N2 - SCIENZE DELL'ESERCIZIO FISICO E DELLO SPORT

Settore Scientifico Disciplinare: M-EDF/02 - METODI E DIDATTICHE DELLE ATTIVITA'
SPORTIVE

APPLICAZIONI TECNOLOGICHE E NUOVI METODI DI VALUTAZIONE DELLA
PERFORMANCE NEGLI SPORT ACQUATICI

Presentata da: Cristian Romagnoli

Coordinatore Dottorato

Carmela Fimognari

Supervisore

Giorgio Gatta

Co-supervisore

Giuseppe Annino

Esame finale anno 2022

INDICE

INTRODUZIONE	6
LA VALUTAZIONE FUNZIONALE	6
STRUMENTI COMUNI PER LA VALUTAZIONE FUNZIONALE	8
<i>Accelerometro e Giroscopio</i>	8
<i>Strain Gauge</i>	10
<i>Catene di misura e reti di sensori</i>	11
<i>Video analisi</i>	14
<i>Encoder Lineare</i>	16
CENNI DI FISICA APPLICATA	18
<i>Cinematica Lineare/Angolare</i>	18
<i>I Principi della Dinamica</i>	20
<i>Cenni di meccanica dei fluidi (galleggiabilità, drag, forza propulsiva)</i>	21
<i>Equilibrio statico e dinamico</i>	25
MODELLI DI PRESTAZIONE DI ALCUNI SPORT ACQUATICI	26
KAYAK.....	26
NUOTO	27
PALLANUOTO	28
CAPITOLO 1	30
A MULTIPROTOCOL WIRELESS SENSOR NETWORK FOR HIGH PERFORMANCE SPORT APPLICATIONS	30
CAPITOLO 2	52
A PILOT STUDY ON THE E-KAYAK SYSTEM: A WIRELESS DAQ SUITED FOR PERFORMANCE ANALYSIS IN FLATWATER SPRINT KAYAKS	52
CAPITOLO 3	83
A NEW MEASUREMENT SYSTEM FOR PERFORMANCE ANALYSIS IN FLATWATER SPRINT KAYAKING	83
CAPITOLO 4	95
ASSESSMENT OF THE PADDLE PROPULSIVE FORCE AND THE KAYAK POWER BALANCE AT DIFFERENT PACES VELOCITIES	95
CAPITOLO 5	115
SPECIFICITY OF WEIGHTLIFTING BENCH EXERCISES IN KAYAKING SPRINT PERFORMANCE: AN INTERESTING PERSPECTIVE FOR NEUROMUSCULAR TRAINING	115
CAPITOLO 6	133
KINEMATIC ANALYSIS OF WATER POLO PLAYER IN THE VERTICAL THRUST PERFORMANCE TO DETERMINE THE FORCE-VELOCITY AND POWER-VELOCITY RELATIONSHIPS IN WATER: A PRELIMINARY STUDY.....	133
CAPITOLO 7	159
FRONT CRAWL STROKE IN SWIMMING: PHASE DURATIONS AND SELF-SIMILARITY	159
CAPITOLO 8	160
PHI-BONACCI BUTTERFLY STROKE NUMBERS TO ASSESS SELF-SIMILARITY IN ELITE SWIMMERS	160

DISCUSSIONE	182
KAYAK.....	182
PALLANUOTO	186
NUOTO	189
CONCLUSIONI	193
RINGRAZIAMENTI	194
LISTA DELLE FIGURE	196
LISTA DELLE TABELLE	200
BIBLIOGRAFIA	202

Sommario

Nello sport di alto livello l'uso della tecnologia ha raggiunto un ruolo di notevole importanza per l'analisi e la valutazione della prestazione. Negli ultimi anni sono emerse nuove tecnologie e sono migliorate quelle pre-esistenti (i.e. accelerometri, giroscopi e software per l'analisi video) in termini di campionamento, acquisizione dati, dimensione dei sensori che ha permesso la loro "indossabilità" e l'inserimento degli stessi all'interno degli attrezzi sportivi. La tecnologia è sempre stata al servizio degli atleti come strumento di supporto per raggiungere l'apice dei risultati sportivi. Per questo motivo la valutazione funzionale dell'atleta associata all'uso di tecnologie si pone lo scopo di valutare i miglioramenti degli atleti misurando la condizione fisica e/o la competenza tecnica di una determinata disciplina sportiva. L'obiettivo di questa tesi è studiare l'utilizzo delle applicazioni tecnologiche e individuare nuovi metodi di valutazione della performance in alcuni sport acquatici. La prima parte (capitoli 1-5), si concentra sulla tecnologia prototipale chiamata E-kayak e le varie applicazioni nel kayak di velocità. In questi lavori è stata verificata l'attendibilità dei dati forniti dal sistema E-kayak con i sistemi presenti in letteratura. Inoltre, sono stati indagati nuovi parametri utili a comprendere il modello di prestazione del paddler. La seconda parte (capitolo 6), si riferisce all'analisi cinematica della spinta verticale del pallanuotista, attraverso l'utilizzo della video analisi 2D, per l'individuazione delle relazioni Forza-velocità e Potenza-velocità direttamente in acqua. Questo studio pilota, potrà fornire indicazioni utili al monitoraggio e condizionamento di forza e potenza da svolgere direttamente in acqua. Infine la terza parte (capitoli 7-8), si focalizza sull'individuazione della sequenza di Fibonacci (sequenza divina) nel nuoto a stile libero e a farfalla. I risultati di questi studi suggeriscono che il ritmo di nuotata tenuto durante le medie/lunghe distanze

gioca un ruolo chiave. Inoltre, il livello di autosomiglianza (self-similarity) aumenta con la tecnica del nuoto.

Parole chiave: Prestazioni sportiva, Biomeccanica, Cinetica, Tecnologia, Sport acquatici

Abstract

In high-level sports, technology has achieved a role of considerable importance for the analysis and performance assessment. In recent years, the developments in new technologies and the improvements in previous ones (i.e. accelerometers, gyroscopes, and software for video analysis) in terms of sample rate, data acquisition, and sensor size, allowed the "wearability" of new sensor systems and their insertion into the sport equipment. Technology has always been at the service of athletes as a support tool to achieve the top in sports results. For this reason, the functional assessment of the athlete associated with the use of technologies aims to assess the improvements of athletes by measuring the physical condition and/or technical skills on a specific sport. This thesis aims to study the use of technological applications and identify new methods of performance assessment in some water sports. The first part (chapters 1-5), focuses on the prototype technology called E-kayak and the various applications in flatwater sprint kayaking. Here, the reliability of the data provided by the E-kayak with other systems available in the literature was verified. In addition, new parameters useful for understanding the paddler's performance model were investigated. The second part (chapter 6), refers to the kinematic analysis of the vertical thrust in the water polo player, through the use of 2D video analysis, for the identification of the Force-velocity and Power-velocity relationships directly in the water. This pilot study will provide useful information for the monitoring and conditioning of strength and power to be carried out directly in the water. Finally, the third part (chapters 7-8) focuses on identifying the Fibonacci sequence (divine sequence) in crawl and butterfly swimming styles. The

results of these studies suggest that the swimming pace maintained during medium/long distances plays a key role. Furthermore, the level of self-similarity increases with the swimming technique.

Keywords: Sport Performance, Biomechanics, Kinetic, Technology, Water Sports

Introduzione

La valutazione funzionale

Lo sport agonistico è una competizione naturale tra gli esseri umani dove attraverso l'allenamento si cerca di raggiungere l'apice della condizione in concomitanza delle competizioni.

Nel corso degli anni si sono succedute molte metodologie di allenamento, che hanno aiutato allenatori ed atleti a prepararsi al meglio per le proprie competizioni. Lo sviluppo della prestazione si ottiene attraverso un processo di allenamento progettato per indurre l'automazione delle capacità motorie e volto al miglioramento delle funzioni strutturali e metaboliche dell'atleta.

L'allenamento prevede la manipolazione del carico esterno attraverso le variabili di intensità, durata e frequenza in relazione alle richieste combinate di forza, potenza, velocità e resistenza, specifiche della disciplina sportiva praticata. Il livello di adattamento all'allenamento è influenzato dai tratti ereditari non solo relativamente alla struttura corporea ma anche alla plasticità della risposta agli stimoli ambientali.

L'unico mezzo in grado di controllare e valutare le caratteristiche fisiologiche e funzionali dell'atleta, i parametri fisiologici (carico interno) e computazionali (carico esterno), le richieste neuromuscolari, i parametri biomeccanici e le richieste metaboliche di una disciplina sportiva, è la valutazione funzionale. Quindi, la valutazione funzionale ha come obiettivi l'indagine delle qualità fisiche che influenzano la prestazione, il controllo e l'ottimizzazione dell'allenamento, la diagnosi funzionale e la ricerca scientifica.

L'unità essenziale della valutazione funzionale è il test, cioè quell'esercizio che in relazione alla sua modalità di esecuzione coinvolge le capacità fisiche specifiche di una determinata disciplina andando

a misurare direttamente o indirettamente i parametri fisici e/o biologici connessi all'esercizio, alla sua modalità di esecuzione e agli strumenti di valutazione utilizzati. La modalità di esecuzione di un test associata alla strumentazione utilizzata ne costituisce il protocollo.

I test per essere utilizzati devono seguire una serie di presupposti scientifici: la validità, la riproducibilità, l'obiettività e la specificità. La validità si riferisce al grado in cui un test misura ciò che dovrebbe misurare ed è una delle caratteristiche più importanti [1,2] ossia, i test che indagano la prestazione fisica dovrebbero misurare le principali abilità sportive, produrre risultati ripetibili, misurare le prestazioni di un atleta alla volta (se non diversamente specificato nel protocollo), apparire significativi, essere di difficoltà adeguata, essere in grado di distinguere tra vari livelli di abilità, consentire una misura accurata, includere un numero sufficiente di prove e resistere al test di valutazione statistica. La riproducibilità è la misura del grado di consistenza o di riproducibilità di un test. Se un atleta possiede un'abilità indagata da un test, i risultati non devono cambiare in due misure successive effettuate a breve tempo l'una dall'altra e non devono essere condizionati da fattori esterni. L'obiettività di un test si riferisce al fatto che il test non deve essere influenzato dall'operatore e/o da fattori ambientali. Infine la specificità di un test è la caratteristica di basarsi, laddove possibile, su condizioni simili a quelle ambientali e fisiche della competizione (dinamiche dell'azione e del gesto sportivo); il test è specifico se riproduce e soddisfa le condizioni della prestazione in termini di coerenza biomeccanica, coordinativa e metabolica.

I test si suddividono in test da campo e test da laboratorio. Il test da campo utilizza strumenti semplici, e forniscono delle indicazioni generalmente corrette sulle qualità fisiche dell'atleta, ma allo stesso tempo non garantiscono tutti i costrutti scientifici di un test; inoltre le misure possono essere affette da errori dovuti alla misurazione dell'operatore.

Differentemente i test da laboratorio con l'ausilio di strumentazioni avanzate sono in grado di fornire dati precisi in riferimento al gesto motorio preso in esame. Il problema principale si riferisce al fatto che il test da laboratorio, molte volte, non tiene conto della specificità del gesto proprio perché viene svolto in un ambiente completamente diverso da quello di allenamento/gara. Per sopperire alle necessità di poter valutare tramite strumenti/sensori gli atleti direttamente sul campo di allenamento/gara la tecnologia si è evoluta, nel tempo, in questa direzione apportando nuove tecniche ma soprattutto nuovi sensori utili al monitoraggio istantaneo della performance.

Strumenti comuni per la valutazione funzionale

Accelerometro e Giroscopio

L'accelerometro venne impiegato per la prima volta nell'ambito delle scienze motorie nel 1981 per misurare le accelerazioni e le decelerazioni sull'asse verticale (y). Il sensore pesava 400 g ed aveva una dimensione di 14x8x4 cm e fu utilizzato per la misura della spesa energetica dell'uomo [3]. A partire dal 1990 si è osservato un aumento dell'uso di accelerometri anche se erano più le limitazioni dovute a costi elevati, scarsa validità, problemi di calibrazione che i vantaggi forniti [4]. Dal 2004 in poi si è verificato un ulteriore incremento dell'utilizzo di accelerometri per l'attività fisica, con un aumento esponenziale della ricerca scientifica in questo ambito [5]. L'accelerometro è un sensore in grado di misurare le accelerazioni statiche (gravità) e le accelerazioni dovute a urti o movimenti applicati sul dispositivo. Esistono diversi tipi di accelerometri, ad esempio quelli piezoresistivi, a effetto tunnel, risonanti, termici ma quelli che trovano più utilizzo nelle applicazioni sportive sono gli accelerometri capacitivi MEMS (Micro ElectroMechanical systems) [6–9], che vengono spesso abbinati a giroscopi per formare le piattaforme IMU (Inertial Measurement Units - Unità di Misura Inerziale). L'accelerometro capacitivo sfrutta la variazione della capacità elettrica di un condensatore

associata con la variazione di distanza tra le sue armature. La massa mobile del sensore è costituita da un'armatura mentre l'altra armatura è solidale alla struttura del dispositivo. La massa viene tenuta sospesa da un elemento elastico che non consente il contatto tra le armature (Figura 1). Quando il sensore subisce un'accelerazione, la massa sospesa sottoposta alla forza di inerzia deforma la molla, e la sua distanza dall'armatura fissa varia. Questo provoca una variazione della capacità del condensatore, che viene rilevata da uno speciale circuito e trasformata in una variazione di tensione elettrica.

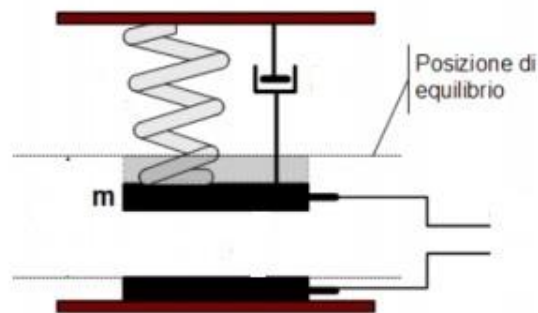


Figura 1: Schema riassuntivo accelerometro capacitivo.

Il giroscopio è un dispositivo in grado di misurare la velocità angolare di un corpo. In passato giroscopi meccanici basati sul principio della conservazione del momento angolare sono stati utilizzati come giocattoli (trottole) e, a partire dal XIX secolo, come strumenti di laboratorio (giroscopi cardanici). Nella seconda metà del XX secolo sono stati prodotti principalmente giroscopi meccanici per la navigazione e per gli aerei (Figura 2) [10,11].

Nel periodo successivo alla II guerra mondiale iniziò lo sviluppo dei sensori inerziali, che portò ad aumentare la funzionalità e l'affidabilità di questi dispositivi riducendo le grandezze, il peso e i costi. La fase più recente è stata l'introduzione dei giroscopi MEMS nel 1995 che proseguì con la

miniaturizzazione degli stessi sulle piattaforme IMU poco costose, leggere e con la possibilità di integrazione con altri sensori (accelerometro-magnetometro) [11].

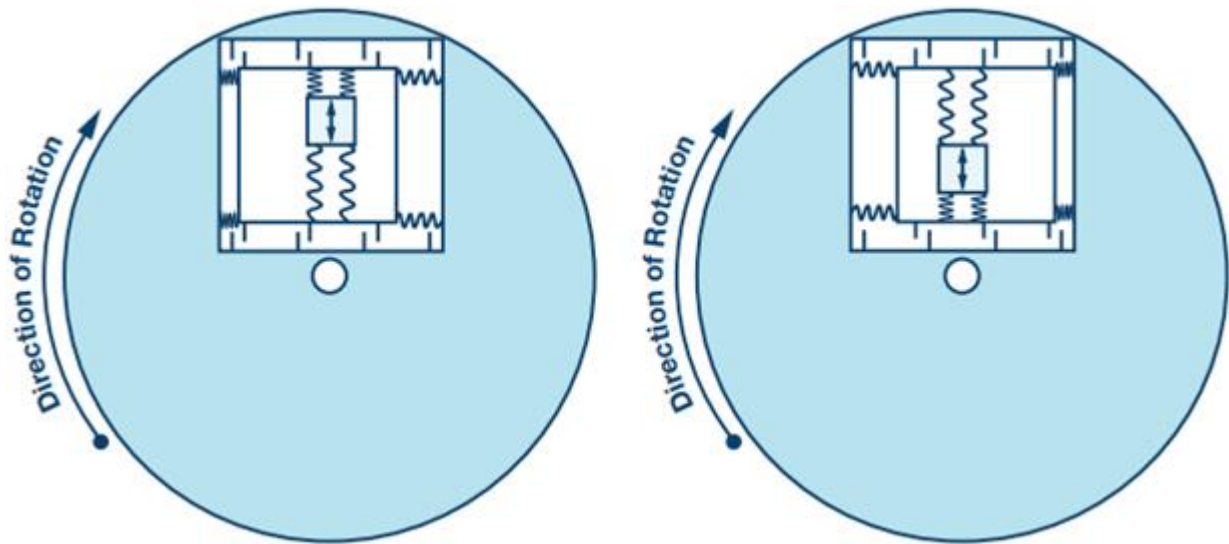


Figura 2: schema di funzionamento del giroscopio

Le applicazioni sportive che utilizzano sistemi integrati con giroscopio e accelerometro (MEMS) su piattaforme IMU sono diverse[12–15], quantificano la velocità angolare ($^{\circ}/s$) e la somma delle accelerazioni lineari (m/s^2) gravitazionali e inerziali lungo gli assi di rilevamento (x,y,z).

Strain Gauge

Per l'analisi della dinamica, o più precisamente della forza applicata durante l'esecuzione di un gesto tecnico sportivo come per esempio nel kayak, canottaggio, golf e hockey trovano largo utilizzo gli strain gauge (o estensimetro). Lo strain gauge è un sensore che basa il suo funzionamento sulla deformazione elastica subita dal materiale metallico che lo costituisce.

Poiché in base alla legge di Hooke la deformazione elastica è proporzionale alla forza applicata, misurando la deformazione possiamo risalire alla forza.

Esistono diversi tipi di estensimetri, per esempio ottici o meccanici; i più diffusi sono gli estensimetri elettrici, che possono essere resistivi, capacitivi, induttivi o fotoelettrici [16]. Tra questi, i più utilizzati sono quelli resistivi, che basano il loro funzionamento sulla variazione della resistenza elettrica quando sono soggetti a deformazione, in base alla seconda legge di Ohm.

Generalmente gli estensimetri vengono disposti in modo da formare un particolare circuito detto ponte di Wheatstone (Figura 3) [23]. Nel ponte di Wheatstone la deformazione di uno o più estensimetri genera una differenza di potenziale tra i punti A e C (Figura 5-2), che viene raccolta e amplificata.

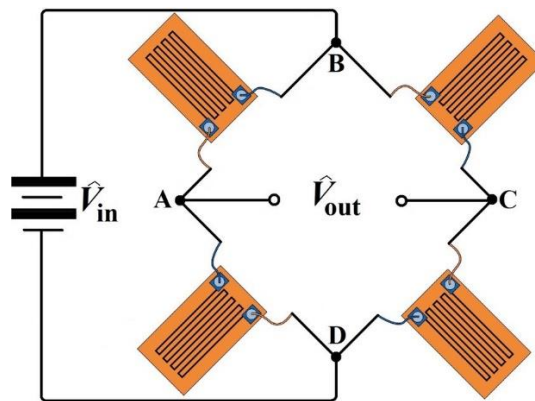


Figura 3: estensimetri disposti a ponte di Wheatstone

Catene di misura e reti di sensori

La tecnologia nello sport si sta sviluppando molto velocemente infatti una valida alternativa alla valutazione svolta in laboratorio è l'utilizzo di sensori cinematici e dinamici (i.e. accelerometro, giroscopio, strain gauge e GPS) supportati anche dall'utilizzo della video analisi. In passato il

movimento poteva essere analizzato solo parzialmente con i primi sistemi di video analisi; invece oggi grazie a sistemi costituiti da sensori di tipo innovativo si può studiare, misurare e valutare interamente ogni singolo parametro biomeccanico del gesto [17].

Molti sistemi di misura utilizzati nello sport utilizzano i Micro-Controller Unit (MCU) ovvero dei dispositivi di piccole dimensioni che contengono un processore (CPU), un orologio e varie memorie. Il MCU è in grado di gestire molte informazioni e memorizzarle in file di piccole dimensioni e di poter comunicare con il terminale finale (PC, tablet, smartphone). Considerato che la CPU è in grado di ricevere in ingresso soltanto segnali digitali, ovvero differenze di potenziale elettrico variabili nel tempo, per le misurazioni si usano i trasduttori (strain gauge, accelerometro, giroscopio) cioè dispositivi che trasformano la grandezza in una differenza di potenziale elettrico leggibile dal sistema. La comunicazione tra i MCU e trasduttori/sensori può avvenire in modalità wireless: ad ogni sensore viene collegato un mini MCU e un trasmettitore che è in grado di elaborare e inviare il segnale all'unità centrale. Si parla in questi casi di, WSN (Wireless Sensor Network, o rete senza fili di sensori) [18].

I trasduttori utilizzati per queste applicazioni sono quelli di tipo MEMS, già descritti in precedenza. La loro miniaturizzazione e il basso costo dei componenti elettronici hanno contribuito ad un elevato utilizzo in ambito sportivo di questi dispositivi, la cui affidabilità è stata validata da un'ampia letteratura scientifica [19–21].

L'IMU fa la sua prima apparizione nel 1930, come supporto alla navigazione aerea [22]; con l'avvento della tecnologia MEMS la piattaforma IMU ha trovato sempre maggiore applicazione nella misura dei parametri cinematici del movimento in molte discipline sportive [23]. Esistono due tipologie di IMU: IMU con 2 sensori e con 3 sensori [24]. L'IMU con due sensori è composto da

giroscopio e accelerometro. Di solito entrambi i sensori hanno 2 o 3 DoF (gradi di libertà) che rappresentano gli assi di misurazione (x,y,z). Il sistema potrà quindi misurare da 4 a 6 movimenti indipendenti, indicati col nome di Gradi di Libertà (in inglese Degrees of Freedom, o DoF).

L'IMU a tre sensori è composto da accelerometro, giroscopio e magnetometro (utilizzato per la misura dell'angolo di imbardata e per la distanza percorsa) tutti tri-assiali per ottenere tutte le informazioni necessarie sui 3 assi (x,y,z) per un totale di 9 DoF (Figura 4) [7,24].

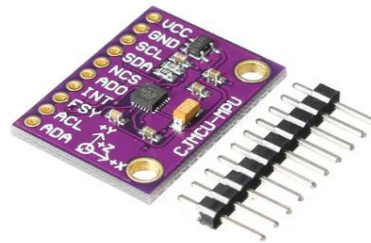


Figura 4: IMU a 9 DoF (accelerometro, giroscopio e magnetometro)

Negli ultimi anni, il Global Positioning System (GPS) ha visto un incremento del suo utilizzo per il monitoraggio dei carichi di lavoro esterno/interno dei giocatori/atleti in diverse discipline [8] per determinare il carico di lavoro dell'atleta si misura non solo la frequenza cardiaca ma anche la distanza percorsa e la velocità [25].

Molto spesso nelle applicazioni sportive il terminale GPS viene abbinato a una IMU [vedi ad esempio sistemi Catapult, E-kayak].

L'abbinamento di questi sensori indossabili facilita così l'analisi del movimento fornendo talvolta un feedback in tempo reale e; essi rappresentano quindi una valida alternativa all'analisi video [26–28].

Chi utilizza queste tecnologie deve tener presente che le misure fornite sono soggette ad errori, che possono in una certa misura essere compensati grazie all'utilizzo di particolari algoritmi (es. filtro di

Kalman) oppure integrando le informazioni ottenute da diversi sensori spesso realizzati con diverse tecnologie (sensor fusion).

Tra gli errori noti possiamo ricordare il drift (deriva) del giroscopio e dell'accelerometro, che è causato sia dai procedimenti matematici di integrazione che dai cambiamenti delle proprietà fisiche dei MEMS [26].

Altri errori possono essere causati dalla posizione del sensore rispetto al corpo: ad esempio gli artefatti dei tessuti molli, che sono sensibili al sito di applicazione, dipendono dal soggetto e variano a seconda del movimento effettuato possono perturbare la misura finale; in questo caso la compensazione dell'errore risulta difficile [11,29–32].

Inoltre risulta essere fondamentale la frequenza di campionamento dei sensori, che deve tener conto delle azioni tipiche della disciplina sportiva; in base al teorema di Nyquist-Shannon [33] la frequenza di campionamento deve essere almeno due volte la frequenza più alta del segnale in esame, questo per minimizzare la perdita di informazioni [34].

Video analisi

I sensori cinematici per essere utilizzati e considerati validi e attendibili devono essere confrontati con il metodo gold-standard, che è dato dai sistemi ottici [35,36]. La ricerca sportiva si è da sempre avvalsa della video analisi per catturare il movimento di un atleta. L'analisi video è in grado di fornire informazioni sulle esigenze fisiologiche e tecniche delle discipline sportive registrando e quantificando il movimento [37,38]. L'analisi riguarda la misura delle durate temporali, della velocità (istantanea/media), dell'accelerazione (istantanea/media), della frequenza dei movimenti (Figura 5).

Di solito le riprese video non vengono solo effettuate in laboratorio ma vengono svolte su campi di gara o di allenamento e quindi al di fuori di un ambiente controllato.

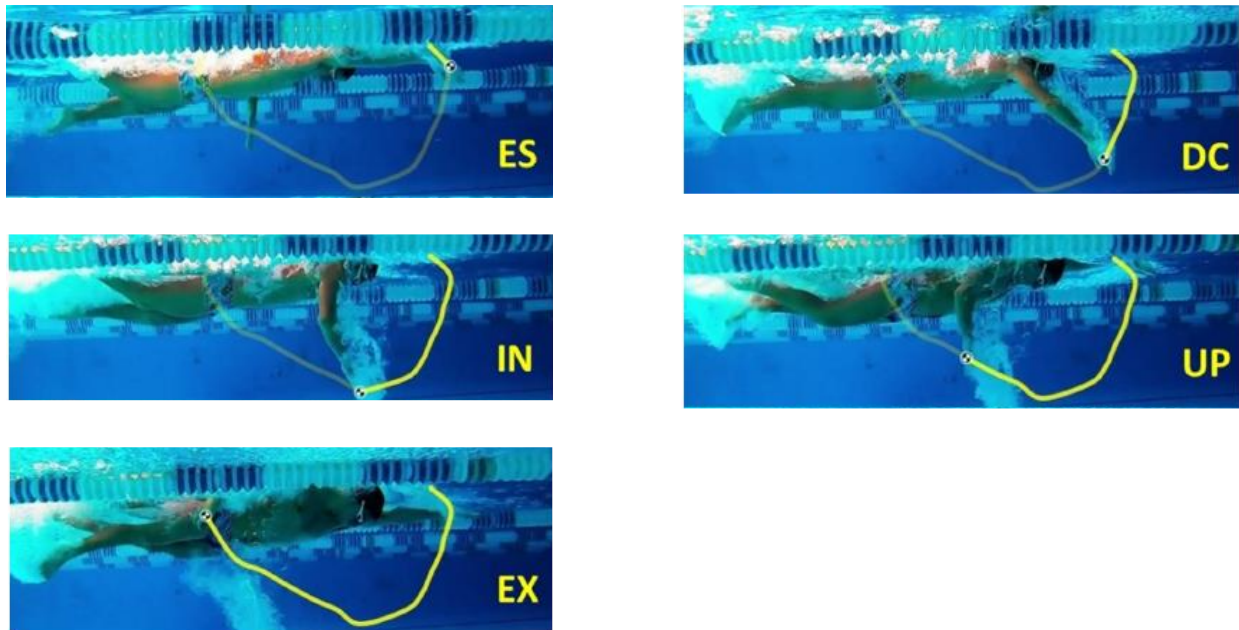


Figura 5: Suddivisione della nuotata crawl nelle fasi: Entry-Stretch (ES), Downsweep-and-catch phase (DC), Insweep phase (IN), Upsweep phase (UP), Exit phase (EX) [39].

Questo implica che l'acquisizione video sia sottoposta a diverse interferenze che possono essere meteorologiche, di misurazione e di ostacoli che possono ostruire la visuale. Un altro fattore da tenere in considerazione è il volume di acquisizione o di azione a cui si riferisce il movimento che si registra il che lo rende, di solito, il fattore limitante nella scelta del sistema di riferimento dell'acquisizione video. Quindi la precisione è inversamente proporzionale alla copertura spaziale del sistema di riferimento[36]. Infatti l'analisi video 2D o 3D prevede sempre una calibrazione del sistema utilizzando il DLT (Direct Linear Transformation) [40], il quale consente di trasformare i pixel in cm permettendo così una corretta analisi computazionale dei parametri cinematici e una stima dei parametri dinamici. Un' ulteriore considerazione da fare è la velocità con cui le azioni motorie

vengono svolte, che le rende più difficili da catturare rispetto ai movimenti lenti o a situazioni statiche. La frequenza di campionamento ottimale per la ripresa di gesti tecnici varia tra 50 e 250 Hz a seconda dell'ambiente in cui si svolge il movimento, e della disciplina sportiva. Secondo Kruk et al. [36] l'utilizzo di Fps (Frame/immagini per secondo) non troppo elevati è utile per non avere una quantità eccessiva di dati e per evitare il bias dovuto ad alte frequenze di acquisizione. Visti e considerati gli aspetti positivi e i fattori limitanti l'analisi video ad oggi risulta essere un valido strumento per l'analisi della prestazione e il controllo del movimento [41,42]; inoltre, il contemporaneo utilizzo dei sensori cinematici e dinamici (IMU, GPS) sincronizzati all'analisi video, fornisce tutte le informazioni necessarie per lo studio della biomeccanica del gesto.

Encoder Lineare

L'encoder è un trasduttore digitale usato per la misura dello spostamento angolare o lineare. È formato da un asse rotante su cui è montato un disco che ha sulla periferia due corone forate. Una sorgente emette una luce infrarossa verso il disco che ruota; quando la luce incontra un foro attraversa il disco e va a eccitare un fototransistor (Figura 6). In questo modo si genera un treno di impulsi per ogni corona che vengono trasmessi ad un microprocessore per la successiva elaborazione.

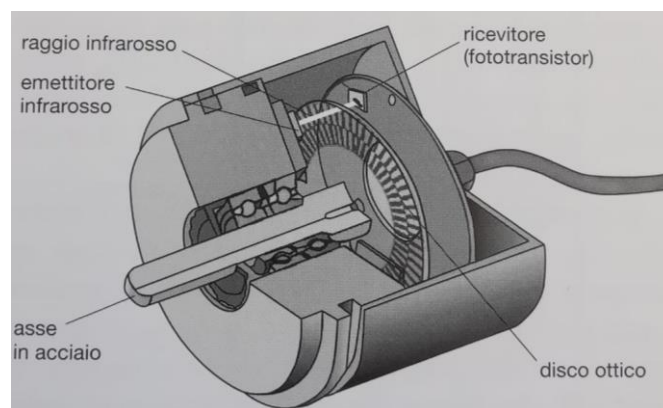


Figura 6: Raffigurazione interna dell'encoder.

Un circuito all'interno del microprocessore è in grado di contare il numero di impulsi e di ricostruire l'angolo di rotazione in funzione del tempo, calcolando in questo modo la velocità angolare. La risoluzione del dispositivo è determinata dal numero di fori: maggiore è il numero di fori presenti sui dischi, più accurato sarà il dato acquisito. Con l'encoder oltre alla velocità angolare è possibile calcolare la velocità lineare, agganciando l'atleta o il pacco pesi ad un cavo con un'eventuale molla di ritorno (Figura 7) [43]. I parametri che è in grado di misurare il sistema sono: lo spostamento del carico, la velocità media durante lo spostamento, il picco di velocità durante lo spostamento ed il tempo impiegato per effettuare lo spostamento. Attraverso opportune elaborazioni matematiche sarà poi possibile ricavare anche l'accelerazione, la forza applicata e la potenza.

Inoltre, è in grado di fornire le relazioni Potenza-Velocità e Forza-Velocità utili per la valutazione neuromuscolare dell'atleta e per il controllo progressivo dell'allenamento durante i macro e mesocicli.

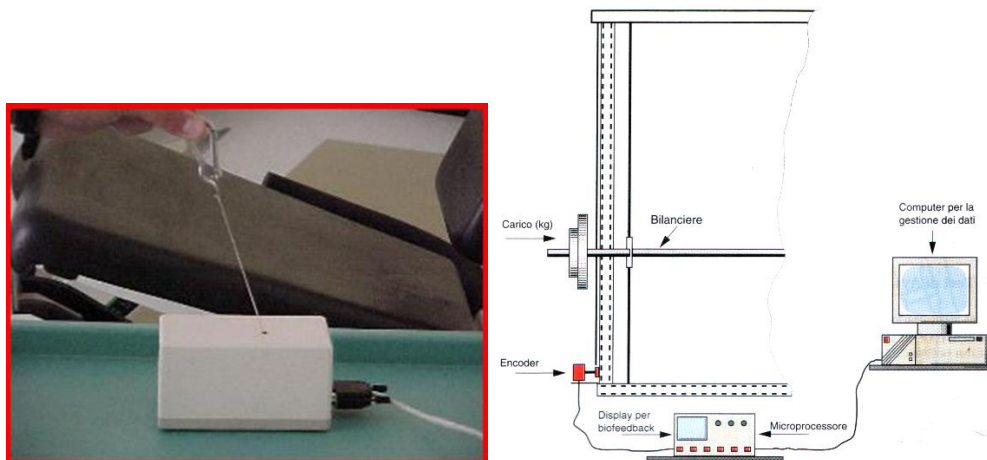


Figura 7: Encoder lineare

Cenni di Fisica Applicata

La chinesologia studia il movimento umano nel suo complesso e la biomeccanica è una sua disciplina. Per biomeccanica si intende la descrizione/studio del movimento degli esseri viventi e le cause che lo determinano, utilizzando la scienza della meccanica [44]. Le forze che agiscono sugli esseri viventi possono creare movimento, essere uno stimolo di crescita (ossificazione) oppure possono sovraccaricare i tessuti danneggiandoli. In fisica la meccanica si occupa della descrizione del movimento ma soprattutto delle forze che vi entrano in gioco.

Cinematica Lineare/Angolare

Il movimento non è altro che il cambiamento della posizione rispetto ad un sistema di riferimento; per la maggior parte delle analisi video (2D) dei movimenti umani, le direzioni utilizzate sono gli assi x , y . La variabile di moto lineare più semplice è la distanza (spazio) ed è una grandezza scalare.

Lo spazio percorso da un oggetto nell'unità di tempo permette di quantificare la velocità media scalare: si definisce la velocità media di un oggetto o punto materiale come il rapporto tra la distanza percorsa e l'intervallo di tempo impiegato ($v_m = \Delta s / \Delta t$). Differentemente dal moto rettilineo uniforme dove la velocità media scalare è costante, in un moto vario (composto da partenze, frenate, cambi di direzione) la velocità media non è costante quindi è più corretto parlare di velocità istantanea. La velocità istantanea rappresenta la derivata dello spazio rispetto al tempo, ossia il valore limite del rapporto $\Delta s / \Delta t$ nell'intorno di un determinato istante per Δt che tende a 0; nella realtà noi consideriamo sempre gli intervalli Δt finiti, ma, quando Δt diventa molto piccolo la velocità così calcolata permette una descrizione molto dettagliata del moto (i.e. GPS). La derivata della velocità rispetto al tempo o come derivata seconda dello spazio è l'accelerazione. L'accelerazione media di un punto materiale è il rapporto tra la variazione di velocità Δv e l'intervallo di tempo Δt in cui essa

avviene $a_m = \Delta v / \Delta t$. In un moto vario anche l'accelerazione come per la velocità, può variare in ogni istante. In questo caso si introduce l'accelerazione istantanea (misurabile con l'accelerometro), in analogia con la velocità istantanea. L'accelerazione istantanea è il valore limite dell'accelerazione media $\Delta v / \Delta t$ nell'intorno di un determinato istante, quando Δt diventa molto piccolo. Quindi nel moto rettilineo uniformemente accelerato l'accelerazione istantanea non cambia ed è uguale all'accelerazione media $A_m = A_i$

La cinematica angolare è utile per lo studio del movimento umano [45] perché è possibile calcolare spazio, tempo e velocità dei movimenti delle singole articolazioni utilizzando le rotazioni attorno a 1, 2 o 3 assi (x,y,z). Le variabili principali della cinematica angolare sono: angolo percorso, velocità angolare e accelerazione angolare.

L'angolo percorso, o angolo, è la quantità che rappresenta il cambiamento di orientazione del corpo, l'unità di misura sono i gradi ($^\circ$) o i radianti (rad). La velocità angolare ($^\circ/s$ o rad/s) è il rapporto tra l'angolo percorso e l'intervallo di tempo ($V_{ang} = D_{ang}/t$). L'accelerazione angolare ($^\circ/s^2$ o rad/s²) è la variazione, nel tempo, della velocità angolare.

Le informazioni che l'accelerazione angolare e la velocità angolare possono fornire sono utili per la descrizione precisa di come si sono verificati i movimenti ad esempio di un'articolazione o di un segmento corporeo o di un kayak.

Quindi, la cinematica lineare e angolare fornisce sufficienti informazioni riguardo lo studio del movimento di oggetti o corpi; infatti un recente studio ha dimostrato che le velocità angolari delle articolazioni o dei segmenti corporei sono di particolare interesse per la biomeccanica applicata allo sport [46].

I Principi della Dinamica

Relativamente alle forze che generano il movimento, le leggi del moto di Newton (moto lineare) rappresentano i principi fondamentali della dinamica. La prima legge di Newton (Principio di Inerzia) afferma che un oggetto tende a rimanere in quiete o in moto rettilineo uniforme se non interviene una forza esterna.

La seconda legge di Newton (anche chiamata principio di proporzionalità) è forse la più importante perché riguarda le forze che generano il movimento. Essa afferma che l'accelerazione di un oggetto è direttamente proporzionale alla forza risultante agente su di esso e inversamente proporzionale alla sua massa: $\vec{F} = m \times \vec{a}$. Nel SI l'unità di misura della forza è il newton (N). Un'applicazione pratica della seconda legge di Newton è la relazione Forza-Tempo: infatti se un atleta applica una forza per un periodo di tempo più lungo, sarà in grado di raggiungere una velocità maggiore rispetto a quando utilizza forze simili in intervalli più brevi di tempo (da tener presente che in diversi movimenti non si ha un tempo illimitato per applicare la forza e ci sono diversi componenti, legate alle diverse caratteristiche dei muscoli, che complicano l'applicazione del 2° principio). La terza legge di Newton (chiamata anche principio di azione e reazione) afferma che per ogni azione c'è una reazione uguale e contraria, quindi stabilisce che se un corpo A applica una forza (detta forza di azione) a un corpo B, il corpo B applicherà a sua volta al corpo A una forza di reazione uguale in modulo e direzione, ma opposta in verso: $\vec{F}_{AB} = -\vec{F}_{BA}$ (un esempio è la ground reaction force).

Considerando la cinematica angolare, le cause (forze) che generano il movimento sono molto simili a quelle menzionate per la cinematica lineare. In effetti, le leggi di Newton hanno analoghi angolari che spiegano come le coppie (torque) creano la rotazione. Quindi ogni principio newtoniano può

essere riformulato usando variabili angolari. Ad esempio l'analogo angolare della terza legge di Newton dice che per ogni coppia (torque) esiste una coppia (torque) uguale e contraria.

L'accelerazione angolare di un oggetto è proporzionale alla coppia (torque) M risultante, è nella stessa direzione ed è inversamente proporzionale al momento d'inerzia I : questa è l'espressione angolare della seconda legge di Newton $\vec{M} = I \times \vec{\alpha}$.

Allo stesso modo, la prima legge di Newton dimostra che gli oggetti tendono a rimanere nel loro stato di movimento angolare a meno che non intervenga una coppia (torque) che sbilanci il sistema. Quasi sempre vengono utilizzate le leggi di Newton per il calcolo delle forze e delle coppie (torque) che agiscono sul soggetto o sui singoli segmenti. La maggior parte delle volte per calcolare o stimare le forze (II legge di Newton) si preferisce misurare dall'analisi video l'accelerazione, utilizzando o la cinematica lineare o angolare, e questo lavoro a ritroso è chiamata dinamica inversa.

Cenni di meccanica dei fluidi (galleggiabilità, drag, forza propulsiva)

Il movimento umano oltre che avere luogo sulla terra può essere effettuato nei fluidi, in particolar modo nell'acqua, come avviene in discipline sportive quali kayak, nuoto, canottaggio, pallanuoto. La fisica che studia il comportamento dei corpi in acqua si divide in idrostatica (che si occupa dei corpi fermi) e idrodinamica (che si occupa dei corpi in movimento).

Quando un corpo si trova in acqua è soggetto a una forza verticale diretta verso l'alto detta spinta idrostatica o di Archimede. In base al celebre principio di Archimede (la sola legge fisica che ci sia giunta dall'antichità greco-romana), la spinta idrostatica è pari al peso del liquido spostato. Quindi la spinta idrostatica avrà stessa direzione ma verso opposto alla forza peso (Eq.1). Se il corpo galleggia, possiamo affermare che le due forze sono in equilibrio, quindi:

$$F_A = -F_p \quad (\text{Eq.1})$$

Dove F_A è il vettore Spinta di Archimede e $-F_p$ è la forza peso generata dal fluido spostato.

Il punto di applicazione della spinta di Archimede è il centro di spinta, o centro di carena, che rappresenta essenzialmente il baricentro del volume d'acqua spostato dall'oggetto.

Nel corpo umano, il tronco costituisce la maggior parte del volume, quindi il centro di galleggiamento si trova 1–2 cm più in alto rispetto al baricentro [45,47]. La galleggiabilità, ovvero il rapporto tra volume emerso e immerso di un nuotatore, varia al variare della composizione corporea. Infatti la densità del corpo umano è simile a quella dell'acqua a causa dell'alto contenuto di acqua nei tessuti. La differenza sostanziale tra i tessuti del corpo umano è relativa alla distribuzione della massa magra e della massa grassa. Infatti, il tessuto magro (muscoli e ossa) possiede una densità maggiore dell'acqua rispetto al grasso corporeo che tende ad essere molto meno denso. Quindi una persona con un'elevata % di massa grassa galleggerà molto più facilmente rispetto ad un soggetto con elevata % di massa magra.

Quando un oggetto/atleta si muove in acqua su di esso agiscono, oltre al peso e alla spinta idrostatica, altre due forze: la propulsione o thrust e la resistenza del mezzo o drag (Figura 8).

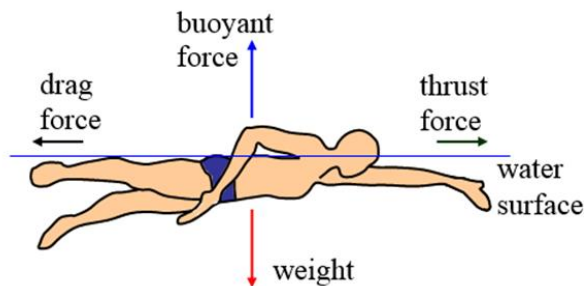


Figura 8: Forze agenti sul nuotatore

A velocità di avanzamento costante, propulsione e resistenza sono in equilibrio. Il drag a sua volta è la somma di 3 tipi di resistenze: drag di attrito, drag di pressione o di forma, drag d'onda [48,49].

Mentre un corpo si muove in acqua l'interfaccia tra acqua e aria genera il drag d'onda. L'onda che si genera davanti si muove in senso contrario all'avanzamento spingendo contro il corpo, rallentando la velocità o aumentando l'energia necessaria per nuotare o pagaiare ad una certa velocità. Anche altre onde si formano, durante l'avanzamento, intorno al corpo a causa della differenza di pressione e disperdono energia. Per esempio nel nuoto il drag d'onda ha un effetto molto importante sulla prestazione; infatti è stato stimato che rappresenta il 50% della resistenza totale che agisce sul nuotatore [50]. Queste onde sono simili a quelle che si formano intorno ad un kayak o ad una nave; sia la lunghezza che l'altezza dell'onda aumentano con l'aumentare della velocità. Il sistema di onde che circonda il kayak/nuotatore si sposterà alla stessa velocità, letteralmente l'atleta porta "le onde con sé". Con l'aumento della velocità la distanza tra la prima onda (onda di prua) e la seconda onda aumenterà fino a quando la lunghezza tra le onde sarà come la lunghezza del nuotatore/ kayak e ci si ritroverà ad avanzare in una conca. In questa situazione un ulteriore aumento di velocità diventa costoso dal punto di vista energetico. Il fattore che causa maggiormente il drag d'onda è il beccheggio (oscillazione positive e negative attorno all'asse y) infatti la riduzione dei movimenti di beccheggio riducono notevolmente il drag d'onda [51].

Il drag di forma è associato all'area di superficie e alla forma del nuotatore/kayak; per ridurlo si deve diminuire il più possibile l'area frontale del nuotatore/kayak. Nel nuoto può essere fatto tenendo bassa la testa [45] mentre per il kayak è opportuno considerare il peso dell'atleta e il modello di imbarcazione [52]. Un' ulteriore riduzione del drag di forma può essere ottenuta allineando il più possibile il corpo/kayak nella direzione di avanzamento. Qualsiasi deviazione da questa linea aumenterà l'area della superficie frontale del corpo/kayak. il drag di forma è proporzionale al quadrato

della velocità: quando la velocità aumenta, anche il drag aumenta, fino a raggiungere un valore tale da equilibrare la forza propulsiva dell'atleta (v. paragrafo successivo).

Il drag di attrito è generato dallo sfregamento dell'acqua sulla superficie del nuotatore/kayak. La viscosità dell'acqua rappresenta la resistenza interna da vincere. I metodi per ridurre questo tipo di drag, visto che non è possibile modificare la viscosità del fluido, sono per esempio modificare la ruvidità del corpo/oggetto per ridurre la resistenza superficiale. In definitiva, la resistenza idrodinamica (D_{hy}) è la somma del drag di attrito (D_a), drag di pressione (D_p), drag d'onda (D_w).

$$D_{hy} = D_a + D_p + D_w \quad (\text{Eq.2})$$

Il movimento in acqua è governato dalla terza legge di Newton; sulla superficie terrestre ad ogni azione corrisponde una forza di reazione vincolare con il terreno, nell'acqua il punto di appoggio dove esercitare la forza deve essere creato e il nuotatore/paddler deve saper sfruttare le caratteristiche fisiche del fluido (densità, viscosità) per poter superare le resistenze passive (drag) che si oppongono al movimento. Quindi è possibile descrivere il nuoto, il kayak tramite forze di azione (propulsive) e forze di reazione (drag).

Nel nuoto e nel kayak l'obiettivo è spostarsi il più velocemente possibile, quindi risulta importante individuare la quantità di forza ma soprattutto di potenza espressa nell'unità di tempo per ogni singolo movimento degli arti superiori. Ecco perché si possono distinguere come per le forze la potenza di azione e la potenza di reazione. La potenza di azione (come la forza di azione) non è uguale e contraria alla potenza di reazione, perché l'acqua non è solida e si muove quando si applicano forze su di essa. Infatti, parte della potenza generata dall'atleta è impiegata per muovere l'acqua piuttosto che per generare propulsione in avanti.

Nel kayak l'efficienza sul colpo è verificata quando la maggior parte dell'energia spesa dal paddler è utilizzata durante la fase di pull-push (tirata-spinta) ed è utile per la propulsione in avanti della barca. La potenza propulsiva generata da una pagaia si misura dalla forza idrodinamica generata dalla pala in acqua e dalla velocità della stessa rispetto all'acqua. Quindi l'efficienza propulsiva della pagaia può essere ottimizzata massimizzando la quantità di forza prodotta dalla pala e riducendo al minimo la quantità di energia persa durante l'avanzamento[53].

Equilibrio statico e dinamico

L'equilibrio è un concetto che deriva dalla I e II legge di Newton. L'equilibrio meccanico si verifica quando è nulla la risultante delle forze che agiscono sull'oggetto. In tal caso il corpo può essere fermo (equilibrio statico) oppure muoversi a velocità costante (equilibrio dinamico). L'equilibrio statico per un punto materiale si verifica quando la risultante delle forze applicate è nulla: $R=0$ (equilibrio statico del centro di massa). La condizione di equilibrio dinamico si verifica quando la velocità istantanea, costante ($a=0$), coincide con la velocità media; ci si trova dunque in una situazione di moto rettilineo uniforme. All'equilibrio dinamico tutta la forza propulsiva prodotta dall'atleta viene impiegata per vincere le resistenze dell'acqua (se presente) e dell'aria: $F = D$.

Anche questo concetto può essere esteso ai moti rotatori: un corpo rigido non sottoposto a coppie esterne rimane fermo $M=0$ (nessuno moto rotatorio) oppure ruota a velocità angolare costante.

Dalla I legge di Newton discende in caso di moto lineare la conservazione della quantità di moto: in assenza di forze esterne $m \cdot \vec{v} = cost$. In caso di moto rotatorio si ha invece la conservazione del momento angolare, ovvero il prodotto del momento di inerzia per la velocità angolare $I \cdot \omega = cost$. Se durante il moto il momento di inerzia diminuisce (ciò è possibile solo se il corpo è articolato), aumenta

la velocità angolare, e viceversa. Atleti quali i tuffatori e i pattinatori su ghiaccio, per esempio, avvicinano gli arti al corpo per ruotare più velocemente, e le allontanano per ruotare più lentamente.

Modelli di prestazione di alcuni sport acquatici

Kayak

Il kayak in acqua piatta è una disciplina sportiva in cui l'azione combinata della pagaia e il movimento degli arti inferiori sul punta piedi permettono l'avanzamento del kayak attraverso l'acqua.

Per massimizzare la velocità dell'imbarcazione l'atleta deve essere in grado di generare elevati gradienti di potenza e forza muscolare durante ogni colpo in acqua della pagaia, nonché mostrare allo stesso tempo solide abilità tecniche e capacità metaboliche inerenti alla distanza di gara (200-500-1000m).

Durante l'avanzamento, il kayak ha una fluttuazione della velocità dovuta all'effetto combinato del movimento dinamico determinato dall'applicazione della forza sulla pala e dalle forze resistive (drag aereodinamico e idrodinamico). Le forze resistive agiscono in direzione opposta al vettore velocità dell'imbarcazione. È noto che l'avanzamento del kayak è prettamente influenzato dalla resistenza idrodinamica rispetto alla resistenza aerodinamica che ha invece, un effetto minimo sulla velocità [48]. L'incremento di velocità del kayak è stato osservato in concomitanza della fase di pull (propulsione) [12] dove la pagaia viene spostata in direzione opposta all'avanzamento del kayak creando una forza maggiore rispetto alle forze di drag presenti. Diversamente, durante le fasi di entrata e di uscita la passata in acqua non è più propulsiva e le forze di resistenza agiscono sul kayak decelerandolo generando così una fluttuazione della velocità. Pertanto, per ottenere prestazioni ottimali, è necessario ridurre al minimo le forze di drag sul kayak e sviluppare i fattori che

contribuiscono a migliorare la fase propulsiva (forza propulsiva). Quindi la velocità media che l'atleta deve mantenere durante la prestazione risulta essere la combinazione intermittente tra forza propulsiva e drag.

Nuoto

La locomozione acquatica di un essere umano è il risultato dell'interazione dei segmenti corporei con l'acqua.

Il nuoto è caratterizzato da una sequenza di azioni coordinate del tronco e degli arti, in uno schema ripetuto e sincrono. L'azione delle braccia durante ciascuno dei quattro stili del nuoto comprende fasi specifiche (Figura 9)[54].

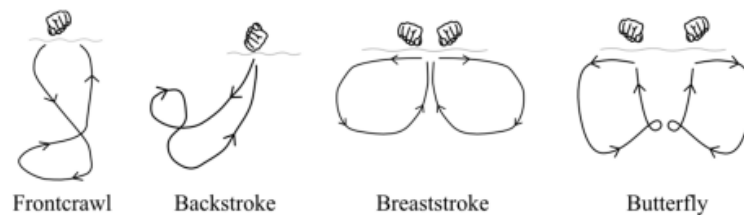


Figura 9: Rappresentazione delle azioni tipiche delle bracciate a stile libero, dorso, rana e delfino[54].

Durante il nuoto un nuotatore crea il "supporto immobile" nel mezzo fluido mobile, sfruttandone la densità e la viscosità, e vince le forze resistive opposte (drag d'onda, di frizione e di pressione). La resistenza idrodinamica si manifesta come: (i) la forza che rallenta e ferma il movimento del nuotatore nell'acqua; e (ii) come la forza di reazione idrodinamica ai movimenti degli arti del nuotatore attraverso l'acqua. Questa forza di reazione idrodinamica è la fonte di propulsione per la locomozione del nuotatore. La velocità di nuoto dipende dall'entità e dalla direzione della forza di reazione

idrodinamica (o forza propulsiva) creata dai movimenti dei segmenti corporei del nuotatore e dall'entità della resistenza idrodinamica attiva. La reazione idrodinamica creata dal nuotatore cambia costantemente valore e direzione durante il ciclo della bracciata a causa dell'alterazione delle fasi di lavoro e delle fasi di recupero. Di conseguenza, ci sono cambiamenti nella forza propulsiva effettiva. Anche il valore della resistenza idrodinamica cambia continuamente all'interno del ciclo della bracciata. Quindi, il nuotatore per poter avanzare in acqua ha bisogno durante ogni ciclo di bracciata di sviluppare una forza propulsiva maggiore o uguale (condizione a velocità costante) delle forze resistive. È noto che generare un'elevata forza propulsiva durante il nuoto non è un compito facile. Infatti, non tutti i componenti della risultante della forza propulsiva contribuiscono a un'efficace produzione della forza propulsiva (o forza di trazione) a causa della deviazione del vettore della forza di reazione dalla direzione del nuoto in determinati momenti delle azioni di trazione. Allo stesso tempo una parte sostanziale dell'energia meccanica delle azioni di trazione viene persa nel trasferimento di energia cinetica alla massa d'acqua che il nuotatore usa come supporto. Di conseguenza, solo una parte del lavoro meccanico svolto da un nuotatore viene utilizzata efficacemente per superare la resistenza idrodinamica[55].

Pallanuoto

La pallanuoto è uno sport molto impegnativo, con intense attività [56] ed è caratterizzato da movimenti complessi: nuoto ad alta velocità (per brevi periodi anche alla massima velocità) [57], azioni veloci e rapide con contrattacchi pronunciati [56,58] svolte con possesso palla e a contatto con l'avversario; frequenti passaggi; tiri in porta; fasi di wrestling e blocchi per mantenere o guadagnare

la posizione in acqua. È nota, l'importanza delle attività diverse dal nuoto (es. tiro, passaggio e lotta), che rappresentano circa il 69% del tempo di gioco [56,59,60] di una partita. La natura intermittente di questa disciplina, unitamente ai limiti imposti dall'ambiente acquatico, rende tecnicamente difficile la valutazione delle capacità fisiologiche dei pallanuotisti. Diversi studi confermano che le frequenze cardiache che sono state registrate durante il gioco [61], insieme ai valori di lattato nel sangue moderatamente alti (fino a 12 mmol/l) suggeriscono che una grande quantità di produzione di energia ha origine dal metabolismo anaerobico lattacido [62]. Molte delle azioni tecniche come il tiro, il passaggio e il wrestling richiedono elevati gradienti di forza degli arti inferiori perché svolte in posizioni verticale e orizzontale. Infatti, è stato dimostrato che i giocatori con livelli più elevati di forza degli arti inferiori sono in grado di generare una maggiore elevazione fuori dall'acqua, quindi lanciando la palla più velocemente [63]. Inoltre, è stato sottolineato che in entrambe le fasi della partita, attacco e difesa, caratterizzati dal tentativo di avvicinamento alla porta (tipico dell'attaccante) e dall'azione opposta di cercare di allontanare l'avversario dalla porta (tipico del difensore) vengono eseguite utilizzando i muscoli di tutto il corpo, ma soprattutto i muscoli degli arti inferiori [56]. Le azioni degli arti inferiori maggiormente coinvolte in queste azioni in acqua sono l'eggbeater kick utilizzato per il mantenimento della posizione e il breaststroke kick utilizzato per le azioni di potenza (salto e tiro). Quindi la riuscita di queste azioni dipende non solo dalla forza ma anche dalla capacità di esercitare la forza alla velocità richiesta dall'azione motoria. Oltre alle capacità tecniche-tattiche e metaboliche, è stato affermato che la forza e la potenza muscolare sono i fattori più importanti che danno un chiaro vantaggio nelle competizioni d'élite [59].

Capitolo 1



A Multiprotocol Wireless Sensor Network for High Performance Sport Applications

Vincenzo Bonaiuto ^{1,*}, Paolo Boatto ³, Nunzio Lanotte ³, Cristian Romagnoli ^{1,4} and Giuseppe Annino ^{1,2}

¹ Sport Engineering Lab, Dept. Industrial Eng., Univ. Rome Tor Vergata, Rome, I00133, Italy

² School of Human Movement Science, Fac. of Med.& Surgery, Univ. Rome Tor Vergata, I00133 Rome, Italy; g_annino@hotmail.com

³ APLAB, Roma, I00196, Italy; paoloboatto@tiscali.it (P.B.); nunziolanotte@aplab.it (N.L.)

⁴ Department for Life Quality Studies University of Bologna, Rimini, I47037, Italy; cristian-romagnoli@outlook.it

* Correspondence: vincenzo.bonaiuto@uniroma2.it; Tel.: +39-06-7259-7402

Received: 22 November 2018; Accepted: 19 December 2018; Published: 19 December 2018

Abstract: The use of a network of wearable sensors placed on the athlete or installed into sport equipment is able to offer, in a real sport environment rather than in the unspecific spaces of a laboratory, a valuable real-time feedback to the coach during practice. This is made possible today by the coordinate use of a wide range of kinematic, dynamic, and physiological sensors. Using sensors makes training more effective, improves performance assessment, and can help in preventing injuries. In this paper, a new wireless sensor network (WSN) system for elite sport applications is presented. The network is made up of a master node and up to eight peripheral nodes (slave nodes), each one containing one or more sensors. The number of nodes can be increased with second level slave nodes; the nature of sensors varies depending on the application. Communication between nodes is made via a high performance 2.4 GHz transceiver; the network has a real-life

range in excess of 100 m. The system can therefore be used in applications where the distance between nodes is long, for instance, in such sports as kayaking, sailing, and rowing. Communication with user and data download are made via a Wi-Fi link. The user communication interface is a webpage and is therefore completely platform (computer, tablet, smartphone) and operating system (Windows, iOS, Android, etc.) independent. A subset of acquired data can be visualized in real time on multiple terminals, for instance, by athlete and coach. Data from kayaking, karting, and swimming applications are presented.

Keywords: inertial sensors; array sensor systems; wireless systems; sport performance assessment

Introduction

High performance sport, i.e., sport at the highest level of competition, requires advanced technology, as each competitor tries to gain the winning edge through incremental improvement. Data acquisition plays a fundamental role in this competitive environment, as it supplies athletes and coaches with quantitative insights into every aspect of performance [1–3].

Sensors used in sport data acquisition range from kinematic (GPS units, accelerometers, gyroscopes, velocity meters, etc.) to dynamic (load cells, strain gages, brakes, etc.) and physiological (heart rate monitors, thermometers, etc.) [4–10]. Several types of sensors are often bundled together: A typical example is the cycling computer that acquires data coming from the global positioning system (GPS), heart rate monitor, power meter, gears, and more [11]. Systems used in sports normally feature a central unit (master node), where the microcontroller (MCU—microcontroller unit) is located, and a series of sensors (slave nodes) [12]. The communication between master and slave nodes can occur

via cables (wired sensor network) or be wireless (wireless sensor network, WSN). WSNs are particularly suitable in sport applications, as cables can hinder the motion of the athlete(s) during training and competitions [13].

Nowadays, several wireless protocols are available on the market; Table 1 illustrates the main features of each of them. These vary in topology, application throughput, complexity of the software interface, ease of configuration, addition of extra sensor nodes, transmission range, and power consumption [14–22]. Concerning the maximum data rate and transmission range, these values must be understood as maximum theoretical values that can be obtained only in an outdoor space free of obstacles and radio interference.

Table 1. Comparison of different wireless communication protocol.

Standard		Max TXRange ¹	Max Data Rate	Application Throughput	Band	Application	Topology
ZigBee	IEEE 802.15.4	100 m	500 kbps	35.0 kbps	2.4 GHz	Wireless Sensors	Star, Mesh
Z-Wave	Proprietary	100 m	100 kbps	6 kbps	900 MHz 2.4 GHz	Wireless Sensors	Mesh
ANT+	Proprietary	30 m	60 kbps	260kbps	2.4 GHz	Wireless Sensors	Star, Tree, P2P, Mesh
Bluetooth	IEEE 802.15.1	10 m	1–3 Mbps	2.1Mbps	2.4 GHz	Wireless Sensors	P2P, Star
Bluetooth 4.0 LE	IEEE 802.15.1	100 m	2 Mbps	305 kbps	2.4 GHz	Wireless Sensors	P2P, Mesh, Star, Broadcast
Bluetooth 5.0 LE	IEEE 802.15.1	400 m	2 Mbps	1360 kbps	2.4 GHz	Wireless Sensors	P2P, Mesh, Star, Broadcast
Wi-Fi	IEEE 802.11a WLAN	5 km	54 Mbps	20 Mbps	5 GHz	PC based data acquisition	Star, Tree, P2P
Wi-Fi 4	IEEE 802.11n	250 m	600 Mbps	72 Mbps	2.4 GHz	PC based data acquisition	Star, Tree, P2P
WiMAX	IEEE 802.16 WWAN	15 km	75 Mbps	4–8 Mbps	2.3-5.8 GHz	Mobile Internet	Star, Tree, P2P

¹(open-air outdoor).

For a long time, in the sport device industry, proprietary and incompatible WSN standards only have been used. Indeed, only in early 2000 was a wireless common communication standard suited for sport and health applications defined and agreed among different main vendors (advanced and adaptive network technology—ANT+ [22,23]). The main features were a very low energy consumption, a high number of connectable nodes, and high robustness to interference. Nowadays, the growing popularity of consumer portable devices, such as tablets and smartphones featuring embedded Bluetooth [23], and more recently, Bluetooth low energy (BLE) [24], has led to a large diffusion of “apps” suited for connection with sport systems. For example, when Apple Inc. supplied BLE in its devices, several fitness products were developed with a MAC iOS software to be compatible with these terminals [25]. Thus, today, the development of a new WSN cannot ignore the use of such personal mobile terminals and should leverage the transmission protocols available on them (typically Wi-Fi and Bluetooth). The use of ANT+ on a mobile phone, for example, would require the use of additional hardware.

Moreover, today, with 75%, the Android operating system (OS) holds the biggest market share for tablets and smartphones, while Windows and MAC iOS are still dominant in laptop and desktop computers [26]. This requires the development of different software tools depending on the nature of the terminal and the relevant OS.

Therefore, from a communication protocol point of view, the constraints in building up an effective WSN suited for sport applications can be identified in the use of personal portable terminals, wide transmission range among the nodes, low power consumption, and easy addition of extra sensor nodes. The transmission range is a particularly severe constraint, as most existing systems for sports are designed for personal area networks (PANs) [27,28] or body sensor networks (BSNs) [29], which cover a very short distance.

In this paper, we present a WSN for sport applications based on a multiprotocol architecture: The communication with the user is based on a Wi-Fi link, while data transmission between the nodes is made via high performance 2.4 GHz modules. Furthermore, the user interface will be implemented on a simple webpage, readable by a web browser on any kind of OS and terminal. The architecture is composed of a main node where, for example, the sensors that have to measure parameters related to the overall performance (i.e., the speed or the acceleration of a boat) are mounted: Inertial measurement unit (IMU), GPS, etc. The slave nodes can be adapted to host different kinds of sensors, for instance, a thermometer, a potentiometer or an encoder. Both the master and slave nodes can be configured to host different kinds of sensors. This means that the whole system can be customized with minimal hardware and software modifications, greatly reducing the development time and cost.

Materials and Methods

Some WSNs for particular sporting applications require, for example, a large number of sensors placed in a specific position and often located at a great distance from each other. In these cases, the design of a WSN must consider the attenuation of the transmitted signal; this is caused not just by the distance between the nodes themselves but also by the presence of obstacles between them as, among others, the bodies of athletes and the sport equipment. In fact, even the structure and the materials used for their manufacture can represent a shield for radio transmission (for example, both the hull and the shaft of a kayak paddle are made of carbon fiber). Ditto, the presence in the nearby area of other radio devices that work in the same frequency band of smartphones, Wi-Fi or Bluetooth networks, etc. They introduce electromagnetic noise and, consequently, a significant reduction in the real range of transmission of the nodes.

For example, a WSN suitable for yacht racing could be composed of nodes mounted in very distant places [30]. Furthermore, the transmission system of the WSN could interfere with other on-board

radio systems. Therefore, the only solution could be to install more nodes at a smaller distance between them: Some of them could, in fact, not collect data from sensors at all and work as simple repeaters of the signal coming from other nodes.

The architecture of the proposed WSN is depicted in Figure 1. The Master Node can be connected with the User Terminal (i.e., tablet, smartphone, PC, etc.) by a Wi-Fi link over a dedicated WLAN and a webpage for realtime feedback of training or download of the whole session data. The master node can communicate with up to eight first level peripheral nodes via 2.4 GHz transceiver ISM band modules (based on the Nordic Semiconductor chip nRF24L01+) which guarantee a real life range in excess of 100 m and an acceptable power consumption. Furthermore, each of the eight first level peripheral nodes can connect to up to eight second level nodes if an increase of sensor nodes or a wider range is required. The system was originally designed for application in elite flatwater kayaking [31]. For this reason, it will be called e-kayak in the following. The main technical specifications of this project are as follows:

- Measurement of boat displacement and velocity by means of high frequency GPS (sampling frequency ≥ 10 Hz);
- Measurement of triaxial acceleration and triaxial angular velocity (sampling frequency ≥ 50 Hz);
- Measurement of force on the paddle and footrest of each athlete (sampling frequency ≥ 50 Hz);
- Real-time visualization of speed and stroke frequency on athlete and coach terminals;
- Wireless data download and system diagnostics from any platform and OS (Windows, MAC iOS, Android);

- Battery time for all the master and slave nodes ≥ 2 h to acquire a whole training session without the need to recharge.

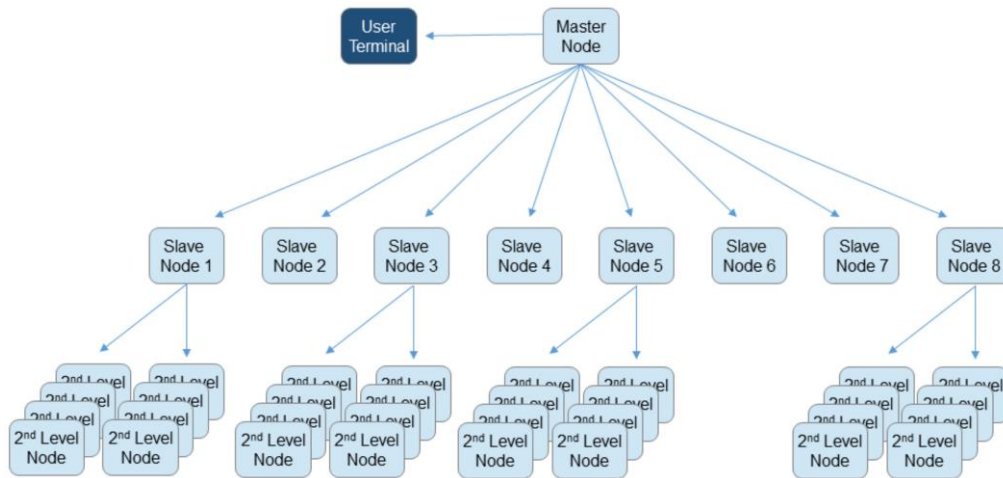


Figure 1. Wireless sensor network (WSN) architecture.

Choice of Radio Transmission Device

For a proper assessment of the performance of a flatwater kayak team, information on both dynamic and kinematic quantities is required. The former ones represent the measure of the forces applied by the athletes while the latter are the result of the action of such forces on the motion of the boat. Each paddle and footrest, which represent the slave nodes for the WSN, has therefore been equipped with strain gauges to measure the intensity and the coordination among these forces. By contrast, the velocity and the triaxial accelerations are measured, respectively, by a high frequency GPS and an IMU placed on the master node. As a result, each boat will be equipped with a master node and two slave nodes for each paddler.

The range constraints in this application are particularly demanding: A racing kayak can have up to four paddlers (K4), each having a paddle and a footrest. Each paddle and footrest, equipped with a force sensor, is a slave node.

Unlike in rowing, the paddle is not attached to the boat, so a wireless connection is required to avoid hindering the motion of the athlete. A typical K4 boat is about 11 m long, so even placing the master node in the middle of the hull, the distance between it and the farthest slave node can be up to 4–5 m, in a very noisy environment with bulky obstacles, namely the bodies of the athletes (Figure 2).



Figure 2. A K4 racing kayak.

This is outside the typical range of both Bluetooth and ANT+, the most widely used protocols for sport applications (see Table 1). A comparative test of the range of some commercially available wireless modules has shown that the one with longer range is the nRF24L01P+PA+LNA, (by Chengdu Ebyte Electronic Technology Co., Ltd., Chengdu, China) (Figure 3).

The module is a low power single chip transceiver for the global, license-free 2.4 GHz ISM band with high-speed communications (up to 2 Mbit/s). It consists of a fully integrated frequency synthesizer (Gaussian frequency shift keying—GFSK modulation), a power amplifier, and a modulator–demodulator block, and it is based on the Enhanced ShockBurst protocol engine [32]. This makes it ideal for building wireless networks in a wide range of applications. Equipped with an external antenna, this module can cover a distance, measured in an open field, in excess of 100 m,

with data loss <1% on a data rate of 1 kbps (declared range of the module is in fact 2500 m). Its power consumption of 100 mW, while higher than other modules, is still compatible with the two hours of battery time required by the project specifications.



Figure 3. The nRF24L01P+PA+LNA module.

All system parameters (e.g., output power, frequency channels, protocol setup, and air data rate) are programmable through the serial peripheral interface (SPI) serial link. The data rate of 250 kbps, 1 Mbps, or 2 Mbps is configurable on air. The same modules can be mounted on master and slave nodes; the network can be composed up to eight peripheral nodes. At power on, all slave nodes transmit and receive over a “handshake” frequency, while the master node scans continuously for new slave nodes on that frequency; once the slave has been detected, its frequency is switched to the “running” frequency by the master node. Using multiple “running” frequencies, it is possible to operate different systems without interference.

Choice of User Communication Protocol

The project specifications require communication between user and system and data download to be carried out from any kind of platform (smartphone, tablet, laptop PC) with any kind of OS (Windows, MAC, Android). While nRF24L01+ is arguably the best choice for data transmission between master and slave nodes, it is not featured in smartphones or laptop computers, so adopting it for user

interaction would mean having to design a plug-in module and a different app for every OS. Wi-Fi modules, on the other hand, are installed by default on virtually every mobile device. Furthermore, a Wi-Fi interface can be designed as a webpage. This means it is readable with any device and OS, as long as a web browser is present. No other app needs to be installed. Finally, data download via Wi-Fi prevents all problems related to connection via cable (USB or similar) in the wet, windy, or snowy environments which are typical of outdoor sports.

The firmware installed on the master node microcontroller and Wi-Fi module generates a purpose-made WLAN. Several users can connect to the WLAN and load the communication webpage (Figure 4). This includes, on the left side of the page, commands for acquisition start–stop, data download, system status (battery level, memory status, number of connected nodes) and, on the right side of the page, a subset of parameters, for instance, speed and stroke frequency, which are refreshed at 5 Hz and shown on a graph.

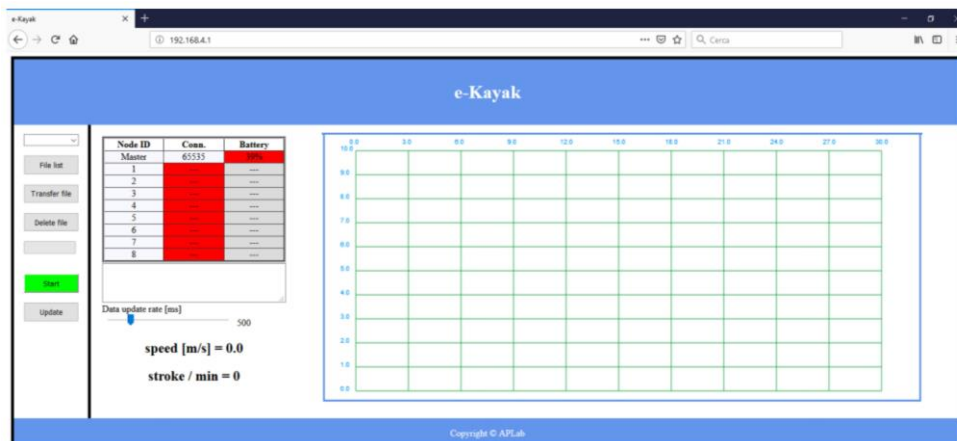


Figure 4. The webpage acts a communication interface.

Thus, in a typical situation, the athlete can have immediate feedback on his training on his smartphone placed in the cockpit of the canoe, while the coach, who usually follows the kayak on a motor boat during training sessions, can manage the acquisition and download data on a PC. Several e-kayak systems can operate at the same time without interference. Each one creates its own WLAN,

identified by a serial number and, if necessary, password protected. A single coach can therefore supervise multiple boats. Data download speed is about 300 kbps (i.e., data from a typical 90 min training session for a K1 boat can be downloaded in less than a minute). Moreover, data download is also possible, if it is required, using a USB cable (up to 6 Mbit/s).

Design of the Master Node

The master node is composed of an MCU, a GPS module, a 9-axis inertial measurement unit (IMU), an nRF24L01P+PA+LNA module, and a Wi-Fi module (Figure 5a).

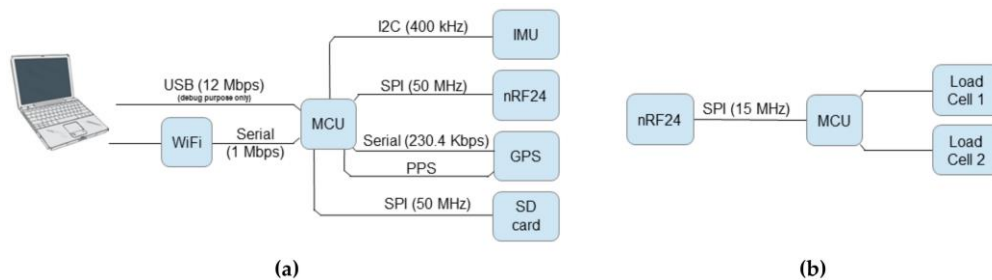


Figure 5. Block scheme of the master node (a) and slave node (b). IMU = Inertial measurement unit, MCU = Microcontroller unit, GPS = Global positioning system, SPI = Serial peripheral interface, PPS = Pulse per second.

The GPS module has a sampling rate of 20 Hz. Since the maximum stroke rate of an athlete during a sprint is about 180 strokes per minute (i.e., 3 Hz), the module can measure speed fluctuations at each stroke (intracyclic speed). The module communicates with the MCU via a serial port at a speed of 230.4 Kbps. The IMU has a sampling frequency of 50 Hz and is connected to the MCU by an I2C (inter-integrated circuit) serial bus link (up to 400 kHz).

The management of the e-kayak WSN is computationally rather demanding. The MCU is tasked with acquiring data from GPS and IMU, communicating with the slave nodes via nRF24L01+ modules and with the user via Wi-Fi, calculating real-time parameters and storing the data in a micro-SD memory card. For this reason, the chosen MCU is Pjrc's Teensy 3.6. It is arguably the most powerful

Arduino clone available on the market, featuring a 32-bit 180 MHz ARM Cortex-M4 processor with a floating-point unit. It also features an on-board micro secure digital (SD) slot and several serial ports for communication with peripherals. Since GPS data, IMU data, and sensors data have different sampling frequencies and time scales, they are synchronized using the GPS receiver PPS (pulse per second) signal.

A custom-made board has been designed (Figure 6a) to accommodate all the main components, as well as a charge circuit and all the necessary interfaces with the commands (switch, button, leads, etc.). The node is placed in a waterproof case for on-board use. The master node is powered by a 3.7 V, 1200 mAh LiPo battery. It can also be connected to a PC via USB cable for system diagnostics.

Design of the Slave Nodes

The main components of a slave node (Figure 5b) are the MCU, the nRF24L01P+PA+LNA module, and the signal conditioning circuits for the force sensors (two channels are available): A load cell or a strain gage bridge placed on the paddle shaft or on the footrest (two sensors in the latter case). Since the computational burden of the master node is much lighter, a smaller MCU, namely an Arduino Nano (based on the 16 MHz ATmega328 processor), has been adopted. The slave node is powered by a 3.7 V, 500 mAh LiPo battery and it is equipped with a battery charge circuit.

In particular, for the e-kayak system, two custom-made boards have been designed, for the paddle nodes and for the footrest nodes, respectively. They only differ in their form factors, the one for the paddle being long and thin enough to be placed inside the shaft (Figure 6b).

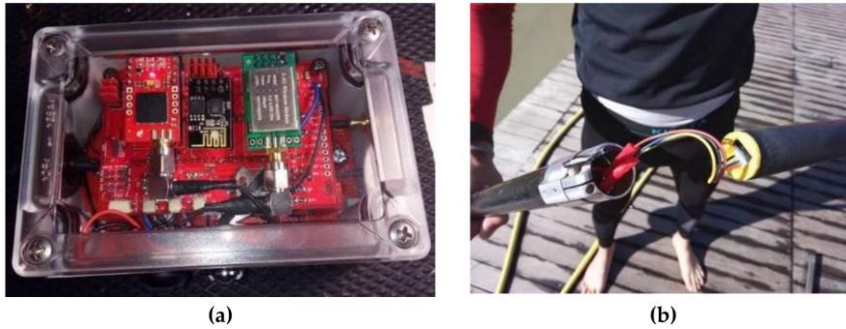


Figure 6. (a) Master node in a waterproof case; (b) slave node placed in the paddle shaft.

Results

The proposed WSN system presents two main features that make it more widely exploitable in several sport applications with respect to other commercially available systems:

- High flexibility in number and type of employable sensors;
- Possibility to cover a wide sensor area by using second level Slave nodes;
- OS independent user interface represented by a simple web browser.

The acquired data can be visualized and analysed on purpose-made apps that are specific to each sport application. In this section, we present applications of the proposed system in different configurations showing acquired data and a brief description of the specific app for the data analysis. Figure 7 depicts the app developed for the e-kayak system equipped with a master node that hosts GPS and IMU and two slave nodes with force sensors on footrest and paddle, respectively. The screen shows all data acquired during a K1 training session: At the top left graph, the data of roll speed (red), yaw speed (yellow), and pitch speed (green, hidden) are shown. The bottom left graph shows the forces on paddle (red) and foot rest (green), while the graphs on the right side of the page depict (from top to bottom) the acceleration on the three axis, the boat's speed, and the travelled distance. All these measurements were taken in synchronous mode, so an increase in the stroke rate and force

(e.g., at about 220 s) corresponds to an increase of the roll speed as well as the boat's acceleration and speed.

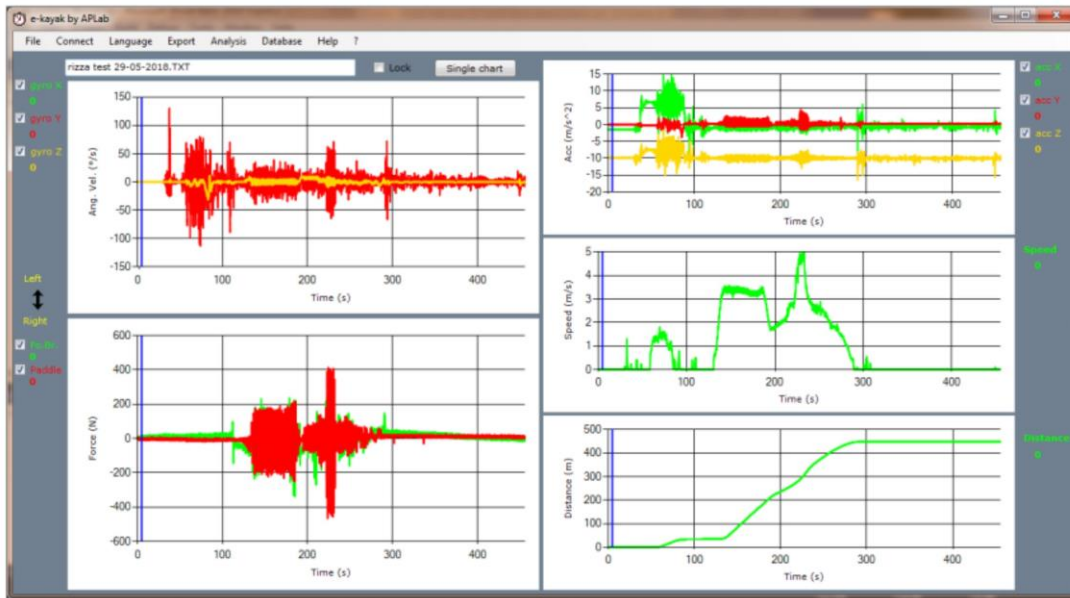


Figure 7. Example of screenshot of the application for e-kayak session analysis.

Figure 8 shows data from a measure of a session of K2 training for which the system was equipped with four slave nodes: Two for the paddles and two for the footrests. In particular, it depicts a detail of an acquisition of the forces applied by the two athletes on their paddles. One can note a rather good synchronization between the athletes and a good symmetry, for both of them, of the force applied on the left paddle (positive side of the waveform) with respect to the right one (negative side of the waveform). On the other hand, there is a remarkable difference in the force applied by the two kayakers.

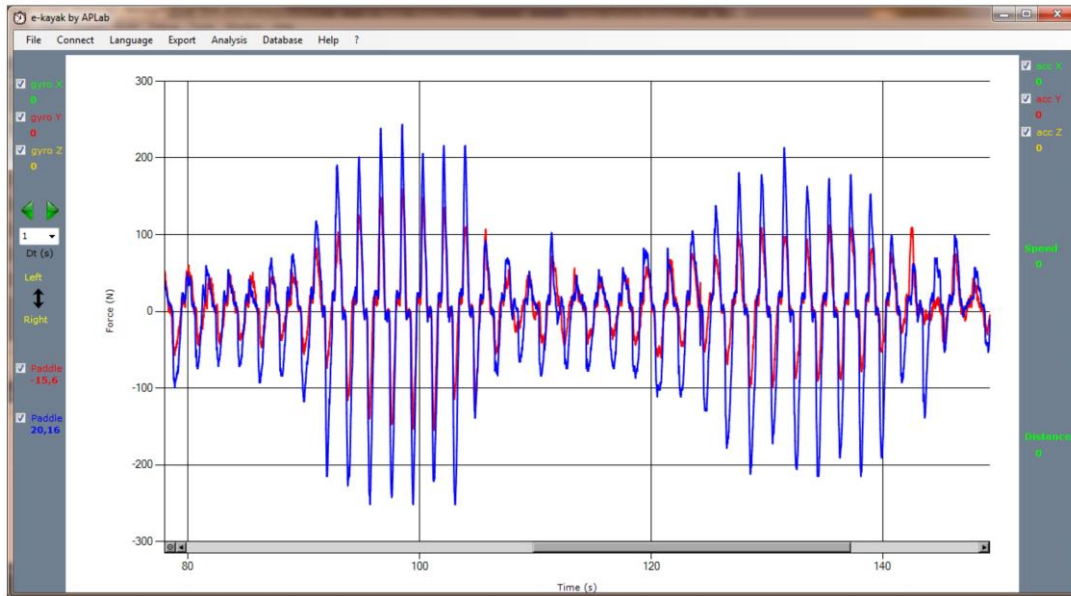


Figure 8. Force on the paddles measured on K2.

Figures 9 and 10 show some screenshots of preliminary measurements of a session of karting race. In this case, the system was equipped only with the master node to acquire data from GPS and triaxial accelerometer and gyroscope. In particular, Figure 9a shows the screenshot of the analysis app where the measures of the time lap, speed in the selected sectors, lap distance, and the average, top, and bottom speed are reported for each lap. Figure 9b shows the curves of the kart's speed, for each lap in a different color, with respect to the position on the track. Finally, Figure 10 shows a screenshot from the same app where the user can, graphically on the map, select the positions of the markers to identify the different sectors on the track. Moreover, the user can analyze the different trajectories together with the speed (the curve at the bottom of the screen) for each lap.

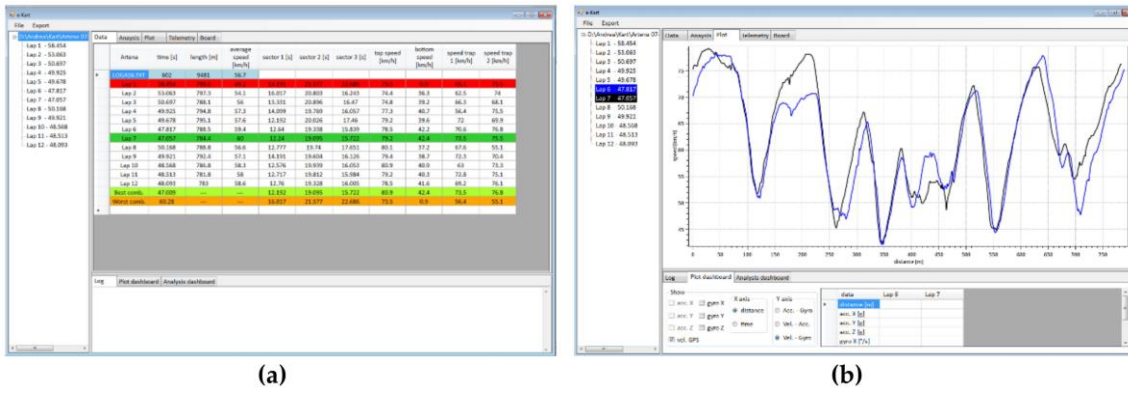


Figure 9. Examples of screenshot of the application for karting session analysis. (a) Analysis app; (b) kart's speed.



Figure 10. Screenshot of the application for karting session analysis.

Figure 11 shows an application of the system for measures of swimming training. In this case, the system was equipped with a master node only. This has been equipped with two differential pressure measurement devices (measuring the difference in pressure between hands' palm and back) for the evaluation of the forces applied by the swimmer with her arms.

The system is placed on the back of the swimmer, as shown in Figure 11a. Thanks to the triaxial accelerometer–gyroscope unit, it is possible to assess the effectiveness of each stroke (see Figure 11b) [33].

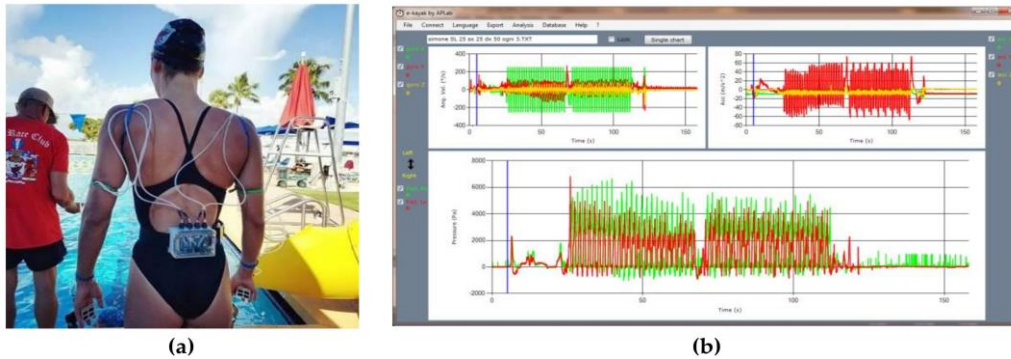


Figure 11. (a) System equipped for swimming; (b) screenshot of the app analysis.

Conclusions

A modular architecture for a WSN designed for sport applications has been introduced, which has better characteristics in terms of range, number of nodes, and interoperability with respect to existing systems. While originally designed for racing kayaks, the system can easily be adapted to rowing, sailing, swimming, and kart racing.

The use of different protocols for communication between nodes and user interaction optimizes the performance of the system without complicating user experience. On the contrary, the user can manage acquisition and data download from any kind of portable device with a web browser. Future improvements of the system will see the integration of heart rate monitors and differential high frequency (50 Hz) GPS with real-time Kinematic and post processing corrections.

Author Contributions: Conceptualization, V.B., N.L., and G.A.; Data curation, C.R.; Methodology, V.B. and G.A.; Software, P.B. and N.L.; Validation, V.B., P.B., N.L., and C.R.; Writing original draft, V.B. and N.L.; Writing review and editing, V.B., P.B., and N.L.

Funding: This research received no external funding.

Acknowledgments: The authors wish to thank Guglielmo Guerrini for devising and initiating the project, the Italian Olympic Committee for funding part of the development of the system, Stefano Grillo at Circolo Canottieri Aniene for support in the tests, and Dario Dalla Vedova at IMSS for providing logistic support and technical advice.

Conflicts of Interest: The authors declare no conflict of interest.

References

1. Baca, A.; Dabnichki, P.; Heller, M.; Kornfeind, P. Ubiquitous computing in sports: A review and analysis. *J. Sports Sci.* **2009**, *27*, 1335–1346. [CrossRef] [PubMed]
2. Baca, A.; Kornfeind, P. Rapid feedback systems for elite sports training. *IEEE Pervas. Comput.* **2006**, *5*, 70–76. [CrossRef]
3. Wei, Y.U.; Fei, Q.; He, L. Sports motion analysis based on mobile sensing technology. In Proceedings of the International Conference on Global Economy, Finance and Humanities Research (GEFHR 2014), Tianjin, China, 27–28 March 2014. [CrossRef]
4. Ermes, M.; Pärkkä, J.; Mäntyjärvi, J.; Korhonen, I. Detection of daily activities and sports with wearable sensors in controlled and uncontrolled conditions. *IEEE Trans. Inf. Technol. Biomed.* **2008**, *12*, 20–26. [CrossRef] [PubMed]

5. Iosa, M.; Picerno, P.; Paolucci, S.; Morone, G. Wearable inertial sensors for human movement analysis. *Expert Rev. Med. Dev.* **2016**, *13*, 641–659. [CrossRef] [PubMed]
6. Avci, A.; Bosch, S.; Marin-Perianu, M.; Marin-Perianu, R.; Havinga, P. Activity recognition using inertial sensing for healthcare, wellbeing and sports applications: A survey. In Proceedings of the 23rd International Conference on Architecture of computing systems (ARCS 2010), Hannover, Germany, 22–25 February 2010.
7. Camomilla, V.; Bergamini, E.; Fantozzi, S.; Vannozzi, G. Trends supporting the in-field use of wearable inertial sensors for sport performance evaluation: A systematic review. *Sensors* **2018**, *18*, 873. [CrossRef] [PubMed]
8. Umek, A.; Kos, A. Wearable sensors and smart equipment for feedback in watersports. *Procedia Comput. Sci.* **2018**, *129*, 496–502. [CrossRef]
9. Bonaiuto, V.; Lanotte, N.; Romagnoli, C.; Silvaggi, N.; Annino, G. Design of a Wireless Wearable DAQ System for the Evaluation of Sports Performances. *Proceedings* **2018**, *2*, 290. [CrossRef]
10. Song, E.Y.; Lee, K.B. IEEE 1451.5 Standard-Based Wireless Sensor Networks. In *Advances in Wireless Sensors and Sensor Networks*; Mukhopadhyay, S.C., Leung, H., Eds.; Lecture Notes in Electrical Engineering, Vol. 64; Springer: Berlin/Heidelberg, Germany, 2010. [CrossRef]
11. Gharghan, S.K.; Nordin, R.; Ismail, M. An ultra-low power wireless sensor network for bicycle torque performance measurements. *Sensors* **2015**, *15*, 11741–11768. [CrossRef] [PubMed]
12. Arefin, M.T.; Ali, M.H.; Haque, A.F. Wireless Body Area Network: An Overview and Various Applications.

J. Comput. Commun. **2017**, *5*, 53. [CrossRef]

13. Dhamdhere, A.; Chen, H.; Kurusingal, A.; Sivaraman, V.; Burdett, A. Experiments with wireless sensor networks for real-time athlete monitoring. In Proceedings of the IEEE 35th Conference on Local Computer Networks (LCN 2010), Denver, CO, USA, 10-14 October 2010; pp. 938–945. [CrossRef]

14. Mukhopadhyay, S.C. Wearable sensors for human activity monitoring: A review. *IEEE Sensors J.* **2015**, *15*, 1321–1330. [CrossRef]

15. Armstrong, S. Wireless connectivity for health and sports monitoring: a review. *Br. J. Sports Med.* **2007**, *41*, 285–289. [CrossRef] [PubMed]

16. Lapinski, M.; Berkson, E.; Gill, T.; Reinold, M.; Paradiso, J.A. A Distributed Wearable, Wireless Sensor System for Evaluating Professional. In Proceedings of the 2009 International Symposium on Wearable Computers, Linz, Austria, 4–7 September 2009. [CrossRef]

17. Gyselinckx, B.; Van Hoof, C.; Ryckaert, J.; Yazicioglu, R.F.; Fiorini, P.; Leonov, V. Human++: autonomous wireless sensors for body area networks. In Proceedings of the IEEE 2005 Custom Integrated Circuits Conference, San Jose, CA, USA, 21 September 2005; pp. 13–19. [CrossRef]

18. Bräysy, V.; Hurme, J.; Teppo, H.; Korpela, T.; Karjalainen, M. Movement tracking of sports team players with wireless sensor network. In Proceedings of the 2010 Ubiquitous Positioning Indoor Navigation and Location Based Service (UPINLBS 2010), Kirkkonummi, Finland, 14–15 October 2010; pp. 1–8. [CrossRef]

19. Watthanawisuth, N.; Lomas, T.; Wisitsoraat, A.; Tuantranont, A. Wireless wearable pulse oximeter for health monitoring using ZigBee wireless sensor network. In Proceedings of

the 2010 ECTI International Conference on Electrical Engineering/Electronics, Telecommunications and Information Technology (ECTI-CON 2010), Computer, Chiang Mai, Thailand, 19–21 May 2010; pp. 575–579.

20. Ali, B.B.; Dugas, É.; Naceur, A.; Romdhani, I. A new Zigbee-based device for measuring visual reaction time in sport activities. In Proceedings of the 2017 International Conference on Engineering & MIS (ICEMIS 2017), Monastir, Tunisia, 8–10 May 2017. [CrossRef]

21. Zulkifli, N.S.A.; Harun, F.C.; Azahar, N.S. XBee wireless sensor networks for Heart Rate Monitoring in sport training. In Proceedings of the 2012 International Conference on Biomedical Engineering (ICoBE 2012), Penang, Malaysia, 27–28 February 2012; pp. 441–444. [CrossRef]

22. Dynastream Innovations Inc. ANT message protocol and usage. *Rev. 4.5*. 2011. Available online: <http://thisisant.com> (accessed on 18 December 2018).

23. Weghorn, H. Efforts in developing android smartphone sports and healthcare apps based on Bluetooth low energy and ANT+ communication standards. In Proceedings of the 2015 15th International Conference on Innovations for Community Services (I4CS 2015), Nuremberg, Germany, 8–10 July 2015. [CrossRef]

24. Bluetooth SIG, Inc. Specifications: The building blocks of all Bluetooth devices. 2018. Available online: www.bluetooth.com/specifications (accessed on 18 December 2018).

25. Higgins, J.P. Smartphone applications for patients' health and fitness. *Am. J. Med.* **2016**, *129*, 11–19. [CrossRef] [PubMed]

26. Android v iOS market share 2018. 16 October 2018. Available online: <https://deviceatlas.com/blog/android-v-ios-market-share> (accessed on 18 December 2018).

27. Gravina, R.; Alinia, P.; Ghasemzadeh, H.; Fortino, G. Multi-sensor fusion in body sensor networks: State-of-the-art and research challenges. *Inf. Fusion* **2017**, *35*, 68–80. [CrossRef]
28. Sharma, S.; Tripathi, M.M.; Mishra, V.M. Survey paper on sensors for body area network in health care. In Proceedings of the International Conference on Emerging Trends in Computing and Communication Technologies (ICETCCT), Dehradun, India, 17–18 November 2017. [CrossRef]
29. Gratton, D.A. *The Handbook of Personal Area Networking Technologies and Protocols*; Cambridge University Press: Cambridge, UK, 2013; ISBN 978-0-521-19726-7.
30. Codeluppi, R.; Golfarelli, A.; Rossetti, A.; Proli, P.; Talamelli, A.; Tartagni, M. A sensor network for real-time windsail aerodynamic control. In Proceedings of the ELMAR-2010, Zadar, Croatia, 15–17 September 2010; pp. 341–344.
31. Bifaretti, S.; Bonaiuto, V.; Federici, L.; Gabrieli, M.; Lanotte, N. E-kayak: a wireless DAQ system for real time performance analysis. *Procedia Eng.* **2016**, *147*, 776–780. [CrossRef]
32. 24 GHz RF System-on-Chip, Transceivers and Audio Streamer. Available online: www.nordicsemi.com/eng/Products/2.4GHz-RF/nRF24L01 (accessed on 18 December 2018).
33. Lanotte, N.; Annino, G.; Bifaretti, S.; Gatta, G.; Romagnoli, C.; Salvucci, A.; Bonaiuto, V. A New Device for Propulsion Analysis in Swimming. *Proceedings* **2018**, *2*, 285. [CrossRef]

Capitolo 2



A Pilot Study on the e-Kayak System: A Wireless DAQ Suited for Performance Analysis in Flatwater Sprint Kayaks

Vincenzo Bonaiuto^{1,*}, Giorgio Gatta², Cristian Romagnoli^{1,2}, Paolo Boatto³, Nunzio Lanotte^{3,4} and Giuseppe Annino^{1,5}

1 Sport Engineering Lab, Department of Industrial Engineering, University Rome Tor Vergata, 00133 Rome, Italy; cristian.romagnoli2@uniroma2.it (C.R.); g_annino@hotmail.com (G.A.)

2 Department for Life Quality Studies, University of Bologna, 47037 Rimini, Italy; giorgio.gatta@uniroma2.it

3 APLAB, 00196 Roma, Italy; paoloboatto@aplab.it (P.B.); nunziolanotte@aplab.it (N.L.)

4 Department of Human Sciences and Promotion of the Quality of Life, San Raffaele Roma Open University, 00166 Rome, Italy

5 Department of Systems Medicine, University Rome Tor Vergata, 00133 Rome, Italy

* Correspondence: vincenzo.bonaiuto@uniroma2.it; Tel.: +39-06-7259-7402

Abstract: Nowadays, in modern elite sport, the identification of the best training strategies which are useful in obtaining improvements during competitions requires an accurate measure of the physiologic and biomechanical parameters that affect performance. The goal of this pilot study was to investigate the capabilities of the *e-Kayak* system, a multichannel digital acquisition system specifically tailored for flatwater sprint kayaking application. *e-Kayak* allows the synchronous measure of all the parameters involved in kayak propulsion, both dynamic (including forces acting on the paddle and footrest) and kinematic (including stroke frequency, displacement, velocity, acceleration, roll, yaw, and pitch of the boat). After a detailed description of the system, we

investigate its capability in supporting coaches to evaluate the performance of elite athletes' through specific measurements. This approach allows for a better understanding of the paddler's motion and the relevant effects on kayak behaviour. The system allows the coach to carry out a wide study of kayak propulsion highlighting, and, at the same time, the occurrences of specific technical flaws in the paddling technique. In order to evaluate the correctness of the measurement results acquired in this pilot study, these results were compared with others which are available in the literature and which were obtained from subjects with similar characteristics.

Keywords: sport; biomechanics; DAQ systems; paddling; flatwater sprint kayaking

Introduction

Nowadays, the use of a simple chronometer or of video analysis no longer represents a suitable system for the assessment of training or a race performance for elite athletes. Indeed, this approach does not allow for investigation of all the parameters involved in the assessment of performance, and it permits qualitative analysis at best. Conversely, a deep "knowledge of performance" by both coach and athlete (i.e., not only the value of the result itself but the way in which this has been obtained [1]) represents a key factor in improving the training procedures of this class of athletes. For this reason, it is possible to obtain better improvements in performance only when athletes and coaches are able to receive live and accurate feedback during training sessions, or an easily understandable full report after training, for deeper analysis. In recent years, several electronic measurement systems specially designed for sport applications have been proposed in the literature or have been made available on the market. With this in mind, there are some "golden rules" that must be taken into account in order to design a suitable electronic system for the monitoring of a sport performance. Firstly, the system has to be accepted by both coach and athlete. Thus, the

system has to be reliable and easy to use, and its output must be easy to understand and able to allow for a deep investigation into the quality of the performance. Furthermore, to be easily accepted by the athlete, the sensors applied on him or her or on the sports equipment must be light, unobtrusive, and not liable to influence in any way, physical or psychological, the performance itself [2–5].

In flatwater sprint kayaking, an effective paddling technique together with good physiological power and a smart race strategy plays a significant role in reaching peak performances among elite athletes. However, the particular features of such a paddling technique make the full comprehension of the way each force is proportionally involved in the boat's propulsion difficult [6]. Kayaking is a cyclic sport where the forces that propel the boat can be identified in the whole muscular kinetic chain of the athlete [7–10]. During acceleration, the athlete needs to generate propulsive forces greater than the resistive forces of air and water acting on the boat; the applied forces have to maximize the velocity and the forward acceleration, while minimizing all the other unnecessary rotations and accelerations along the axes of the boat. Furthermore, in contrast to rowing, where the oar is constrained to the hull via an oarlock, in kayaking the force transferred by the athlete to the water through the paddle during the stroke is transmitted to the boat through the body of the paddler itself via the seat and footrest [11,12]. Hence, measuring the force on the paddle or the stroke rate alone is not enough for the coach to identify the best actions with which to improve the performances for this class of athletes. For this reason, even if the dynamic behaviour of the blades in the water can be measured, the proportion with which each of these forces contributes to the boat's motion is widely debated and, consequently, the study of its propulsion very complicated [12–14].

A useful key for good comprehension of the biomechanical parameters upon which the performance of the kayaker depends could be given by an accurate and simultaneous measure of the forces exerted by the upper body musculature on the paddle and those applied by the legs on the footrest together with the kinematics of the boat. This means that an in-depth study of dynamic and kinematic parameters of both athlete and boat could allow the coach to give practical tips which will refine the paddling technique and help to avoid specific technical flaws.

In recent years, several studies [10–21] have been published on force–time curve development performed by kayakers on ergometers (non-specific conditions), in lab measurements, and on boats (specific race conditions). These papers (Table 1) describe the use of particular digital acquisition (DAQ) systems, with sensors applied on the boat either on the boat paddle or on the footrest. The table provides a brief description of each system together with information about the presence of kinematic or dynamic sensors and the capability of each system to operate under standard training conditions (on water).

Specifically, in 2009 Mickael Begon et al. [7] presented a kinematic analysis of the anteroposterior forces applied to the footrest, the seat, and the paddle of a kayak by using a special ergometer instrumented with seven uniaxial force sensors and two goniometers. The ergometer was provided with a trolley sliding forward and backward along a static frame. The aim of this study was the assessment of the paddling performances, the analysis of the involved forces, and the coordination between the left and right sides. F. Nates et al. (2015) [20] presented a study in which, by using a special kayak ergometer (the Poitiers-B kayak ergometer), they installed six degree of freedom (DOF) force sensors for the measurement of the contact force between the athlete's hands and the paddle shaft. This allowed for a tridimensional study of the forces applied on the paddle and improvement of the knowledge in both the drive and recovery phases.

Table 1. State of the art on DAQ systems developed for kayaking Legend: Dyn, dynamic; Kin, kinematic.

Authors	Brief Description	Dyn	Kin	On Water
Vos, J.A. et al. (1974) [7]	Strain gauges installed on both the paddle and footrest. A telemetry system allowed data transmission to a computer located at the shore. The study, initially formulated for rowing, has been applied to kayaking.	Yes	No	Yes
Campagna, P.D. et al. (1986) [15]	One of the first examples of an instrumented ergometer for kayaking. It has been demonstrated that this system is able to replicate open water paddling action very closely.	No	Yes	No
Aitken et al. (1992) [8]	Four strain gauges are attached near each blade for the measurement of the shaft bending. A data recorder system provides memorization of the acquired data for an offline download.	Yes	No	Yes
Pelham et al. (1993) [16]	Accelerometry measurement system based on electromagnetic force–balance accelerometers.	No	Yes	Yes
Begon, M., et al. (2009) [17]	Instrumented kayak ergometer for the measurement of the contact forces between the athlete and the ergometer.	Yes	Yes	No
Limonta, E. et al. (2010) [18]	Kayak simulator based on an automatic motion analysis system. It performs a three-dimensional kinematic analysis of the paddler’s movements.	No	Yes	No
Sturm, D. et al. (2010) [19]	A wireless (Bluetooth)-based sensor system is able to perform the measurement of the paddle bending by using four strain gauges. The measurement of the pressure of the foot on a custom-built footrest is obtained by force-sensitive resistor (FSR) sensors.	Yes	No	Yes
Gomes, B. et al. (2011) [6]	The <i>FPaddle</i> system measures the strain on the shaft via two couples of strain gages, with one placed on the bending plane of the blade and the other on a perpendicular plane. A wireless system provides the data transmission.	Yes	No	Yes
Gomes, B. et al. (2015) [13]	An <i>FPaddle</i> system instrumented with two strain gauges is integrated with a triaxial accelerometer placed inside the boat.	Yes	Yes	Yes

Nates, F.M. et al. (2015) [20]	A special kayak ergometer is designed with six degree of freedom (DOF) force sensors for the measurement of the contact force between the athlete's hands and the paddle shaft.	Yes	No	No
Luo Niu et al. (2019) [21]	The measurement of the force on the shaft is obtained by the use of Fiber Bragg Grating (FBG) optical fiber sensors enclosed in the material of the blades.	Yes	Yes	No

In 2010, Sturm et al. [19] were involved in the design of a system consisting of force sensors positioned on both the paddle and footrest and wirelessly connected to a central unit via a Bluetooth radio link. The goal of this study was to present a measuring tool able to record, in a training session of flatwater kayaking, the strength on the paddle and footrest. The forces on the paddle were measured by means of four strain gauges connected in a Wheatstone full-bridge, while, for the measure of the forces on the footrest, force-sensitive resistor (FSR) sensors were employed. The measures obtained by the proposed system were compared to those achieved using a Dansprint kayak ergometer [22], showing a good correlation between the power (measured by the ergometer) and the force on the paddles (measured by sensors).

In 2011, Gomes et al. [14] investigated the intracyclic velocity variation as well as the kayak's motion using a triaxial accelerometer in K1, K2, and K4 boats. In the same year, Gomes et al. [6] presented the *FPaddle* system. This is a wireless system that allows the measurement of the paddle forces in a specific environment. Later, in 2015, the same authors presented an updated version of the *FPaddle* system (with only two strain gages) where the paddling force profile and the force–time curves were studied together with triaxial accelerometry [13].

Finally, Luo Niu et al. (2019) [21] proposed to evaluate kayak paddling performance by use of a custom-built paddle instrumented with a special optical fiber technology, namely, Fiber Bragg Grating (FBG) strain sensors [23]). Through this new technology system, it is possible to measure handgrip load and blade load distribution in on-water kayaking in real time. The proposed technology

seems to be very promising for the measurements of forces on the paddle. Nevertheless, it seems to be obtrusive (it is still a cabled system) and it cannot be employed in standard training conditions. In fact, the presence of the cables does not allow for a specific assessment of the performance [3,19]. In kayaking, the main kinematic parameters which are useful in the investigation of performance include velocity, acceleration, intra-cyclic velocity, roll, and pitch of the boat. In addition, the dynamic parameters have to include stroke frequency, forces acting on the paddle and footrest, the symmetry between the forces on the right and left side for both the paddle and footrest, and the synchronization among these forces [12–14].

As previously shown, most of these systems cannot simultaneously measure the kinematic and dynamic parameters that affects the kayaker's performance. In particular, as reported in Table 1, only three of them are able to obtain both measurements, and, among these, only one has been designed for on-water use [13].

In this context, the aim of this pilot study was to investigate the capabilities of a wireless multichannel portable DAQ (the *e-Kayak* system) in supporting coaches to evaluate the performance of elite athletes. The system is tested on a couple of athletes through specific measurements during on-water training and simulating specific race phases in a specific flatwater kayak environment. In particular, the measurement results presented in this paper are related to some different tests, i.e., a slow-pace test (100 m and 150 m for the female and male subjects, respectively), a 50 m fast-pace test for the female subjects only, and, for the male subjects, a 40 m speed test simulation starting from the race blocks. In the slow-pace tests, the subjects are asked by the coach to perform the test with care taken to perform the proper paddling technique (i.e., performing a specific work on the technical gesture). The tests are carried out in a lake with a negligible level of water currents, and the system synchronously acquires the force signal on both the paddle and footrest, the position and the boat's

speed by a Global Position System (GPS) device and three-axis acceleration, and the yaw, pitch, and roll by an inertial measurement unit (IMU) installed inside the boat.

The goal of the test was the evaluation of the type of parameters supplied by it in order to verify their usefulness for the measurement of the performance and the identification of technical flaws. Moreover, the test verifies the usability of the system as per the readability of the output by the coaches and easiness of the setup and calibration procedures.

Materials and Methods

Measurement System

The DAQ used for measurements here is the “*e-Kayak* system”, which was developed in the framework of a project carried out on behalf of the Italian Olympic Committee. We have employed a version customized for flatwater sprint kayaking of the DAQuino system [24,25], a modular architecture easily customizable for particular sport application that allows for the connection of up to eight slave nodes to a master one via a high performance 2.4 GHz wireless link (ISM Band). The design of this new system was inspired by previous experience gained using a first preliminary prototype developed in 2016 [26]. Although that prototype presented the same class of sensors (IMU, GPS, and force sensors) of the DAQuino system, the modular architecture, the maximum available sample rate of most of the new employed sensors, the unobtrusiveness in the position of the force sensors, and the new implemented communication protocol make the new system more reliable and effective. For example, in the previous prototype system, the slave node for the measurement of the force exerted on the paddle was installed on the outside in the middle of the shaft (a barycentric but rather obtrusive position) while the connection with the footrest was implemented by a wire.

Furthermore, in a manner different from the previous system, the modular architecture of the new system easily allows its use on K2 and K4 boats.

In particular, the new system is equipped with a 9-axis IMU, a high sample rate GPS device, and a pair of force sensors applied on the paddle and footrest for each of the kayakers belonging to the crew of the boat. Hence, as depicted in Figure 1, the system designed for a K1 boat (i.e., a kayak with only one paddler) presented in this paper is composed of a master node (M) and two slave nodes equipped with force sensors and installed on the paddle (S1) and footrest (S2).

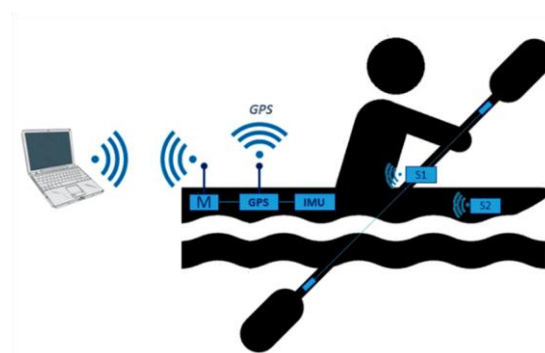


Figure 1. Block scheme of the *e-Kayak* system. Legend: GPS, Global Positioning System; IMU, inertial measurement unit; S1, paddle; S2, footrest.

The master node handles the data stream from the dynamic sensors on the slave nodes and the acquisition of the kinematic data from the IMU and GPS. Moreover, it provides, via a wi-fi link over a dedicated WLAN (Wireless Local Area Network), a communication interface on the user terminal (i.e., a tablet, smartphone, or PC, etc.) for real-time feedback on a reduced set of parameters. The same wi-fi link can be used to download the data of the whole training or race session.

Since the interface is a webpage, it can be used with any operating system and any device, as long as a web browser is present. In addition, the master node manages the synchronization of the data acquisition; due to the large amount of computational resources needed to carry out all these tasks,

the node has been designed to host a high-performance micro controller unit (MCU, 32 bit 180 MHz ARM Cortex-M4 Pjrc's Teensy 3.6). The wi-fi transmission is based on the module ESP8266 (Espressif Systems Co., Ltd., Shanghai, China), while the communication with the slave nodes is granted by nRF24L01P+ modules (Nordic Semiconductor [27]). These modules are low power single chip transceivers in the global license-free 2.4 GHz ISM band with high-speed communications capability (up to 2 Mbit/s). They are suitable for deploying wireless networks in several application fields. In the *e-Kayak* system, they have been equipped with an external antenna that increases the transmission range of the device in order to overcome the signal losses due to the boat and the body of the athlete itself.

The GPS device which is installed in the system is based on the Venus822A chip by Skytraq Technology Inc. Taiwan. It has been designed for quad-GNSS (Global Navigation Satellite System) applications and can work with an up to 50 Hz update rate when it is running at top speed (this feature is valid if it processes signals from the US satellite system GPS only). In the described system, it is employed with an update frequency set at 20 Hz that provides an accurate measurement of the velocity fluctuations at each stroke (intracyclic velocity). Finally, the IMU is a nine DOF device that allows a sampling frequency of up to 50 Hz based on the MPU 9250 by TDK Co., Tokyo, Japan. LiPo batteries power the master as well as each of the slave nodes, allowing an operating time of more than 2 h. The user can monitor the battery charge level on the master and the slave nodes using the web interface. The master node is placed in a waterproof case for on board use (Figure 2c) and is installed inside the boat and fastened to the central rail on the back of the seat. Since its weight is limited (about 450 g), it can be compensated with an appropriate sizing of the ballast.

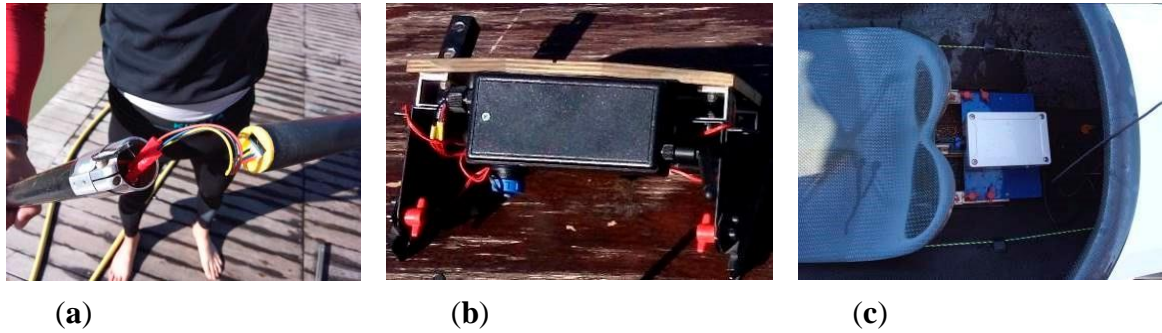


Figure 2. *e-Kayak* system: (a) paddle node, (b) footrest node, and (c) master node installed on the boat.

Both the paddle and footrest nodes are composed of a microcontroller unit (16 MHz ATmega328 processor, Atmel, San Jose, CA, USA), a radio circuit (again based on the module nRF24L01P+), and a signal conditioning circuit based on the instrumentation amplifier INA326 (Texas Instruments, Dallas, TX, USA) connected to the force sensors for signal amplification and noise filtering.

In particular, for the measure of the deformation of the shaft, these sensors (four waterproof strain gauges (KFW-5-120, Kyowa, Tokyo, Japan)) are connected in a Wheatstone full-bridge configuration and each pair of them is placed in the left and right side of the shaft at the same distance from the tip blades (i.e., at 53 cm). Each pair is placed parallel to the bending plane of the nearby blade. Of the two strain gauges composing a pair, one measures the tensile strain ($+\epsilon$) and the other the compressive strain ($-\epsilon$). The full bridge configuration ensures temperature and lead resistance compensation. The force applied on the blade can thus be measured by measuring the bending strain on the shaft.

The paddle's slave node has been designed to be installed inside the shaft of the paddle (Figure 2a). Its weight is only 30 g, and since it can be placed in a barycentric and unobtrusive position, it does not affect in any way the movements of the kayaker. Figure 3 depicts a scheme of the instrumented paddle. Conversely, for the measurement of the forces on the footrest, the same strain gauges used in

the paddle are connected in a Wheatstone half-bridge configuration and are placed, in order to measure the strain caused by the forces applied by the legs, on the back of the footrest itself. Each slave node (paddle and footrest) is individually calibrated before each training session according to the procedure described by Aitken [8] and Nilsson [28] and accurately described by Gomes et al. in [13]. Such a calibration procedure for the paddle consists of statically loading it, in specific positions for both sides, with calibrated masses by finding the relationship between the force applied on the paddle shaft and the signal measured on the circuit. The footrest is calibrated with a similar procedure by loading it with calibrated masses. The setup of the system takes a few minutes to position the master node on the boat and to carry out the zero adjusting procedure of the IMU. The system, though for the kinematic part only, has been widely tested during a few high level competitions both in training as well as under race conditions. Although a deep and complete study on the usability of such a system has still not been carried out, this experience has resulted in a rather easy-to-use system, and both the setup and the calibration procedures also seem to be affordable for non-technician people.



Figure 3. Block scheme of the paddle slave node (where d is the distance of the strain gauge sensor from the tip blade).

The acquisition software is simply a web page, and it allows for immediate monitoring by both athlete and coach of a restricted number of parameters, including instantaneous stroke rate, boat speed, and travelled distance. A more efficient visualization application (Figure 4) allows for analysis of all the dynamic and kinematic data acquired during the whole training session. The data of the angular accelerations are depicted in the top graph on the left side of the screen, while the forces on the paddle

(red) and footrest (green) are shown in the bottom left corner. The three charts on the right side show, from top to bottom, the acceleration, the instantaneous velocity, and the distance travelled. A synchronized marker allows the user to highlight specific events of the session and show the measured value for each of the acquired parameters. The instrumented paddles were for both athletes BRACA-SPORT Mod. BRACA-IV; the kayak used for the female subject was NELO4, while for the male subject it was PLASTEX.

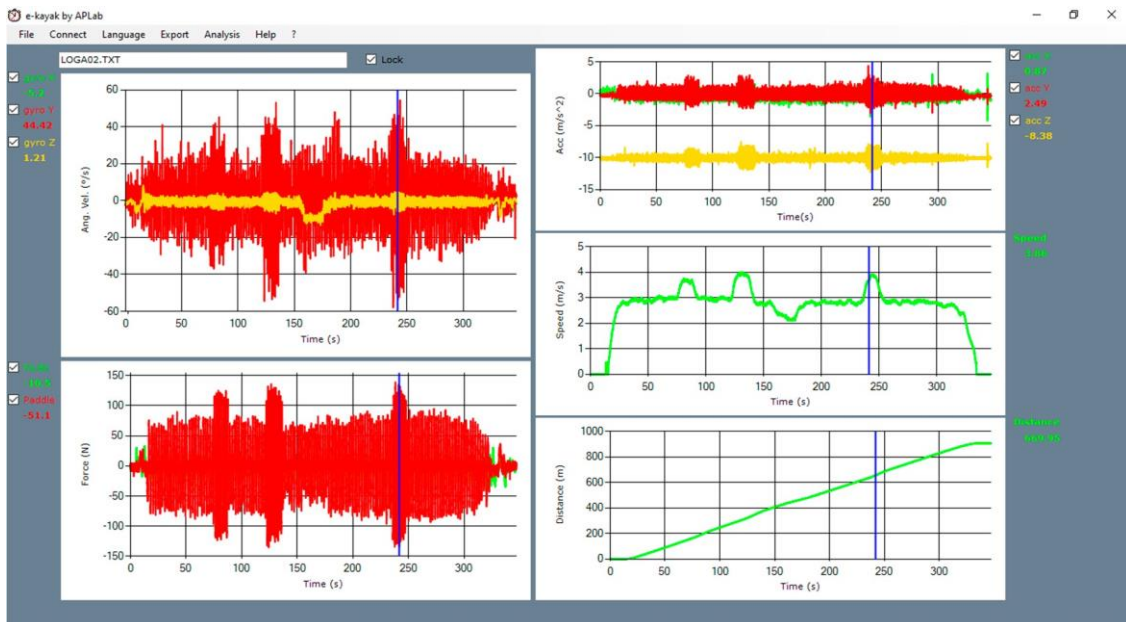


Figure 4. Screenshot of the *e-Kayak* data visualization software.

Methods

The data were collected during training sessions of K1 boats in flat water. The force on both the paddle and footrest, as well as the kinematic data from the IMU, were synchronously acquired at a sampling frequency of 50 Hz while the velocity and the distance were sampled from the GPS at a frequency of 20 Hz. The data were acquired during on-water training sessions at different paces; two athletes (female, age 24, height 163 cm, weight 67 kg; male, age 28, height 185 cm, weight 85 kg) with international level flatwater kayak competition experience were involved in the sessions. The subjects, after a brief period of warmup and familiarization with the instrumentation, were asked to

perform a standard training session featuring repetitions at different lengths and with increasing force intensity and stroke rate; the subjects also simulated some specific race phases (e.g., the starting phase). The athletes were asked to use their usual paddling technique in terms of stroke length and rate during the tests. Each subject performed three different repetitions, each followed by complete recovery; the best repetition for each athlete was taken into account in this study. Written informed consent was obtained after familiarization and explanation of the benefit and risks involved in the procedures adopted. The study was approved by the Ethical Committee of the School of Sports and Exercise Science at the University of Rome “Tor Vergata”, Faculty of Medicine and Surgery. Moreover, all the tests were carried out in accordance with the Declaration of Helsinki.

Data Analysis

The collected data were analyzed using the previously described visualization software, while some of the procedures for the data analysis were automated using a custom program (Matlab R2018b by The MathWorks Inc., Natick, MA, USA). The former provided the smoothing and filtering of the acquired data by a fourth-order low-pass Butterworth filter, while the latter was employed to automatically detect the strokes by analysis of the paddle force–time curves and for the computation of all the parameters (i.e., time values and forces). Each pulse of the force–time curve was identified as a force impulse when all the following features had been detected: the peak force was above a specific threshold (fixed at 70% of the maximum value of force) and the curve showed a fast rise followed by a falling to its resting value. The sum of the wet time and aerial time represents the stroke duration. The onset and the end of the force application were automatically detected by software routine. In particular, they were identified as the points where the force–time curve respectively leaves (paddle entry into the water) or returns (paddle exit) to its resting value. Moreover, two

consecutive pulses in the force–time curve were identified as different strokes only if a time interval was measured (equal to the glide time) at which such a curve remained at the resting value.

Results

The *e-Kayak* system was installed on the boats of the two kayakers and some measurements results acquired during the tests are reported in this paper. In order to evaluate the capabilities of the system, parameters were identified among the parameters that the system is able to measure which, in the literature, are considered more affordable for the assessment of propulsion in kayaking. Among the parameters that can be measured for the assessment of performance in elite kayaking, the most significant ones are undoubtedly the force applied to the paddle by the kayaker as well as the stroke rate and good boat buoyancy and velocity [12]. In particular, with regard to the paddling analysis, several studies can be found in the literature that identify some specific parameters that can be used for an evaluation of the most effective technique. Among others, it is possible to identify the underwater phase duration (wet time (s)), the aerial phase duration (recovery time (s)), the time to force peak (time to peak (s)), the force impulse (i.e., the area under the force–time curve during the wet phase (N·s)) and the ratio between the average force and the peak one ($F_{\text{average}}/F_{\text{peak}}$ ratio) [12,13,29].

Tables 2 and 3 give a summary of the biomechanical parameters measured from the tests at, respectively, slow and fast paces for the female subject while Tables 4 and 5 show the same parameters measured for the male subject.

Table 2. Female 100 m—slow pace (stroke rate (SR) = 62 str/min; velocity = 3.67 ± 0.26 m/s).

Biomechanical Variables	Left Paddle	Right Paddle
Force peak (N)	108.40 \pm 5.04	106.46 \pm 6.36
F _{average} (N)	77.19 \pm 3.03	77.86 \pm 5.44
F _{average} /F _{peak} ratio (%)	71.43 \pm 2.37	73.15 \pm 3.21
Force impulse (N·s)	38.12 \pm 2.24	38.75 \pm 4.56
Time to peak (ms)	0.18 \pm 0.03	0.17 \pm 0.03
Stroke time (ms)	0.99 \pm 0.07	0.99 \pm 0.11
Wet time (ms)	0.51 \pm 0.02	0.51 \pm 0.05
Recovery time (ms)	0.47 \pm 0.07	0.47 \pm 0.08
TWet/TStroke ratio (%)	52.55 \pm 4.30	52.29 \pm 4.42

Table 3. Female 50 m—fast pace (SR = 82 str/min; velocity = 3.76 ± 0.10 m/s).

Biomechanical Variables	Left Paddle	Right Paddle
Force peak (N)	142.25 \pm 10.56	137.28 \pm 9.93
F _{average} (N)	99.22 \pm 7.36	103.09 \pm 7.94
F _{average} /F _{peak} ratio (%)	69.81 \pm 2.80	75.12 \pm 2.84
Force impulse (N·s)	46.20 \pm 4.17	47.76 \pm 6.37
Time to peak (ms)	0.21 \pm 0.03	0.18 \pm 0.02
Stroke time (ms)	0.74 \pm 0.04	0.74 \pm 0.04
Wet time (ms)	0.49 \pm 0.05	0.48 \pm 0.03
Recovery time (ms)	0.25 \pm 0.05	0.27 \pm 0.02
TWet/TStroke ratio (%)	65.71 \pm 5.55	63.87 \pm 1.62

Table 4. Male 150 m—low pace (SR = 63 str/min; velocity = 3.24 ± 0.08 m/s).

Biomechanical Variables	Left Paddle	Right Paddle
Force peak (N)	166.39 \pm 17.67	156.98 \pm 13.58
F _{average} (N)	114.73 \pm 9.46	111.86 \pm 8.32
F _{average} /F _{peak} ratio (%)	69.14 \pm 2.53	71.35 \pm 2.14
Force impulse (N·s)	48.68 \pm 6.69	52.74 \pm 5.16
Time to peak (ms)	0.16 \pm 0.02	0.16 \pm 0.01
Stroke time (ms)	0.97 \pm 0.19	0.98 \pm 0.04
Wet time (ms)	0.44 \pm 0.04	0.49 \pm 0.02
Recovery time (ms)	0.52 \pm 0.15	0.49 \pm 0.03
TWet/TStroke ratio (%)	46.36 \pm 3.96	49.83 \pm 2.00

Table 5. Male 40 m—fast pace (SR = 90 str/min; velocity = 4.14 ± 0.25 m/s).

Biomechanical Variables	Left Paddle	Right Paddle
Force peak (N)	310.94 \pm 13.16	301.13 \pm 23.06
F _{average} (N)	217.57 \pm 10.53	221.69 \pm 14.01
F _{average} /F _{peak} ratio (%)	69.97 \pm 1.66	73.74 \pm 2.75
Force impulse (N·s)	76.06 \pm 5.97	82.74 \pm 6.54
Time to peak (ms)	0.14 \pm 0.01	0.15 \pm 0.02
Stroke time (ms)	0.66 \pm 0.03	0.67 \pm 0.02
Wet time (ms)	0.37 \pm 0.03	0.39 \pm 0.04
Recovery time (ms)	0.29 \pm 0.01	0.28 \pm 0.01
TWet/TStroke ratio (%)	56.45 \pm 1.79	56.96 \pm 2.54

Figure 5 depicts these paddling phases, namely, the drive or underwater (wet) phase (Figure 5b–d) followed by an air or recovery phase (Figure 5a, e); in particular, in the wet phase it is possible to identify three different sub-phases, namely, the paddle entry into the water (Figure 5b), the catch (Figure 5c), and the pull (Figure 5d). Figure 6 depicts the aforementioned parameters and, via gray coloration, highlights the paddle force impulses of the right and left side, respectively. The force impulse is the area under the force–time curve.



Figure 5. Kayak paddling stroke phases: (a) entry, (b) catch, (c) pull, (d) exit, (e) recovery.

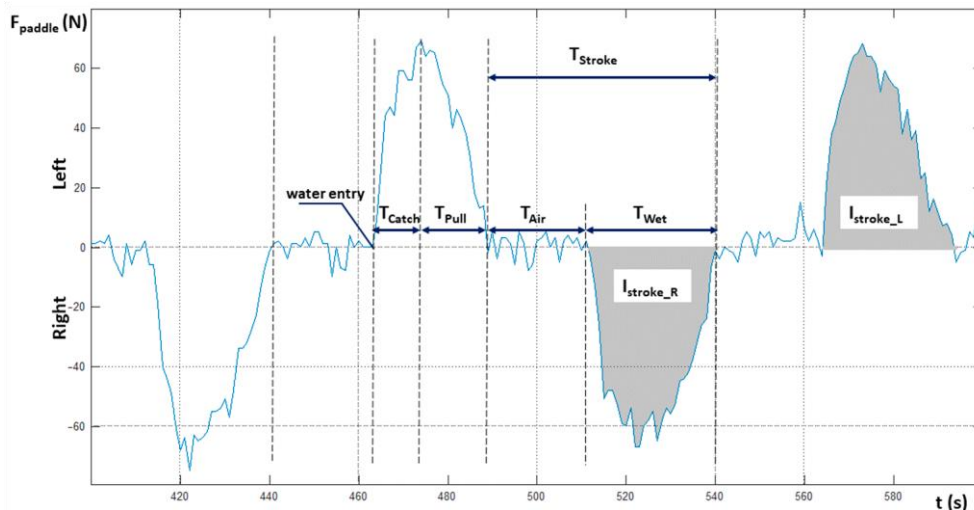


Figure 6. Kayak paddling stroke phases. Legend: T_{catch} [s] = length of the catch phase, T_{pull} [s] = length of the pull phase, T_{air} [s] = length of the air (recovery) phase, T_{wet} [s] = length of the wet phase ($T_{catch} + T_{pull}$), T_{stroke} [s] = length of the stroke phase ($T_{air} + T_{wet}$), I_{stroke_R} = right stroke pulse, I_{stroke_L} = left stroke pulse.

Discussion

Tables 2 and 3 report the measured biomechanical variables for the female subject paddling a K1 over different lengths (ranging 50 to 100 m) at slow and fast paces, respectively. It is worth observing that with an increase of about 32.25% for the stroke rate (SR) of the subject, the peak force increases by 30.36%, the force impulse (FI) by 22.43%, and the product FI-SR by more than 61.92%. Nevertheless, the resulting increase in the boat's velocity is only about 2.45%. This is mainly due to a difference in the operating conditions that occurred between the two tests (i.e., changes in water current intensity). In any case, it is worth noting a reduction in the time of the paddle in the water (T_{wet}), which it is possible to observe also by the decrease in the $T_{\text{wet}}/T_{\text{stroke}}$ ratio of about 12.37% (from 52.42% to 64.79%). Hence, the increase in the SR was obtained by performing a more significant decrease in the T_{wet} rather than the recovery time. This result could be justified by a higher imbalance in the values of the left/right roll that was measured during the fast pace paddling.

Tables 4 and 5 report the same biomechanical variables for the male subject under similar training conditions (lengths ranging from 40 to 150 m). In this case, it is possible to observe that with an increase of 46% for the SR average increase were measured of 89% for the peak force, 56.66% for the FI, and 128% for the FI-SR product. At the same time, the boat's velocity showed a significant increase of 27.7%. The fast pace data of Table 5 are relative to a test where the subject was simulating a race start phase, i.e., the first 40 m were performed at maximal intensity.

In stark contrast to the female subject, the increase in SR was obtained in this case with a more significant reduction of the recovery time with respect to T_{wet} . Conversely, according to Baker [12], a measured value for the $T_{\text{wet}}/T_{\text{stroke}}$ ratio of above 75% represents a signal of a too fast transfer between the two strokes with negative effects on the paddling efficiency (it is also taken into account that this could lead to an early onset of fatigue).

The shape of the paddle's force–time curve provides significant information about the paddling technique of the kayaker. As reported in Baker [12], there are two possible shapes that can occur: curves that present a double peak (“*bimodal force curve*”) and curves with a single peak (“*unimodal force curve*”). The *bimodal force curve* is characterized by the presence of an initial small peak in the rise phase of the curve followed by a slight fall and a further rise to reach a new peak. Such a shape is an indicator of a possible technical flaw, i.e., a light flexion, immediately after the catch, of the elbow, which should be perfectly extended, or an early pushing of the top hand in the stroke. Both flaws are often the consequence of an over-aggressive catch. In fact, this could be justified by the elastic response of the shaft, which is particularly noticeable when the kayaker tries to reduce the recovery time and to accelerate the paddle to reach the water as fast as possible [13]. Figure 7 depicts a force curve relative to the female subject involved in a fast pace training session where, highlighted by the green arrows, it is possible to note a couple of occurrences of a *bimodal force curve*. Both of these occurrences are located in the right side of the force curve and could be correlated to the right-handed nature of the athlete. In each of them, the amplitude of the second peak is lower than that of the first one: this, according to what is suggested by Baker, could be the confirmation of the use of a shaft with a proper degree of stiffness.

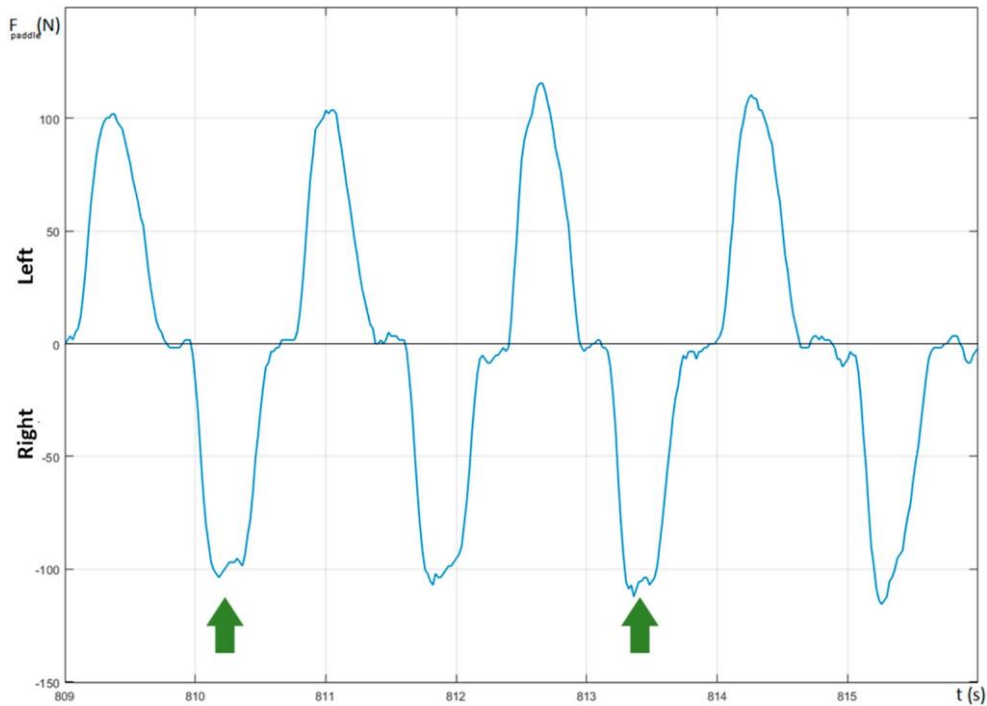


Figure 7. Bimodal (highlighted by arrows) and unimodal paddle force curves.

The force impulse multiplied by the stroke rate is equivalent to the total work done by the kayaker in moving the boat. Hence, the higher this product the faster the boat. Consequently, the measure of only one of these two factors cannot give a correct assessment of the paddling performance (i.e., a high value for the impulse area with a low stroke rate will result in a slow boat). Generally, the higher the stroke frequency, the lower the impulse for the same applied force, as a consequence of the proportional decrease in wet time.

The shape of an ideal force curve should be a bell shape because this allows, by regular and efficient application of force, for it to be transformed into a smooth acceleration of the boat. Moreover, as in this case the velocity waveform presents a sinusoidal shape, if the intracyclic velocity variation is low, this reduces the energy expended by the athlete for the propulsion [12,30]. Conversely, as described by Gomes in [13], a fast rise time for the stroke force, together with the same peak value of the paddling force, should result in a higher value for the force impulse and, consequently, a faster boat. Thus, in order to obtain the best effectiveness in paddling, both the catch time (known as the

catch slip) and the exit time (known as the release slip) should be taken into account. In fact, these should be as fast as possible so that the applied force quickly reaches its maximum value, which has to be maintained for the whole pull time. In this case, starting from a bell, the force waveform should tend to assume a rectangular shape. For this purpose, it is useful to monitor the $F_{\text{aver}}/F_{\text{peak}}$ ratio parameter, which is widely used in rowing [31]. In this study, the values of this parameter increased with the increase in SR and the average velocity for both subjects. Moreover, the delay between the paddle entry in the water and the start of the kayak's acceleration decreased. Finally, at the end of the wet phase, the delay between the start of the kayak deceleration and the end of the force application decreased with increasing SR. This result suggests that at low SR, keeping the paddle in the water at the end of the wet phase could slow down the kayak.

The measurement of the peak force value represents another significant parameter for the evaluation of the water resistance of the boat while the simultaneous study of both the acceleration and force–time waveforms is a helpful key for evaluating the paddling technique and highlighting the effectiveness of the pulling, together with any imbalance in the boat's movement. It is also useful for assessing progress in eliminating any technical flaws.

Figure 8 shows the measurement of forward acceleration (red curve) together with the measurement of the roll (light blue) and the force on the paddle (dashed). It is possible to notice that the peaks of the roll curve occur mostly in correspondence with the peaks of the paddle force and acceleration. It is worth noting that these rotations could also occur for particular body movements of the kayaker and that their intensity could not be directly connected to the amplitude of the forward acceleration.

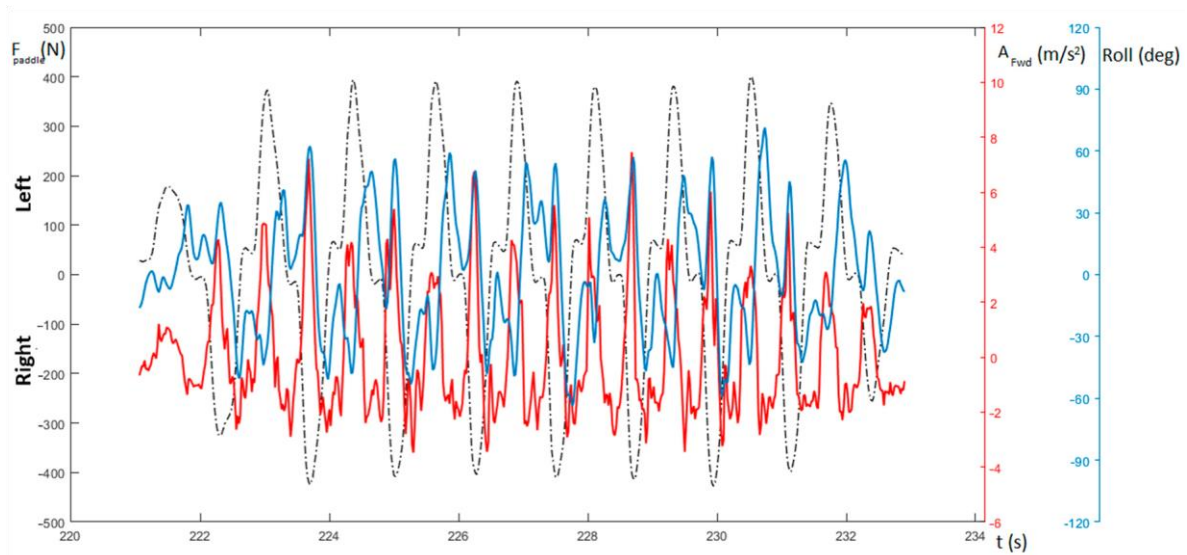


Figure 8. Measure of force on the paddle (F_{paddle} —dashed), roll (light blue), and the boat’s acceleration (A_{fwd} —red).

The kayak velocity is mostly influenced by yaw and roll rather than pitch. In any case, even if it is clear that the rotations of the boat should be as small as possible, it is not easy to identify a paddling technique that represents the best trade-off between a great force applied on the paddle and a limited roll. This can only be obtained with a specific study of the athlete’s movements, and, for this purpose, the *e-Kayak* system seems to be a useful tool for such an analysis.

As depicted in Figure 8, the male subject showed a slight imbalance in the force pulled on the paddle. The forward acceleration curve (the red curve in the figure) confirms this left/right force imbalance with values of the acceleration peaks for the right side generally presenting a higher value with respect those of the left one. This disparity will cause a rotation of the boat around its vertical axis, thus increasing the resistance to the forward motion of the hull (i.e., affecting both the surface and wave drag), and, consequently, resulting in a deceleration [32]. Figure 9 shows that for the male subject, the measurement of the velocity and paddling force of the first strokes occurs immediately after the start. The mean value of the velocity increases until it reaches the final value. The velocity of the kayak presents a fluctuant wave shape because it will tend, inside each stroke cycle, to increase when

the paddle force applied by the kayaker exceeds the drag force, and, successively, to fall when, during the air phase, no paddle force is being applied (intracyclic velocity). The peak velocity inside each stroke cycle is reached before the blade exits from the water. In particular, as suggested by Kendal [30], it is possible to see that the velocity increases during the pull phase of the stroke and that it decreases before the exit of the blade from the water. This could point to the presence of a period near the end of the traction phase where the produced force is not enough to maintain the speed of the kayak. The minimum value of the velocity occurs near the re-entry of the blade in the water. Furthermore, it is possible to note a difference between the value of the reduction in the velocity for the right and left sides, respectively. This asymmetry could be caused by the different coordination and strength between the dominant and non-dominant parts of the body. Furthermore, the velocity peaks are concurrent with the force peaks, whereas the minimum values of the speed are recorded in the phase just before the paddle entry. The amplitude of the ripple for the velocity waveform represents an optimal indicator of the boat's run: the lower such a value the better the efficiency of the paddling, because, as reported above, high variations in the velocity are an indication of inefficient energy handling [14]. Again, in Figure 9, it is possible to notice that at time 226 s and when highlighted by the green arrow, there is a significant fluctuation in the velocity. This is probably due to a movement forward and then backward of the body of the athlete. A velocity variation of such a shape is generally present at the start of the race because to make the kayak accelerate the athlete tends to move the body forward. As a matter of fact, because later the body mass must be moved back during the race, this body movement will cause a following deceleration of the boat.

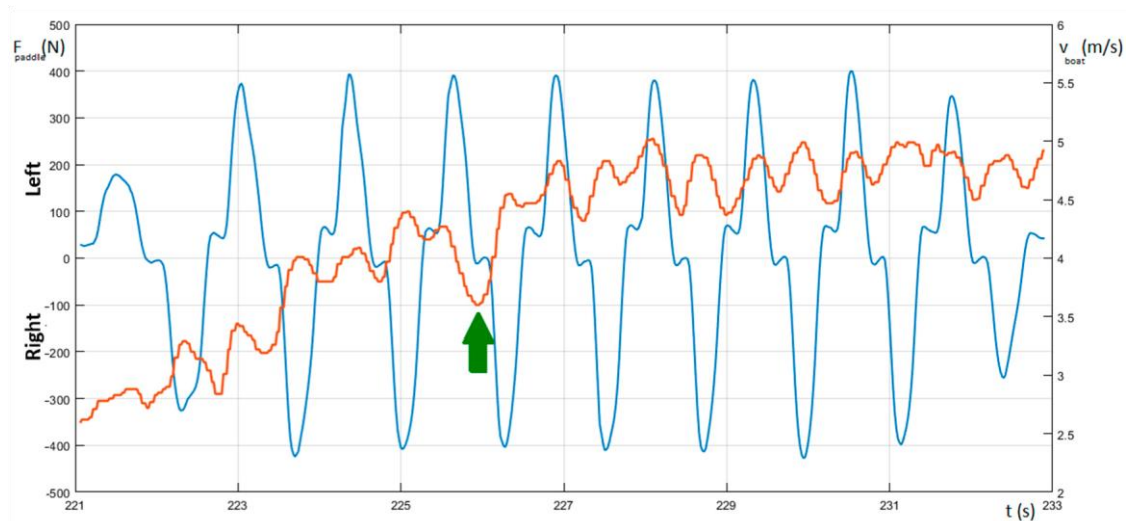


Figure 9. Measure of force on the paddle (F_{paddle} —blue) and the boat's velocity (v_{boat} —red).

Since the introduction of the wing paddle, paddling techniques have widely changed, and involve to a much greater degree the musculature of the body trunk and the legs in force production. In fact, because the force exerted by the kayaker with the paddle acts far from the axis of the craft, every stroke will create a momentum which tends to turn the kayak [30]. Although this is somewhat compensated for by the particular design of the hull, it also has to be balanced by a force exerted by the leg on the footrest on the active side. Moreover, the same force can give useful aid to the kayaker in stabilizing the torso rotations that occur during each stroke movement. The exact timing between these movements which can be used to improve the effects of the paddling force is still debated among coaches. In any case, it has been shown in the literature that it is important to investigate the synchronization and the timing of movements between the upper and lower body of the athlete in order to maximize performance.

Figure 10 shows the force–time curves of the paddle (orange curve) and footrest (blue curve) by which it is possible to study the anticipation or the delay of each foot pressure with respect to the paddle entry in the water. Figure 11 depicts a detail of the same curves, where it is possible to focus on the level of coordination between the legs and arms during each stroke and measure the relative

anticipation (T_{Dpf1}) or delay (T_{Dpf2}). In the same figure, highlighted by the green arrow, it is possible to note an example of the force exerted on the footrest that has been applied by the kayaker just before the beginning of the stroke.

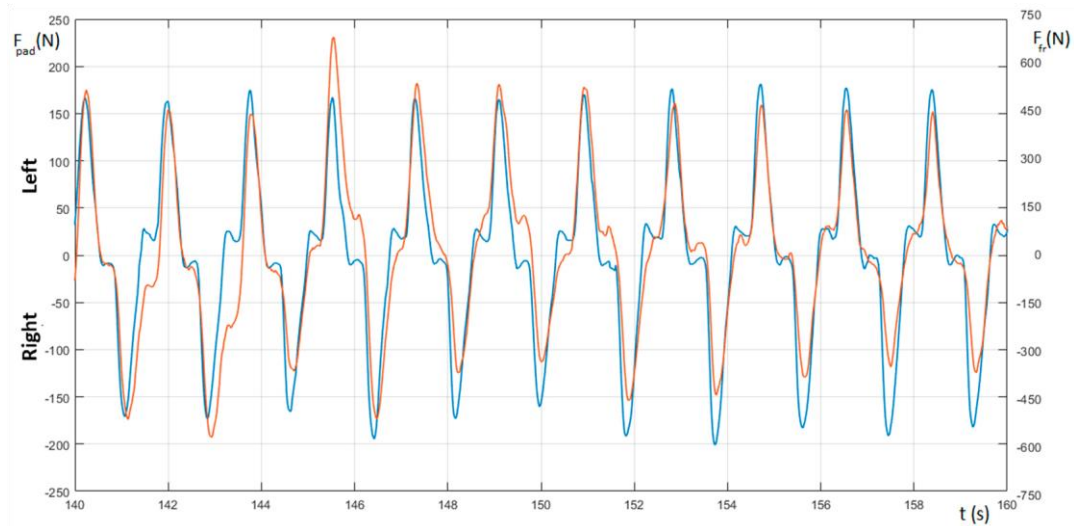


Figure 10. Measure of force on the paddle (F_{pad} —orange) and the footrest (F_{fr} —blue).

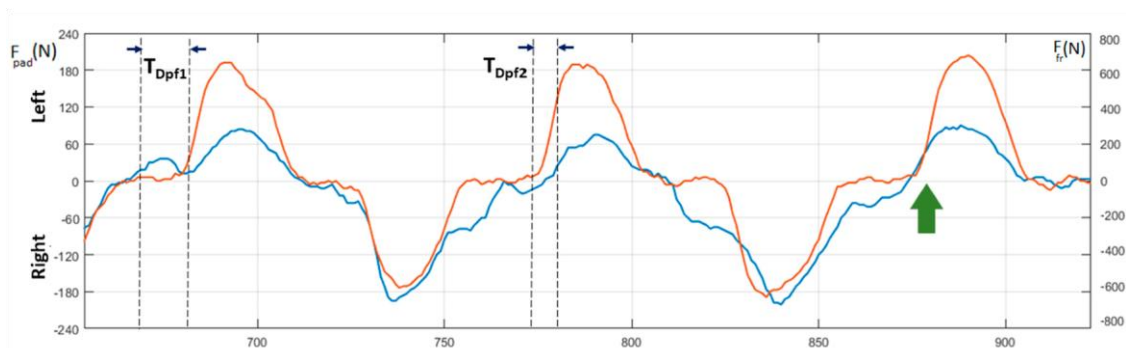


Figure 11. Detail of the force on the paddle (orange) and footrest (blue). Legend: F_{pad} [N] = force impressed on the paddle, F_{fr} [N] = force impressed on the footrest, T_{Dpf1} = leg-arm anticipation time [s], T_{Dpf2} = leg-arm delay time.

No foot straps were used to maintain the position of the feet on the footrest, but we preferred to use the original footrest configuration as usually employed by the subjects in races or training. For this reason, as the shape of deformation detected by the strain gauges strongly depends on the position of force applied on the footrest, the amount of the measured force depends not only on the intensity of

the pressure but also on the position of each foot with respect to the position of the force sensor. As a consequence, this force–time curve could not produce reliable values. In addition, it is worth noting that this position could not be the same for the length of the whole test. Consequently, these curves have to be taken into account for the timing of the gesture only, while the intensity of the measured forces as well as their symmetry between the two legs cannot be seen to reflect a real occurrence. On the other hand, though this could represent a limitation for the *e-Kayak* system, it is worth noting that this force is required, as discussed above, only for balancing the rotation of the boat. For this reason, the synchronization with the paddling force represents a parameter that can better provide a useful performance indicator with respect to that provided by the level of applied force. There are only a few studies available in the literature, [17,33] and all of them evaluate the forces on the footrest’s ergometers.

Conclusions

In flatwater sprint kayaking, paddler performances can be improved by a more effective paddling technique that consists of improvement in the propulsive power together with a reduction in the water drag by a proper checking of yaw and roll. This paper has presented a pilot study on the *e-Kayak* system, a multichannel DAQ system suited for flatwater sprint kayaking. The system manages the synchronous acquisition of both dynamic and kinematic parameters, allowing for an accurate assessment of paddling technique in real–life environments. The collected data allow a deep investigation into the assessment of paddling and can give useful evidence to differentiate between the skill levels of the athletes, while also allowing live feedback during training. Because in this specific field an acknowledged reference system is not still available, in order to evaluate the reliability of the system, the measurement results achieved in this pilot study were compared with

those available in the literature which were obtained by a system with similar features [13] for the same class of athletes. The performed comparison showed a good correspondence, for each stroke and for each of the cases depicted in this study, in the mean values of the force with respect to the exerted velocity, while the values of the other parameters were in a similar range in both studies. This suggests that the *e-Kayak* system can provide data of great interest to improving the knowledge of propulsion phases, namely, the wet and the recovery phases, during paddling. The possibility of highlighting, in fast time, several technical flaws, as for example those that are due to a lack of synchronization between arms and legs or those consequences of an over-aggressive catch, can support coaches to provide more effective suggestions to athletes in order to improve the paddling technique or in the identification of more suitable equipment. Moreover, the system seems to be highly promising for the development of objective criteria for the selection of crew members in team boats (K2 or K4 boats).

Author Contributions: Conceptualization, V.B., G.A. and G.G.; data curation, V.B and C.R. methodology, V.B., G.A. and G.G.; software, P.B. and N.L.; validation, V.B., P.B., N.L. and C.R.; writing—original, V.B. and C.R.; writing—review and editing, V.B. and C.R.; supervision, V.B., G.A. and G.G. All authors have read and agreed to the published version of the manuscript.

Funding: The development of the system discussed in this work was partially funded by the Italian Olympic Committee.

Acknowledgments: The authors wish to thank Guglielmo Guerrini for devising and initiating the project, Stefano Grillo at Circolo Canottieri Aniene for support in the tests, Giampiero Pastore and

Dario Dalla Vedova at IMSS (Medicine and Science Institute) for providing logistical support and technical advice.

Conflicts of Interest: The authors declare no conflict of interest.

References

1. Salmonia, A.W.; Schmidt, R.A.; Walter, C.B. Knowledge of results and motor learning: A review and critical reappraisal. *Psychol. Bull.* **1984**, *95*, 355–386. [CrossRef]
2. Tonacci, A.; Sansone, F.; La Spina, R.; Billeci, L.; Domenici, C.; Conte, R.; Pratali, L.; Sposta, S.-M.; Giardini, G. Feasibility of using a smart unobtrusive wearable system for the autonomic characterization of endurance trail runners. In Proceedings of the 2017 IEEE 7th International Conference on Consumer Electronics-Berlin (ICCE-Berlin), Berlin, Germany, 3–6 September 2017; pp. 224–226.
3. Amor, J.; James, C. Unobtrusive Wearable Technology for Health Monitoring. In *Wearable Technologies: Concepts Methodologies Tools and Applications*; IGI Global: Hershey, PA, USA, 2018; pp. 562–577.
4. Chambers, R.; Gabbett, T.J.; Cole, M.H.; Beard, A. The use of wearable microsensors to quantify sport-specific movements. *Sports Med.* **2015**, *45*, 1065–1081. [CrossRef] [PubMed]
5. Kos, M.; Kramberger, I. A wearable device and system for movement and biometric data acquisition for sports applications. *IEEE Access* **2017**, *5*, 6411–6420. [CrossRef]
6. Gomes, B.; Viriato, N.; Sanders, R.; Conceição, F.; Vilas-Boas, J.P.; Vaz, M. Analysis of the on-water paddling force profile of an elite kayaker. In Proceedings of the Biomechanics in Sports 29, Porto, Portugal, 27 June–1 July 2011; Volume 1.

7. Vos, J.; Kimmich, H.; Mäkinen, J.; Ijsenbrandt, H.; Vrijens, J. Telemetry of dynamic forces in endurance sports. In *Proceedings of the Biotelemetry II*; Karger Publishers: Basel, Switzerland, 1974; pp. 106–108.
8. Aitken, D.A.; Neal, R.J. An on-water analysis system for quantifying stroke force characteristics during kayak events. *Int. J. Sport Biomech.* **1992**, *8*, 165–173. [CrossRef]
9. Mimmi, G.; Rottenbacher, C.; Regazzoni, M. Evaluating paddling performances through force acquisitions with a specially instrumented Kayak ergometer. *J. Biomech.* **2006**, *39*. [CrossRef]
10. Logan, S.M.; Holt, L.E. Sports performance series: The flatwater kayak stroke. *Strength Cond. J.* **1985**, *7*, 4–11. [CrossRef]
11. Harfield, P.; Halkon, B.; Mitchell, S.; Phillips, I.; May, A. A novel, real-time biomechanical feedback system for use in rowing. *Procedia Eng.* **2014**, *72*, 126–131. [CrossRef]
12. Baker, J. Evaluation of biomechanic performance related factors with on-water tests. In *Proceedings of the International Seminar on Kayak-Canoe Coaching and Science*; University of Gent Press: Gent, Belgium, 1998; pp. 50–66.
13. Gomes, B.B.; Ramos, N.V.; Conceição, F.A.; Sanders, R.H.; Vaz, M.A.; Vilas-Boas, J.P. Paddling force profiles at different stroke rates in elite sprint kayaking. *J. Appl. Biomech.* **2015**, *31*, 258–263. [CrossRef] [PubMed]
14. Gomes, B.; Viriato, N.; Sanders, R.; Conceição, F.; Vaz, M.; Vilas-Boas, J.P. Analysis of single and team kayak acceleration. In *Proceedings of the 29th International Conference on Biomechanics in Sports*, Porto, Portugal, 27 June–1 July 2011; Volume 1.
15. Campagna, P.; Holt, L.; Alexander, A. A kayak ergometer for dry-land testing and conditioning. In *Proceedings of the 4th International Symposium on Biomechanics in Sports*, Halifax, Canada, 1986; ISBS: Halifax, Canada, 2008.

16. Pelham, T.; Holt, L.; Burke, D.; Carter, A. Accelerometry for paddling and rowing. In Proceedings of the 11th International Symposium on Biomechanics in Sports, Amherst, MA, USA, 23–26 June 1993; Volume 1.
17. Begon, M.; Colloud, F.; Lacouture, P. Measurement of contact forces on a kayak ergometer with a sliding footrest–seat complex. *Sports Eng.* **2009**, *11*, 67–73. [CrossRef]
18. Limonta, E.; Squadrone, R.; Rodano, R.; Marzegan, A.; Veicsteinas, A.; Merati, G.; Sacchi, M. Tridimensional kinematic analysis on a kayaking simulator: Key factors to successful performance. *Sport Sci. Health* **2010**, *6*, 27–34. [CrossRef]
19. Sturm, D.; Yousaf, K.; Eriksson, M. A wireless, unobtrusive Kayak Sensor Network enabling Feedback Solutions. In Proceedings of the 2010 International Conference on Body Sensor Networks, Singapore, 7–9 June 2010.
20. Nates, F.M.; Colloud, F. A 6-component paddle sensor to estimate kayaker’s performance: Preliminary results. In Proceedings of the 33rd International Conference of Biomechanics in Sports, Poitiers, France, 29 June–3 July 2015.
21. Niu, L.; Kong, P.W.; Tay, C.S.; Lin, Y.; Wu, B.; Ding, Z.; Chan, C.C. Evaluating On-water Kayak Paddling Performance using Optical Fiber Technology. *IEEE Sens. J.* **2019**, *19*, 11918–11925. [CrossRef]
22. Available online: <http://www.dansprint.com/uk/Dansprint-Ergometer/Dansprint-PRO-Kayak.html> (accessed on 2 January 2020).
23. Campanella, C.; Cuccovillo, A.; Campanella, C.; Yurt, A.; Passaro, V. Fibre bragg grating based strain sensors: Review of technology and applications. *Sensors* **2018**, *18*, 3115. [CrossRef] [PubMed]

24. Bonaiuto, V.; Boatto, P.; Lanotte, N.; Romagnoli, C.; Annino, G. A Multiprotocol Wireless Sensor Network for High Performance Sport Applications. *Appl. Syst. Innov.* **2018**, *1*, 52. [CrossRef]
25. Bonaiuto, V.; Boatto, P.; Gatta, G.; Lanotte, N.; Romagnoli, C.; Annino, G. *A Multipurpose DAQ System for Sports Applications*; Sport Engineering: Sheffield, UK, in press.
26. Bifaretti, S.; Bonaiuto, V.; Federici, L.; Gabrieli, M.; Lanotte, N. E-kayak: A wireless DAQ system for real time performance analysis. *Procedia Eng.* **2016**, *147*, 776–780. [CrossRef]
27. Available online: www.nordicsemi.com/eng/Products/2.4GHz-RF/nRF24L01 (accessed on 2 January 2020).
28. Nilsson Johnny, E.; Rosdahl Hans, G. New Devices for Measuring Forces on the Kayak Foot Bar and on the Seat during Flat-Water Kayak Paddling: A Technical Report. *Int. J. Sports Physiol. Perform.* **2014**, *9*, 365–370. [CrossRef] [PubMed]
29. McDonnell, L.K.; Hume, P.A.; Nolte, V. An observational model for biomechanical assessment of sprint kayaking technique. *Sports Biomech.* **2012**, *11*, 507–523. [CrossRef] [PubMed]
30. Kendal, S.J.; Sanders, R.H. The technique of elite flatwater kayak paddlers using the wing paddle. *J. Appl. Biomech.* **1992**, *8*, 233–250. [CrossRef]
31. Warmenhoven, J.; Cobley, S.; Draper, C.; Smith, R. Over 50 Years of Researching Force Profiles in Rowing: What Do We Know? *Sports Med.* **2018**, *48*, 2703–2714. [CrossRef] [PubMed]
32. Michael, J.S.; Smith, R.; Rooney, K.B. Determinants of kayak paddling performance. *Sports Biomech.* **2009**, *8*, 167–179. [CrossRef] [PubMed]
33. Tornberg, Å.B.; Håkansson, P.; Svensson, I.; Wollmer, P. Forces applied at the footrest during ergometer kayaking among female athletes at different competing levels—A pilot study. *BMC Sports Sci. Med. Rehabil.* **2019**, *11*, 1. [CrossRef] [PubMed]

Capitolo 3



A New Measurement System for Performance Analysis in Flatwater Sprint Kayaking

Vincenzo Bonaiuto ^{1*}, Giorgio Gatta ², Cristian Romagnoli ^{1,2}, Paolo Boatto ³, Nunzio Lanotte ^{3,4}
and Giuseppe Annino ^{1,5}

1- Sport Engineering Lab, Department Industrial Engineering, University of Rome Tor Vergata, I-00133 Rome, Italy; cristian.romagnoli2@uniroma2.it (C.R.); g_annino@hotmail.com (G.A.)

2- Department for Life Quality Studies University of Bologna, I-47037 Rimini, Italy, giorgio.gatta@unibo.it (G.G)

3- APLAB, I-00196 Rome, Italy; paolo.boatto@aplab.it (P.B.); nuziolanotte@aplab.it (N.L)

4- Department of Human Science and Promotion of Quality of Life, San Raffaele Open University of Rome, I-00166 Rome, Italy

5- School of Neuroscience, Faculty of Medicine and Surgery, University of Rome Tor Vergata, I-00133 Rome, Italy

* Correspondence: vincenzo.bonaiuto@uniroma2.it; Tel.: +39-06-7259-7402

† Presented at the 13th conference of the International Sports Engineering Association, Online, 22–26 June 2020.

Published: 15 June 2020

Abstract: The full comprehension of the impact with which each force is involved in kayak propulsion is very difficult. The measure of the force on the paddle or the stroke rate only is often not enough for the coach to identify the best actions useful to improve the performances of a kayaker. To this purpose, the synchronous measurement of all parameters involved in the kayak propulsion, both dynamic (force acting on paddle and foot brace) and kinematic (stroke frequency, displacement, velocity, acceleration, roll, yaw, and pitch of the boat) could suggest to the coach more appropriate strategies for better understanding of the paddler's motion and the relevant effects on the kayak behaviour. Some simulation models, as well as measurement systems of increasing complexity, have been proposed in the recent years. In this paper, we present the

e-Kayak system: A multichannel Digital Acquisition (DAQ) system specifically customized for flatwater kayaking. The system will be described in depth and its capability investigated through specific measurement results.

Keywords: Wireless Sensor Network; performance analysis; biomechanics; flatwater kayaking

Introduction

In flatwater sprint kayaking, fully comprehending the effectiveness of the paddling technique on the kayak's propulsion can be often very hard [1]. Kayaking is a cyclic sport, where the whole muscular kinetic chain of the athlete is involved to produce the forces that move the boat [2–5]. Moreover, different from rowing, where the force generated by the rower on the oar is transmitted to the hull through the oarlock, in kayaking the force exerted by the athlete to the paddle during the stroke is transmitted to the hull through his body itself via seat and footrest [6–8]. The kayaker, during the acceleration phase, has to generate propulsive forces greater than the resistive force offered by the water acting on the boat and, to a lesser extent, the resistance offered by the air. Furthermore, because the forces that the kayaker applies with the paddle act far from the axis of the craft, it is worth to note that each stroke will create a momentum, which will tend to turn the kayak [9]. Although these rotations are somewhat compensated for by the particular design of the hull, they also have to be balanced by the kayaker applying a force through the leg on the footrest on the active side. The same force can provide useful assistance to the kayaker in stabilizing the torso rotations that occur during each stroke movement. Consequently, a good paddling technique should be able to maximize the velocity and the forward acceleration, while minimizing all the other unnecessary rotations and accelerations along the axes of the boat. For this reason, only measuring the force on the paddle or the stroke rate is not enough for the coach to identify the findings that affect the paddling technique

and to find the best actions to improve performance for this class of athletes [7,8,10,11]. For this purpose, to give the athlete useful suggestions in modifying his paddling technique, the coach has to investigate the effectiveness of it with respect to the resulting speed and the energy expenditure by the athlete. Therefore, he requires a DAQ (Digital Acquisition) system that allows the simultaneous measurement of the kinematics of the boat together with all the forces involved in the propulsion of the kayak: The forces exerted by the upper body musculature of the kayaker on the paddle and those applied by his legs on the footrest. In recent years, several simulation models [7–13], as well as electronic measurement systems specially designed for sprint kayaking [14–21], have been proposed in literature, or they are available on the market. Some of the measurement systems allow for the study of the force-time curves performed in laboratories on ergometers (non-specific conditions) or in specific race conditions (on water). Among them, some are provided by kinematic and others by dynamic sensors applied either on the boat or on the paddle or footrest. Therefore, most of these systems cannot simultaneously measure both kinematic and dynamic parameters and among these, only one has been designed for on water use [16]. In this paper, we present a new electronic measurement system suited for flatwater kayaking application. The system allows measuring both kinematic and dynamic parameters, allowing the coaches to study the propulsion of the kayak and support the athletes in improving their performance.

Materials and Methods

Measurement System

The e-Kayak system is a digital acquisition system based on the DAQuino [22–24]. This is a modular DAQ architecture composed of up to eight slave nodes connected to a master one via a high

performance 2.4 GHz wireless link (ISM Band). Such a system is a versatile architecture, easily customizable for specific sport applications complying with the particular features required by coaches and researchers. The system hosts, inside the master node, a 9-axis IMU (Inertial Measurement Units) and a GPS (Global Positioning System), while force sensors have been applied on the paddle and footrest, the force sensors respectively hosted by two different slave nodes. Therefore, the system will be composed of a master node and pairs of slave nodes for each of the kayakers belonging to the crew of the boat. Figure 1 depicts a possible configuration of the system designed for a K2 boat (i.e., with two paddlers in the kayak).

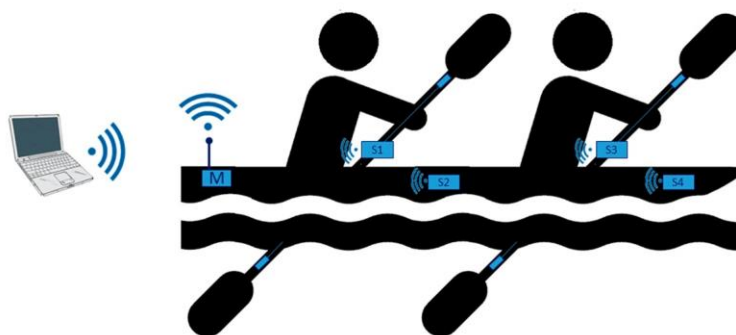


Figure 1. DAQuino configuration for K2 kayaking.

The master node is the core of the system. It has to manage the data collection from IMU and GPS (kinematic data) and by the sensors located on the slave nodes (dynamic data) and store them in a local digital memory. Moreover, by a simple webpage over a dedicated WLAN, the user is able to monitor a reduced set of parameters for an immediate feedback, download the whole training or race session, and verify the state of charge of the batteries on both master node and slave nodes. The GPS device (based on the Venus822A chip by Skytraq Technology Inc.) allows frequency update up to 50 Hz, and the IMU (based on the MPU 9250 by TDK Co.) a maximum sampling frequency of 50 Hz. The master node's weight is very limited (about 450 g); it can be easily compensated with an

appropriate sizing of the ballast. The slave node for the measure of the deformation of the shaft has been designed to be installed inside it (weight 30 g only). A proper design allows its installation in a barycentric and unobtrusive position. The force sensor consists of four waterproof strain gauges (KFW-5-120—Kyowa) connected in Wheatstone full-bridge configuration. In particular, each pair of them has been placed, in the left and right side of the shaft, at a distance of 53 cm from the tip blades. The measure of the forces on the footrest is carried out by using the same strain gauges connected in a Wheatstone half-bridge configuration on the back of the footrest itself. The setup of the whole system requires a few minutes for positioning the master node on the boat and for the zero adjusting procedure of the IMU.

```

Strokes Number= 32.00
Delta Time= 30.74 s
Stroke Rate= 62.46
Mean Velocity= 3.67 m/s
Max Paddle Force= 81.60 N
Travelled Distance= 111.30 m

```

#	Peak Force	Mean Force	Wet Time	Air Time	TimeToPeak	Mean/Peak	Mean Acc	Force Impulse
1	69.60	52.45	0.34	0.34	0.00	75.35	0.79	17.83
2	72.00	52.89	0.54	0.36	0.20	73.46	1.08	27.50
3	73.20	57.70	0.52	0.32	0.16	78.82	1.36	28.85
30	76.80	51.89	0.52	0.52	0.20	67.56	1.17	25.94
31	73.20	51.41	0.52	0.52	0.14	70.23	1.22	25.70
32	74.40	52.96	0.48	0.00	0.14	71.18	1.22	24.36
----- Mean values -----								
	75.75	54.72	0.51	0.47	0.18	72.29	1.22	27.07
----- Dev Std -----								
	4.03	3.07	0.04	0.08	0.03	2.91	0.15	2.50

Figure 2. DAQuino: Example of report.

Methods and Data Analysis

The e-Kayak system has been tested on several training sessions and, in this paper, some measurement results on a female athlete (A written informed consent was obtained after familiarization and explanation of the benefit and risks involved in the procedures adopted. The study was approved by the Ethical Committee of the School of Sports and Exercise Science—University of Rome “Tor Vergata”—Faculty of Medicine and Surgery. Moreover, all the tests were carried out

in accordance with the Declaration of Helsinki.) (age 24, height 163 cm, weight 67 kg) will be presented in order to highlight the capabilities offered by the system. These measurements have been collected during a training session of K1 boats in flat water, and some of them will be reported in this paper. The system has been installed on a NELO4 boat while a paddle BRACA-SPORT Mod. BRACA-IV has been equipped with the force sensors. Both the dynamic sensors and the kinematic ones from the IMU have been synchronously acquired at a sampling frequency of 50 Hz. The velocity and the distance have been measured through the GPS at the update frequency of 20 Hz that allows measuring the fluctuations of the velocity at each stroke (intra-cyclic velocity). The collected data have been analyzed using a custom program (Matlab R2018b by The MathWorks Inc., USA) used to automatically detect, by the analysis of the paddle force–time curves, the length of the strokes. The same software has been used for the computation of those parameters (i.e., time values and levels of force) that are commonly used by the coaches for the performance assessment.

Results

Figure 2 depicts the output report of the software that, in the first section, quotes some data of the trial under test as the number of strokes, the stroke rate, the mean velocity, and the displacement. Later, for each stroke, it has reported the peak and mean level of the force, the wet and recovery time, the time taken to reach the peak level of force, the ratio between the values of peak and mean force, the value of the mean acceleration during the peak, and the area of the force pulse.

Figure 3 depicts the force measured on the paddle (blue) versus the forward acceleration of the boat (orange). The measure of the forward acceleration acquired synchronously with the force impressed by the paddler is an interesting parameter in the assessing of the effectiveness of the paddling because

it allows for evaluation of the progression of the boat in the presence of a possible imbalance between the left and right arm [6].

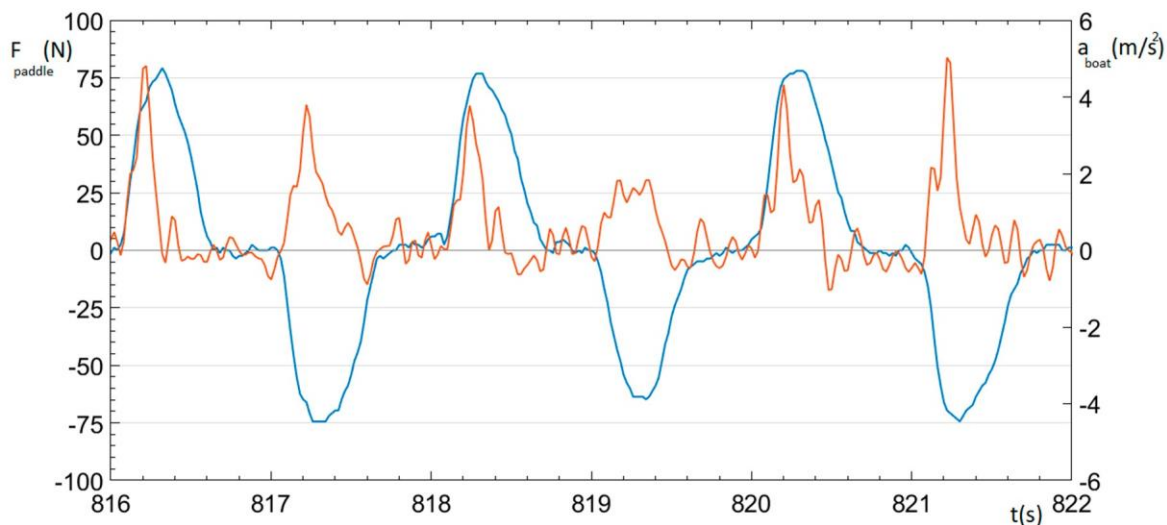


Figure 3. Boat's forward acceleration (orange) vs. force on the paddle (blue).

Figure 4 depicts the force measured on the paddle (blue) versus the velocity of the boat (orange). In particular, it depicts an acquisition of the first thirty seconds of a simulation of the start of a race. As you can see, it is possible to observe the increase, in the first part of the figure, of the velocity until it reaches the steady-state value.

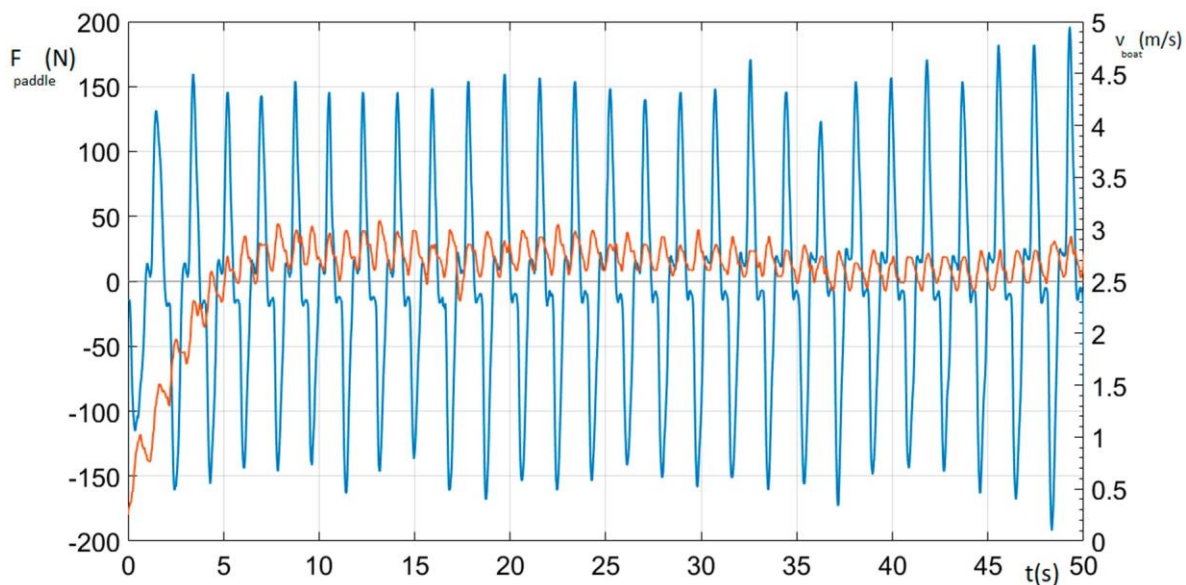


Figure 4. Boat's velocity (orange) vs. force on the paddle (blue).

Discussion

In Figure 3, the positive side of the curve represents the force exerted by the left arm while the negative represents that exerted by the right one. The forward acceleration curve (orange) results for most of the strokes are proportional to the force impressed. The subject shows a negligible imbalance in the force pulled on the paddle with a slight prevalence on the left side. When this unbalance is bigger, it will cause a rotation of the boat around its vertical axis, thus increasing the resistance to forward motion of the hull by affecting both surface and wave drag and, consequently, the forward acceleration presents a more noticeable reduction.

The mean velocity represents a fundamental appearance in the assessment of the propulsive effectiveness of the kayaker. The importance of investigating the synchronization and timing of the movements between the upper and lower body of the athlete in order to maximize performance has been widely reported in the literature. The exact timing between these movements to improve the effects of the paddling force is still debated among coaches.

The measure of velocity compared with the force signal (Figure 4) represents a useful key in the assessment of the effectiveness of the paddling technique, where the goal is to prove if it has been obtained an improvement in the velocity with the same amount of force exerted by the athlete. In particular, in the figure, you can note that the velocity, starting from zero, reaches the steady state after about 7 s. It is worth noting the fluctuant wave shape of the velocity inside each stroke (intra-cyclic velocity) increasing when the paddle force applied by the kayaker exceeds the drag force and, successively, falling down when, during the air phase, no force applied on the paddle has been measured.

Conclusions

In flatwater sprint kayaking, the paddler performances can be improved by a more effective paddling technique that consists of the improvement of the propulsive power together with a reduction of the water drag by a proper checking of yaw and roll. This paper presented the e-kayak system, a multichannel DAQ system suited for flatwater sprint kayak. The system manages the synchronous acquisition of both dynamic and kinematic parameters, allowing an accurate assessment of the paddling technique in specific training environment providing feedback to both athletes and coaches that is useful in supporting them to improve the knowledge of propulsion phases. Moreover, it allows us to highlight, quickly, several technical flaws, identify the best equipment and support, in K2 or K4, and provide helpful criteria for the selection of crews' members.

Acknowledgments: The authors wish to thank Guglielmo Guerrini for devising and initiating the project, Stefano Grillo at Circolo Canottieri Aniene for support in the tests, Giampiero Pastore and Dario Dalla Vedova and IMSS for providing logistic support and technical advice.

Conflicts of Interest: The authors declare no conflict of interest.

References

1. Gomes, B.; Viriato, N.; Sanders, R.; Conceição, F.; Vilas-Boas, J.P.; Vaz, M. Analysis of the on-water paddling force profile of an elite kayaker. In Proceedings of the ISBS-Conference Proceedings Archive, Porto, Portugal, 27 June–1 July 2011; Volume 1.
2. Vos, J.; Kimmich, H.; Mäkinen, J.; Ijsenbrandt, H.; Vrijens, J. Telemetry of dynamic forces in endurance sports. In *Proceedings of the Biotelemetry II*; Karger Publishers: Basel, Switzerland, 1974; pp. 106–108.

3. Aitken, D.A.; Neal, R.J. An On-Water Analysis System for Quantifying Stroke Force Characteristics during Kayak Events. *Int. J. Sport Biomech.* **1992**, *8*, 165–173.
4. Mimmi, G.; Rottenbacher, C.; Regazzoni, M. Evaluating paddling performances through force acquisitions with a specially instrumented Kayak ergometer. *J. Biomech.* **2006**, *39*, S543.
5. Logan, S.M.; Holt, L.E. Sports Performance Series: The flatwater kayak stroke. *Natl. Strength Cond. Assoc. J.* **1985**, *7*, 4–11.
6. Michael, J.S.; Rooney, K.B.; Smith, R.M. The dynamics of elite paddling on a kayak simulator. *J. Sports Sci.* **2012**, *30*, 661–668.
7. McDonnell, L.K.; Hume, P.; Nolte, V. A deterministic model based on evidence for the associations between kinematic variables and sprint kayak performance. *Sports Biomech.* **2013**, *12*, 205–220.
8. Kendal, S.J.; Sanders, R.H. The Technique of Elite Flatwater Kayak Paddlers Using the Wing Paddle. *Int. J. Sport Biomech.* **1992**, *8*, 233–250.
9. Limonta, E.; Squadrone, R.; Rodano, R.; Marzegan, A.; Veicsteinas, A.; Merati, G.; Sacchi, M. Tridimensional kinematic analysis on a kayaking simulator: Key factors to successful performance. *Sport Sci. Health* **2010**, *6*, 27–34.
10. Nakashima, M.; Kitazawa, A.; Nakagaki, K.; Onoto, N. Simulation to clarify the effect of paddling motion on the hull behavior of a single kayak in a sprint race. *Sports Eng.* **2016**, *20*, 133–139.
11. Nakashima, M.; Ito, S.; Nakagaki, K. Simulation of sprint canoe paddling. *Sports Eng.* **2019**, *22*, 1.

12. Nakashima, M.; Yamazaki, S.; Yue, J.; Nakagaki, K. Simulation analysis of paddling motions in a single kayak: Development of a comprehensive dynamic model of a paddler, paddle and hull. *Proc. Inst. Mech. Eng. Part P: J. Sports Eng. Technol.* **2014**, *228*, 259–269.
13. Harfield, P.; Halkon, B.; Mitchell, S.; Phillips, I.; May, A. A Novel, Real-time Biomechanical Feedback System for Use in Rowing. *Procedia Eng.* **2014**, *72*, 126–131.
14. Baker, J. Evaluation of biomechanic performance related factors with on-water tests. In *Proceedings of the International Seminar on Kayak-Canoe Coaching and Science*; University of Gent Press: Gent, Belgium, 1998; pp. 50–66.
15. Warmenhoven, J.; Cobley, S.; Draper, C.; Smith, R. Over 50 Years of Researching Force Profiles in Rowing: What Do We Know? *Sports Med.* **2018**, *48*, 2703–2714.
16. Gomes, B.B.; Ramos, N.V.; Conceição, F.A.; Sanders, R.; Vaz, M.A.; Vilas-Boas, J.P. Paddling Force Profiles at Different Stroke Rates in Elite Sprint Kayaking. *J. Appl. Biomech.* **2015**, *31*, 258–263.
17. Gomes, B.; Viriato, N.; Sanders, R.; Conceição, F.; Vaz, M.; Vilas-Boas, J.P. Analysis of single and team kayak acceleration. In *Proceedings of the ISBS-Conference Proceedings Archive*, Porto, Portugal, 27 June– 1 July 2011; Volume 1.
18. Pelham, T.; Holt, L.; Burke, D.; Carter, A. Accelerometry for paddling and rowing. In *Proceedings of the ISBS-Conference Proceedings Archive*, Amherst, MA, USA, 23–26 June 1993; Volume 1.
19. Begon, M.; Colloud, F.; Lacouture, P. Measurement of contact forces on a kayak ergometer with a sliding footrest–seat complex. *Sports Eng.* **2009**, *11*, 67–73.

20. Sturm, D.; Yousaf, K.; Eriksson, M. A wireless, unobtrusive Kayak Sensor Network enabling Feedback Solutions. In Proceedings of the 2010 International Conference on Body Sensor Networks, Singapore, 7–9 June 2010.
21. Niu, L.; Kong, P.W.; Tay, C.S.; Lin, Y.; Wu, B.; Ding, Z.; Chan, C.C. Evaluating On-Water Kayak Paddling Performance Using Optical Fiber Technology. *IEEE Sens. J.* **2019**, *19*, 11918–11925.
22. Bonaiuto, V.; Boatto, P.; Lanotte, N.; Romagnoli, C.; Annino, G. A Multiprotocol Wireless Sensor Network for High Performance Sport Applications. *Appl. Syst. Innov.* **2018**, *1*, 52.
23. Bonaiuto, V.; Boatto, P.; Gatta, G.; Lanotte, N.; Romagnoli, C.; Annino, G. A Multipurpose DAQ System for Sports Applications. *Sport Eng.* **2020**, submitted.
24. Bonaiuto, V.; Gatta, G.; Romagnoli, C.; Boatto, P.; Lanotte, N.; Annino, G. A Pilot Study on the e-Kayak System: A Wireless DAQ Suited for Performance Analysis in Flatwater Sprint Kayaks. *Sensors* **2020**, *20*, 542.

Capitolo 4

Assessment of the paddle propulsive force and the kayak power balance at different paces velocities

Cristian Romagnoli^{1,2}, Massimiliano Ditroilo³, Vincenzo Bonaiuto², Giuseppe Annino^{4,5}, Giorgio Gatta¹

¹ Department for Life Quality Studies, University of Bologna Italy, ² Sport Engineering Lab, Dept. Industrial Engineering University of Rome “Tor Vergata” Italy, ³ School of Public Health Physiotherapy and Sports Science, University College Dublin, Dublin, ⁴ Department of Medicine Systems, University of Rome “Tor Vergata” Italy, ⁵ Centre of Space Bio-Medicine, University of Rome “Tor Vergata” Italy.

(In Third Revision)

Abstract

This study determined the propulsive force (F_p) and its timing of application during the paddle stroke and confirmed the dynamic balance between propulsive power and drag power ($P_p=P_d$) in kayaking performance.

Ten male sub-elite paddlers participated in the study. The athletes carried out three trials of 50m at three different velocities: 2.70-3.00 (m/s); 3.01-3.50 (m/s) and 3.51-4.00 (m/s). A constant velocity during each trial was maintained and the section between 15-40m of the total pool length was considered for later analysis. Data were collected using the E-kayak system, an instrumented paddle and 2D video analysis.

It was observed that the propulsive force (F_p) increases in intensity (up to 85.09-90.05% of the peak force) as the velocity increases. The dynamic balance between P_d and P_p was confirmed with a Bland and Altman plot (estimated bias: 0.2; LoA: 12.8 and 13.3 W). The related comparisons between the power parameters (P_p , P_d) showed no significant difference ($p>0.05$) in each velocity considered.

By applying the dynamic balance theory between $P_p = P_d$ on the data obtained from the interaction between (three devices), it is possible to acquire essential information (F_p , P_p) to monitor the flatwater kayaking performance.

Key words: flatwater kayaking, performance analysis, GPS unit, 2D video analysis, timing of force application

Introduction

In all cyclic forms of locomotion, such as swimming, kayaking, rowing and cycling (di Prampero, 1986; Zamparo et al., 2002), intracycle velocity fluctuations occur due to the intermittent application of force. However, if the average intracycle velocity is constant over a period of time, a particular distance can be covered at an overall constant velocity. In this case the propulsive power (developed by the athlete) and the drag power (acting on the athlete and/or the equipment) must be in balance (Gatta et al., 2016; Toussaint & Beek, 1992). In kayaking performance, this condition occurs when the paddler keeps the kayak at maximum constant velocity for as long as possible (Borges et al., 2013; Goreham et al., 2021; Paquette et al., 2020), as it happens during the 1000m race competition (Goreham et al., 2021; Paquette et al., 2020). Interestingly, Gomes et al (2018) compared the size and shape of a kayak to that of the body of a swimmer, therefore the cyclic propulsive action of the paddler can be associated to the stroke in swimming and analyzed in a similar fashion to the drag swimming model in order to verify the dynamic balance.

In the flatwater kayaking context, the drag power ($P_d = F_d \cdot v = k \cdot v^3$) is the product between drag force ($F_d = k \cdot v^2$) and kayak velocity (v); while the propulsion power ($P_p = F_p \cdot v_p$) is obtained by multiplying the paddle propulsive force (F_p) by velocity in water (v_p). Therefore, the accurate measurement of F_p is central in competitive kayaking because it relates to the useful force that allows the kayak to move forward and thus at the kayak velocity.

In the literature some studies have tried to identify the phases of F_p application (Kendal & Sanders, 1992; McDonnell et al., 2012; Michael et al., 2009; Plagenhoef, 1979; Qiu et al., 2005). Commonly 4 phases of the paddle stroke are described: catch (entry)-immersion (pull)- extraction (exit)-release (aerial), and the force applied in each phase is not constant (Cox, 1992; Kendal & Sanders, 1992; Logan & Holt, 1985; Mann & Kearney, 1980; McDonnell et al., 2012; Qiu et al., 2005). Most of these studies reported that the F_p is mostly generated during the immersion and extraction phases, with differences in the phase duration and the displacement of the paddle in the water. In fact, Aitken and Neal (1992) and Mann and Kearney (1980) have suggested that the optimum force is generated when the paddle shaft is vertically in the water during the pull phase. In contrast, Qiu et al (2005) have suggested another partition of the paddle stroke: the preparation phase, the catch phase, the power phase and the recovery phase. Their observation indicate that the pull phase (propulsion) consists of the catch phase and the power phase (vertical point of the paddle in water and the water-out point). Whereas McDonnell et al (2012) considered the pull phase ranging between the immersion phase and the extraction phase. While the other phases create no propulsion (McDonnell et al., 2013).

Although, different studies have already shown the presence of a delay between force application and positive acceleration (Gomes et al., 2015; Michael et al., 2009), to date, no study has described the F_p , including its timing of application, and the dynamic balance between P_p and P_d , useful for

monitoring the paddling performance. It is known that the underwater phase of the paddle does not fully contribute to the propulsion and that current technology does not allow to accurately measure propulsive force and propulsive power parameters (Gomes et al., 2015; Sturm, 2012). The identification of the propulsive phase is going to provide useful information about the paddle position in relation to the water and the boat. This has the potential to allow coaches and athletes to make the mechanical paddling action more effective, i.e. increasing the duration of the propulsive phase and the power developed to maintain the required kayak velocity.

Applying the theory of dynamic balance ($F_p * v_p = k * v^3$) to the action of the paddler allows to accurately measure force and power variables that contribute to the kayaking performance, especially in middle- and long-distance races (Gatta et al., 2016). The determination of these variables, along with more established parameters, such as anthropometry, race distance, athlete experience (Jackson, 1995; López-Plaza et al., 2017), can help profiling the propulsive power of each paddler and in turn identifying the optimal dimension of the paddle that optimises performance.

Accordingly, the aims of this study were: a) to identify and measure the F_p and its timing of application, as well as the velocity during the paddle stroke (analyzed from the end of immersion phase to the start of extraction phase); and b) to verify the dynamic balance ($P_p=P_d$) using an instrumented paddle, a GPS unit and 2D video analysis (Bonaiuto et al., 2020). It was hypothesized that a) F_p is different from mean force (F_m) (that is typically investigated) and that b) F_p allows to obtain propulsive power (P_p) which is in balance with drag power (P_d) when a kayak moves at an overall constant velocity.

Materials and Methods

Subjects

Ten male sub-elite paddlers participated in the study [Age: 21.37 ± 2.19 (yrs), Height: 182.57 ± 5.04 (cm), weight: 82.14 ± 6.98 (kg), Kayak experience 9.75 ± 2.71 (yrs)]. The tests were conducted during the autumn 2020, when the paddlers were in the preparation period of their training. The study was approved by the University of XXX Institutional Review Board. Testing procedures were fully explained to each participant before obtaining individual written informed consent.

Procedures

The testing sessions were conducted in the morning in a 50m long outdoor swimming pool (Average Temperature of the water $22 \pm 0.5^{\circ}\text{C}$).

The athlete, after a period of 2 weeks in order to familiarize with the different paces, carried out three 50m trials at three different velocities with the same boat (K1 NELO Cinco ML): slow pace 2.7-3.0 (m/s); moderate pace 3.01-3.5 (m/s) and fast pace 3.51-4 (m/s). A 3 min rest period was allowed between trials. The test was preceded by a warm-up for the upper limbs that was completed in about 25 mins and included joint mobilization, shoulder circumduction, shoulder horizontal abduction and adduction and paddling in water. The 50m trial included an acceleration phase (0-15m), a constant velocity phase (15-40m) and a deceleration phase until stop (40-50m). The constant velocity phase of the fastest trial at each velocity range was used for later analysis.

Data collection was carried out using the E-Kayak system (APLab, Rome, Italy), incorporating a data acquisition system connected to a paddle (Braca IV min) instrumented with strain gauges and sampling at 240 Hz. The paddle was calibrated as previously recommended (Gomes et al., 2015; Sturm, 2012). The data acquisition system houses a GPS unit sampling at 20Hz to monitor the Kayak velocity. Additionally, 2D video analysis (sampling at 240 Hz) was employed to acquire kinematics and spatio-temporal variables relative to the paddle. Specifically, four video-cameras (Casio Exilim

zr3700, LTD Japan) were placed sideways to the kayak action on the pool deck at a distance of 3.5 m from one other. Moreover, these video-cameras were synchronized, between them, using a flashing visible light as reference before each test. The size of the images obtained by the camera was 432 x 320 pixels. The calibration factor has been carried out by using a 2D-direct linear transformation (Brewin & Kerwin, 2003) with horizontal reference object the distance (212 cm) between the external edge of the markers M1 and M2 on the visible side of the boat, as depicted in Figure 1 (calibration factor = 0.69 pix/cm).

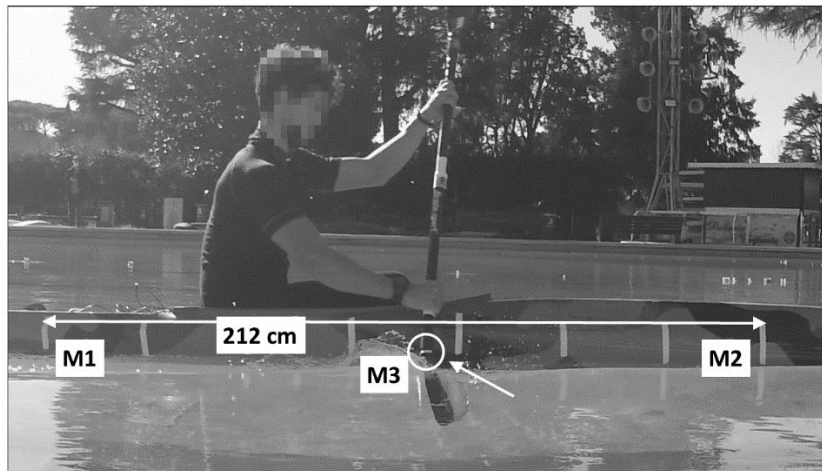


Figure 1. Horizontal reference object: the reference distance between the markers M1-M2 (212 cm). M3 is the marker used to measure the paddle displacement.

Figure 1 also shows the marker M3 placed on the shaft at 60 cm from the paddle's tip that has been used to measure the paddle displacement (S_p).

If the perpendicular orientation of the boat to the camera was lost, the video was discarded. The Biomovie ERGO© software 5.5 (Infolabmedia, Aosta, Italy) was used to synchronize data coming from the E-Kayak system and the 2D video analysis (Bonaiuto et al., 2020). The synchronization has

been obtained manually exploiting the first variation of the signal force from the E-kayak system and the start of the first entry of the paddle in the water observed by the video.

The instrumented paddle was the same used for training and competition for the majority of athletes. Only two of them could not use their usual paddle, however they familiarized with Braca IV min for a period of two weeks before the start of the testing session.

Variable extraction

These variables were measured for each athlete:

The mean force, propulsive force and peak force (F_m ; F_p ; F_{pk}) of the stroke paddle were measured with the E-kayak system. Partially based on subdivision of the paddle stroke as described by McDonnell et al (2012), F_p was instead identified from the end of the immersion phase to the start of the extraction phase with 2D video analysis, when the paddle moves in opposite direction to the movement of the kayak.

The average kayak velocity (V_k) measured with the E-kayak system.

The paddle displacement (S_p) measured with 2D video analysis it represents the horizontal paddle displacement observed between the end of the immersion and the start of the extraction phase.

The entry phase time (T_{en}), the dynamic propulsive time (T_p) and the extraction time (T_{ex}) and the wet time (T_w) were measured with 2D video analysis (Figure 2)

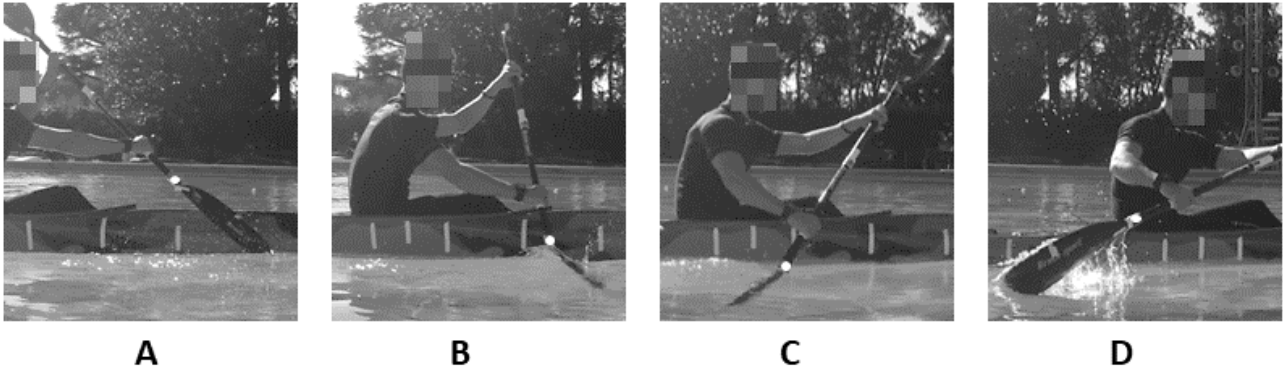


Figure 2. The underwater paddle phase ($A+B+C+D= T_w$) is divided in *entry* ($A+B = T_{en}$), *dynamic propulsive* ($B+C= T_p$) and *exit* ($C+D= T_{ex}$) time. The corresponding positions are: *catch* (A), *end immersion* (B), *start extraction* (C) and *release* (D).

These variables were calculated for each athlete:

Drag power (P_d), drag force (F_d) and drag constant (k_d) were calculated following the models proposed in the literature (Gatta et al., 2016; Gomes et al., 2015).

The kayak drag power was calculated as follows:

$$P_d = k_d * V_k \text{ (W)} \quad (\text{Eq.1})$$

the drag constant (k_d) and the drag force (F_d) relatively to the kayak:

$$k_d = \frac{F_d}{V_k^n} \quad (\text{Eq.2})$$

$$F_d = k_d * V_k^n \text{ (N)} \quad (\text{Eq.3})$$

The average paddle velocity was calculated theoretically:

$$V_{pt} = \frac{P_d}{F_p} \text{ (m/s)} \quad (\text{Eq.4})$$

where the P_d represent drag power of the kayak and F_p represent the propulsive force

The propulsive power developed from the athlete was obtained:

$$P_p = F_p * V_{pa} \quad (\text{Eq.5})$$

From the measured values of S_p and T_p , it is possible to calculate the average paddle velocity developed by the athlete as follows:

$$V_{pa} = \frac{S_p}{T_p} \text{ (m/s)} \quad (\text{Eq.6})$$

where S_p and T_p represent the paddle displacement (m) and the dynamic propulsive time (s).

Statistical Analysis

Results are presented as Mean \pm SD, unless otherwise specified. The Kolmogorov-Smirnov test was used to validate the assumption of normality. Student's paired t-test was used to detect significant differences between $P_p - P_d$ and $V_{pa} - V_{pt}$. Bland and Altman plots (Bland & Altman, 2007) were used to analyze the level of agreement between $V_{pt} - V_{pa}$ and $P_p - P_d$. In addition, the effect sizes (ES) were also calculated using Cohen's d to define the intra-observer difference between two trials for each range's velocity (Cohen, 1988), where small effect was 0.1, moderate 0.3 and large was 0.5 (Cooper & Hedges, 1993).

The statistical analysis was carried out using IBM-SPSS 20.0 (SPSS, Inc. Chicago, IL, USA). The level of statistical significance was set at $p < 0.05$.

Results

The descriptive results of kinematic (T_{en} , T_p , T_{ex} , T_w , S_p , V_{pa}) and dynamic (F_p , F_m , F_{pk}) variables are presented in Table 1 for each velocity range. Table 2 compares P_d vs P_p , and V_{pa} vs V_{pt} at each velocity. No significant differences were observed.

Table 1. Summary of kinematic and dynamic variables (Mean \pm SD).

Velocity (m/s)	T_{en} (s)	T_p (s)	T_{ex} (s)	T_w (s)	S_p (cm)	V_{pa} (m/s)	F_p (N)	F_m (N)	F_{pk} (N)	SR (spm)
From 2.70 to 3.00 (2.94 \pm 0.10)	0.13 \pm 0.03 (24.94%)	0.23 \pm 0.02 (44.14%)	0.16 \pm 0.03 (30.92%)	0.52 \pm 0.03	0.153 \pm 0.01	0.67 \pm 0.08	139.33 \pm 22.71 (85.09%)	104.71 \pm 15.51	163.85 \pm 27.19	68.06 \pm 8.10
From 3.01 to 3.50 (3.32 \pm 0.14)	0.12 \pm 0.02 (25.34%)	0.19 \pm 0.02 (40.36%)	0.16 \pm 0.04 (34.30%)	0.47 \pm 0.03	0.14 \pm 0.01	0.74 \pm 0.07	181.71 \pm 33.97 (86.74%)	129.00 \pm 21.44	210.71 \pm 44.78	75.18 \pm 7.10
From 3.51 to 4.00 (3.74 \pm 0.15)	0.13 \pm 0.02 (29.51%)	0.15 \pm 0.03 (36.05%)	0.15 \pm 0.03 (34.44%)	0.43 \pm 0.03	0.13 \pm 0.01	0.85 \pm 0.16	213.00 \pm 36.64 (90.05%)	153.22 \pm 24.03	237.33 \pm 42.04	82.07 \pm 6.80

T_{en}=Entry time (catch+ immersion); **T_p**=dynamic propulsive time; **T_{ex}**=extraction time; **T_w**= wet time; **S_p**=propulsive displacement of paddle; **V_{pa}**=paddle velocity; **F_p**=propulsive force; **F_m**=mean force; **F_{pk}**=peak force; SR=stroke rate. **T_{en}**, **T_p** and **T_{ex}** are also expressed in percentage of **T_w** and **F_p** in percentage of **F_{pk}**.

Table 2. Mean values (\pm SD) of propulsion power (P_p) and drag power (P_d); and paddle velocity determined with the 2D video analysis (V_{pa}) and paddle velocity calculated theoretically (V_{pt}). P values from the paired t-test are also reported.

Velocity (m/s)	P_p (W)	P_d (W)	p
From 2.70 to 3.00	92.41 \pm 12.11	89.40 \pm 11.51	0.53
From 3.01 to 3.50	132.89 \pm 19.79	130.25 \pm 17.78	0.69
From 3.51 to 4.00	179.22 \pm 22.38	182.06 \pm 22.62	0.67

Velocity (m/s)	V_{pt} (m/s)	V_{pa} (m/s)	p
From 2.70 to 3.00	0.65 \pm 0.07	0.67 \pm 0.08	0.66
From 3.01 to 3.50	0.72 \pm 0.08	0.74 \pm 0.07	0.61
From 3.51 to 4.00	0.87 \pm 0.17	0.85 \pm 0.16	0.75

The intra-observe magnitude, calculated between two trials, showed at low effect for T_p (0.18), T_{ex} (0.19) and moderate effect for T_{en} (0.30) in the velocity range between 2.7 to 3.00 m/s. In the velocity range from 3.01 to 3.50 m/s the ES was low for T_{en} (0.05), T_p (0.10) and moderate effect for T_{ex} (0.32). Lastly, in the velocity range between 3.51 to 4.00 m/s the ES is low for T_{en} (0.09), T_p (0.12) and T_{ex} (0.09)

Bland and Altman plots show that the values of P_p are in agreement with P_d (Figure 3), and that V_{pa} is in agreement with V_{pt} (Figure 4). The estimated bias for the power is 0.2 W and the limits of agreement are 12.8 and 13.3 W while for velocity the estimated bias is 0.002 m/s and the limits of agreement are -0.069 and 0.074 m/s.

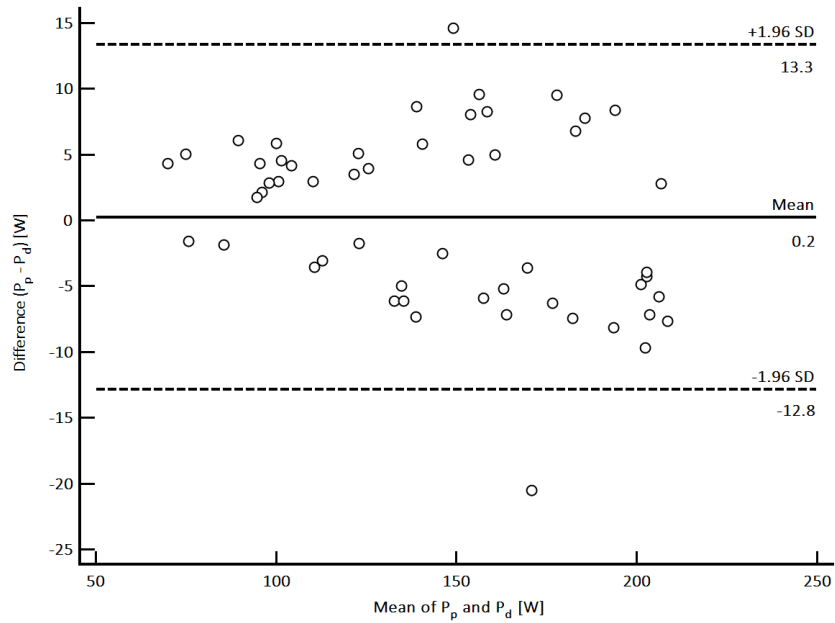


Figure 3. Bland–Altman plot of drag power (P_d) and propulsive power (P_p). Bias and random error lines (95% limits of agreement, LOA) are included.

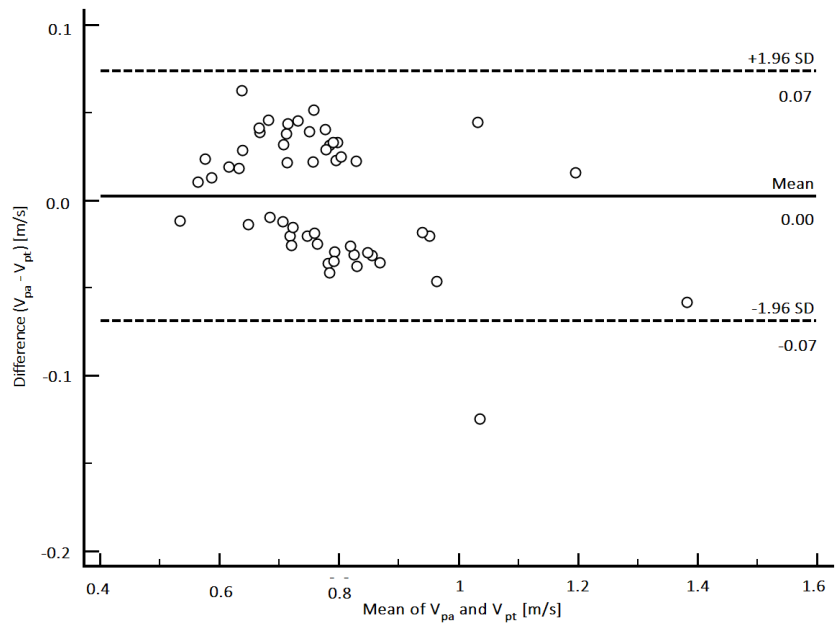


Figure 4. Bland–Altman plot of average paddle velocity developed by the athlete (V_{pa}) and average paddle velocity calculated theoretically (V_{pt}). Bias and random error lines (95% limits of agreement, LOA) are included.

Discussion and Implication

The aim of this study was to identify and measure the F_p and its timing of application in kayaking and to verify the dynamic balance ($P_p=P_d$) of the system at constant velocity. Taking into account the kinematic subdivision of paddle stroke proposed by McDonell (2012), it was possible to differentiate propulsive from non-propulsive phase of the stroke. Unlike McDonell's model where the pull phase (propulsive) occurs from the immersion to the extraction phase, in this study it appears to occur from the end of the immersion to the start of the extraction phase. Furthermore, paddle displacement and dynamic propulsive time (S_p , T_p) were measured in the pull phase (propulsive) in order to calculate paddle velocity (V_{pa}) and the relative propulsive power (Eq. 5,6) while in the immersion and extraction phase were not observed the paddle displacements e therefore were considered as non-propulsive phases.

From the percentage variations of T_{en} , T_p , T_{ex} in each singular stroke (Table 1), it can be observed that as F_m increases, the duration of T_p decreases from 44.14 to 36.05% while the non-propulsive phases (T_{en} and T_{ex}) increase their duration from 55.86 to 63.95%. These percentages are lower than the 60-80% reported in the literature (Kendal & Sanders, 1992; Mann & Kearney, 1980; Plagenhoef, 1979). This difference is likely to be related to the different time partition of propulsive and non-propulsive phases.

The increase in power generated by the athlete, and in turn the kayak velocity, corresponds to a decrease in the T_p (Table 1). The paddler needs to apply high levels of force in a short period of time. By pushing the surface of the paddle against the water a reaction force is produced useful to generate propulsion (F_p) that can be transferred to the boat. The 2D analysis allowed to calculate the paddle displacement during the propulsive phase (Table 1). The results are in agreement with previous studies by Kendal and Jackson (Jackson, 1995; Kendal & Sanders, 1992), with reported displacements between 0.12 and 0.22 m (Table 1). The synchronization between the 2D video analysis and the E-Kayak enabled the identification and separation of propulsive force from the other non-propulsive force components, and therefore the propulsive power generated by the athlete on the paddle could be calculated.

Despite different previous studies described the paddle stroke as Catch-Pull-Exit (Gomes et al., 2015; Kendal & Sanders, 1992; McDonnell et al., 2012; Michael et al., 2009), they only considered the mean force produced during the paddle stroke. In this study, for the first time, the F_p required to maintain the constant pace velocity is measured at 85.09-90.05% of F_{pk} (Table 1). However, it is worth to note that the kayak velocity does not depend on the F_p only, but the paddling technique and the boat-athlete interaction are relevant aspects that have been taken into account (Baudouin & Hawkins, 2002, 2004; Jackson, 1995; Michael et al., 2009). Therefore, it is difficult to individualize a general threshold value for propulsive phase.

The results of dynamic balance showed no significant difference (Table 2) (Figure 3 and 4) between the parameters measured and those calculated theoretically. Importantly, to verify the dynamic balance between P_p and P_d at constant pace velocity only F_p was considered, the average force values were excluded. Additionally, the comparison between the V_{pa} (measured through 2D video analysis),

and V_{pt} , did not yield significant differences at any velocity (Table 2 and Figures 3,4), thus supporting the dynamic balance condition.

This study provides a new approach to measure and monitor the kayak performance through the introduction of a new dynamic parameter like F_p . The spatial-temporal identification of F_p of the paddler may help practitioners to improve the mechanical propulsion of the paddle stroke. Finally, the propulsive power developed by the athlete and the drag power produced by the kayak validate the hypothesis that, at constant pace velocity, the interaction between both powers is in equilibrium. Furthermore, the paddler's F_p plays a key role in the calculation of P_p .

There are limitations in the interpretation of the results of this study. First of all, it was conducted in a pool environment, however this was unavoidable as it was not possible to set the cameras along the race course. Secondly, only three velocity bands were considered in this study because the pool is 50m long and the paddler can reach and maintain only relatively low velocities (until 4m/s). Additional studies using the same methodology proposed and performed in a competition facility could be conducted at greater velocities. Finally, two kayakers could not use their training paddle as it was different from the one available for testing. This may have affected their results; however, they were allowed to familiarise with the paddle for testing during the 2 weeks preceding the testing session.

Conclusion

This study used the E-kayak system incorporating an instrumented paddle, and 2D video analysis, to determine for the first time the spatial, temporal, and magnitude of the F_p during the stroke, and the dynamic balance between propulsive and drag power at constant velocity.

The new subphases partition proposed in this study will allow the coaches, the trainers, and sports biomechanists to focus their attention to increase the propulsive phase by adapting the trainings to improve the power and the technique of the paddling. By a forecasting point of view, the possibility to identify the real propulsive force related to the paddle velocity will allow to choose the best paddle useful to carry out a training mainly focused on the stroke propulsive force or a training focused directly on the paddling velocity. Further studies, could be addressed to investigate how the well-known dry-land exercises (e.g., bench press and prone bench pull) and relative training methodologies could affect the propulsive force development and the paddling velocity.

Acknowledgments

The authors wish to thank Claudio Schermi, president of the kayak club “Circolo Canottieri EUR”; Paolo Boatto and Nunzio Lanotte (Aplab company) for their assistance with E-Kayak system; Luca Ghelardini, Claudio Ghelardini and Lucia Lissoni for their assistance during the study.

Disclosure statement

The authors declare that they have not competing interests.

Funding

This research did not receive any specific grant from public or private institutions, companies or agencies.

References

- Aitken, D. A., & Neal, R. J. (1992). An On-Water Analysis System for Quantifying Stroke Force Characteristics during Kayak Events. *Journal of Applied Biomechanics*, 8(2), 165–173. <https://doi.org/10.1123/ijsb.8.2.165>
- Baudouin, A., & Hawkins, D. (2002). A biomechanical review of factors affecting rowing performance. *British Journal of Sports Medicine*, 36(6), 396–402. <https://doi.org/10.1136/bjism.36.6.396>
- Baudouin, A., & Hawkins, D. (2004). Investigation of biomechanical factors affecting rowing performance. *Journal of Biomechanics*, 37(7), 969–976. <https://doi.org/10.1016/j.jbiomech.2003.11.011>
- Bland, J. M., & Altman, D. G. (2007). Agreement Between Methods of Measurement with Multiple Observations Per Individual. *Journal of Biopharmaceutical Statistics*, 17(4), 571–582. <https://doi.org/10.1080/10543400701329422>
- Bonaiuto, V., Gatta, G., Romagnoli, C., Boatto, P., Lanotte, N., & Annino, G. (2020). A Pilot Study on the e-Kayak System: A Wireless DAQ Suited for Performance Analysis in Flatwater Sprint Kayaks. *Sensors (Basel, Switzerland)*, 20(2). <https://doi.org/10.3390/s20020542>
- Borges, T. O., Bullock, N., & Coutts, J. A. (2013). Pacing characteristics of international Sprint Kayak athletes. *International Journal of Performance Analysis in Sport*, 13(2), 353–364. <https://doi.org/10.1080/24748668.2013.11868653>
- Brewin, M. A., & Kerwin, D. G. (2003). Accuracy of scaling and DLT reconstruction techniques for planar motion analyses. *Journal of Applied Biomechanics*, 19(1), 79–88.

Cohen, J. (1988). *Statistical power analysis for the social sciences*.

Cooper, H., & Hedges, L. V. (1993). *The Handbook of Research Synthesis*. Russell Sage Foundation.

Cox, R. W. (1992). *The science of canoeing: A guide for competitors and coaches to understanding and improving performance in sprint and marathon kayaking*. Coxburn Press.

Di Prampero, P. (1986). The energy cost of human locomotion on land and in water. *Int. J.*

Gatta, G., Cortesi, M., & Zamparo, P. (2016). The Relationship between Power Generated by Thrust and Power to Overcome Drag in Elite Short Distance Swimmers. *PLOS ONE*, *11*(9), e0162387. <https://doi.org/10.1371/journal.pone.0162387>

Gomes, B. B., Conceição, F. A. V., Pendergast, D. R., Sanders, R. H., Vaz, M. A. P., & Vilas-Boas, J. P. (2015). Is passive drag dependent on the interaction of kayak design and paddler weight in flat-water kayaking? *Sports Biomechanics*, *14*(4), 394–403. <https://doi.org/10.1080/14763141.2015.1090475>

Gomes, B. B., Machado, L., Ramos, N. V., Conceição, F. A. V., Sanders, R. H., Vaz, M. A. P., Vilas-Boas, J. P., & Pendergast, D. R. (2018). Effect of wetted surface area on friction, pressure, wave and total drag of a kayak. *Sports Biomechanics*, *17*(4), 453–461. <https://doi.org/10.1080/14763141.2017.1357748>

Gomes, B. B., Ramos, N. V., Conceição, F. A., Sanders, R. H., Vaz, M. A., & Vilas-Boas, J. P. (2015). Paddling force profiles at different stroke rates in elite sprint kayaking. *Journal of Applied Biomechanics*, *31*(4), 258–263. <https://doi.org/10.1123/jab.2014-0114>

- Goreham, J. A., Miller, K. B., Frayne, R. J., & Ladouceur, M. (2021). Pacing strategies and relationships between speed and stroke parameters for elite sprint kayakers in single boats. *Journal of Sports Sciences*, *0*(0), 1–8. <https://doi.org/10.1080/02640414.2021.1927314>
- Jackson, P. S. (1995). Performance prediction for Olympic kayaks. *Journal of Sports Sciences*, *13*(3), 239–245. <https://doi.org/10.1080/02640419508732233>
- Kendal, S. J., & Sanders, R. H. (1992). The technique of elite flatwater kayak paddlers using the wing paddle. *Journal of Applied Biomechanics*, *8*(3), 233–250. <https://doi.org/10.1123/ijsb.8.3.233>
- Logan, S. M., & Holt, L. E. (1985). Sports Performance Series: The flatwater kayak stroke. *Strength & Conditioning Journal*, *7*(5), 4–11.
- López-Plaza, D., Alacid, F., Muyor, J. M., & López-Miñarro, P. Á. (2017). Sprint kayaking and canoeing performance prediction based on the relationship between maturity status, anthropometry and physical fitness in young elite paddlers. *Journal of Sports Sciences*, *35*(11), 1083–1090. <https://doi.org/10.1080/02640414.2016.1210817>
- Mann, R. V., & Kearney, J. T. (1980). A biomechanical analysis of the Olympic-style flatwater kayak stroke. *Medicine and Science in Sports and Exercise*, *12*(3), 183–188.
- McDonnell, L. K., Hume, P. A., & Nolte, V. (2012). An observational model for biomechanical assessment of sprint kayaking technique. *Sports Biomechanics*, *11*(4), 507–523. <https://doi.org/10.1080/14763141.2012.724701>
- McDonnell, L. K., Hume, P. A., & Nolte, V. (2013). A deterministic model based on evidence for the associations between kinematic variables and sprint kayak performance. *Sports Biomechanics*, *12*(3), 205–220. <https://doi.org/10.1080/14763141.2012.760106>
- Michael, J. S., Smith, R., & Rooney, K. B. (2009). Determinants of kayak paddling performance. *Sports Biomechanics*, *8*(2), 167–179. <https://doi.org/10.1080/14763140902745019>

- Paquette, M., Bieuzen, F., & Billaut, F. (2020). Effect of a 3-Weeks Training Camp on Muscle Oxygenation, V̇O₂ and Performance in Elite Sprint Kayakers. *Frontiers in Sports and Active Living*, 2. <https://doi.org/10.3389/fspor.2020.00047>
- Plagenhoef, S. (1979). Biomechanical Analysis of Olympic Flatwater Kayaking and Canoeing. *Research Quarterly. American Alliance for Health, Physical Education, Recreation and Dance*, 50(3), 443–459. <https://doi.org/10.1080/00345377.1979.10615632>
- Qiu, Y., Wei, W., Liu, A., & Cao, J. (2005). COMPARATIVE RESEARCH ON THE STROKE RHYTHM OF MEN AND WOMEN KAYAKERS IN THE INTERNATIONAL COMPETITION. *ISBS - Conference Proceedings Archive*. <https://ojs.ub.uni-konstanz.de/cpa/article/view/1152>
- Sturm, D. (2012). *Wireless Multi-Sensor Feedback Systems for SportsPerformance Monitoring: Design and Development*. <http://urn.kb.se/resolve?urn=urn:nbn:se:kth:diva-101159>
- Toussaint, H. M., & Beek, P. J. (1992). Biomechanics of Competitive Front Crawl Swimming. *Sports Medicine*, 13(1), 8–24. <https://doi.org/10.2165/00007256-199213010-00002>
- Zamparo, P., Minetti, A. E., & di Prampero, P. E. (2002). Mechanical efficiency of cycling with a new developed pedal–crank. *Journal of Biomechanics*, 35(10), 1387–1398. [https://doi.org/10.1016/S0021-9290\(02\)00071-4](https://doi.org/10.1016/S0021-9290(02)00071-4)

Capitolo 5

Specificity of weightlifting bench exercises in kayaking sprint performance: an interesting perspective for neuromuscular training

Cristian Romagnoli^{1,2}, Giorgio Gatta², Niloofar Lamouchideli³, Antonino Bianco⁴, Stefano Loddo⁵, Anas Alashram⁶, Vincenzo Bonaiuto², Giuseppe Annino^{2,7,8} and Elvira Padua⁹

¹ Department for Life Quality Studies University of Bologna, Italy.

² Sport Engineering Lab, Dept. Industrial Engineering, University of Rome "Tor Vergata", Italy.

³ Department of Human Neuroscience, University of Rome "La Sapienza", Italy.

⁴ Department of Psychology, Educational Science and Human Movement, Sport and Exercise Sciences Research Unit, University of Palermo, Italy.

⁵ Coach of the Italian Canoe/Kayak Federation (FICK), Italy.

⁶ Department of Physiotherapy, Isra University, Amman, Jordan

⁷ Department of Medicine Systems, University of Rome "Tor Vergata", Italy.

⁸ Centre of Space Bio-Medicine, "Tor Vergata" University of Rome, Italy.

⁹ Department of Human Science and Promotion of Quality of Life, San Raffaele Open University of Rome, Italy.

(In revision)

Abstract

This study aims to compare the power-load and velocity-load neuromuscular parameters performed in prone bench pull and bench press exercises to identify which of them meet the gesture specificity in sprint flatwater kayak performance. Ten elite kayakers participated in this study. Power-load, velocity-load relationships, the maximum dynamic strength and the kayak sprint performance test were assessed. The power-load and velocity-load relationships showed significant differences between the prone bench pull and bench press for each considered load. The kayakers showed a significant correlation between maximum power performed on the prone bench pull and the maximum velocity reached in the kayak sprint ($r=0.80$, $p<0.01$) and the stroke frequency ($r=0.61$,

$p < 0.05$). Conversely, the maximum power performed on the bench press did not show any correlation with the kinematic parameters analyzed. In addition, the maximum dynamic strength in the prone bench pull and bench press did not show any correlation with the maximum velocity and stroke frequency. Furthermore, no significant difference was observed in both the bench exercises for the maximum dynamic strength ($p > 0.05$). The results of this study suggest that the maximal muscular power expressed in prone bench pull exercise only seems to be more specific in kayak velocity performance compared with maximal dynamic strength and with all dynamic parameters recorded in the bench press. This will allow coaches and trainers to use specific bench exercises for specific neuromuscular kayakers' adaptations in the whole competitive season.

Key words Optimal load, Power-based training, Sprint performance, Propulsive force, Resistance training

INTRODUCTION

Canoeing / kayaking is a sport where the use of upper limbs is predominant in the propulsion phase of the boat while the action of lower limbs counteract only the consequent kayak rotations (Baker, 2012; Begon et al., 2010; Mann & Kearney, 1980). To maximize kayak velocity, paddler generates high propulsive power by applying forces on the paddle blade during each stroke (Aitken & Neal, 1992; Michael et al., 2008). During the race, the kayak shows a changeable velocity (ranging from 4.63 to 5.38 m/s) generated by the paddler actions against the drag forces (Gomes, Ramos, et al., 2015; Kendal & Sanders, 1992; Zumerchik, 1997). Therefore, to increase the kayak velocity, the paddler, dipping and pulling backwards the blade (pull phase), has to produce a propulsive force greater than the drag force (P. S. Jackson, 1995; Millward, 1987). Conversely, during the recovery

phase, where no forces are applied on the boat, only the decelerating drag forces (friction, form, wave drag) intervene (Bonaiuto et al., 2020). Therefore, it is possible to deduce that the kayak mean velocity is the consequence of the combined effects of the propulsion and the drag forces (Michael et al., 2009; Pendergast et al., 2005). So, in order to improve the propulsion phase to reduce the race time performance, the kayaker needs to condition the strength and power of upper limbs muscles through the prone bench pull (PBP) and bench press (BP) exercises (Akca & Muniroglu, 2008; Bielik et al., 2017; Bjerkefors et al., 2018; García-Pallarés et al., 2009; Hamano et al., 2015; McKean & Burkett, 2010, 2014; Pearson et al., 2009; Ualí et al., 2012; Winchcombe et al., 2019). Uali et al. (Ualí et al., 2012) reported that heavy resistance training, performed in bilateral bent pull and in one-arm cable row, were significantly correlated with the start phase of kayak sprint performances. In addition, Liow and Hopkins (Liow & Hopkins, 2003), using both bench press and bilateral dumbbell prone lifts exercises have shown that the heavy resistance training seems to be more effective to condition the start phase (0 to 15m) of kayak sprint performance while an explosive power training (low loads performed at high contraction velocity) could be more effective to maintain kayak velocity. However, it is necessary to take in account that BP and PBP exercises present some distinctive biomechanical and neuromuscular features that make them as antagonistic exercises to each other (Pearson et al., 2009; Sánchez-Medina et al., 2014). In this context, it should be more appropriate to consider these differences in specific strength and power conditioning and assessments in those sport disciplines that use upper limbs differently in pushing or pulling actions (Sánchez-Medina et al., 2014). According to these considerations, it could be relevant to know which of both bench exercises and relative training methods (strength-based vs power-based training) are more specific to improve the kayak maximum velocity performance. Thus, the aim of this study is to compare the power-load (p-l) and velocity-load (v-l) relationships expressed in BP and PBP exercises, verifying which of their dynamic

parameters, 1RM and maximum power (Pmax), is more correlated with the maximum velocity reached during flatwater kayak performance.

Material and Methods

Participants

Ten elite male kayak athletes [age: 28.88 ± 2.26 (yrs), height: 1.85 ± 0.04 (m), weight: 84.93 ± 5.96 (kg), Body Mass Index: 24.60 ± 1.46 (kg/m²)] have been involved in the study. They are members of the Italian Federation Canoe-Kayak (FICK) team with wide experience in international competitions. During the study period (May), the subjects trained ten times a week, including four dry-land training and seven water sessions. The study was approved by the University of Bologna Institutional Review Board and it is conformed to the Declaration of Helsinki.

Testing procedure

In order to determine 1RM, power-load and velocity-load relationships, a linear encoder (Bosco et al., 1995) has been used during increasing load tests performed on the PBP and BP exercises. Regarding the water tests, three trials on 50m all-out kayak sprint test (KST) were assessed to measure maximum velocity and stroke frequency. Each athlete was evaluated in five sessions (1RMPBP, 1RMBP, PBP_{p-1 & v-1}, BP_{p-1 & v-1} and KST assessment) separated by 24 hours of rest for each load test while 48 hours of rest between the last load session and KST.

Power- load and Velocity- load relationships

Before the strength and power tests, the athletes performed a warm-up for the upper limbs that was completed in 20' (5-8' for static/dynamic stretching and joint mobilization and 5-12' for shoulder circumduction, shoulder horizontal abduction and adduction).

The standard procedure to assess power-load, velocity-load relationships and maximum strength through the 1RM were determined in the PBP and BP exercises as suggest by Sreckovic et al (Sreckovic et al., 2015).

During the PBP, the subject was in the prone position on a bench with their head supported and the arms were stretched out grabbing the barbell. The pull phase started with both straight elbows and the goal was to pull with maximum effort until the barbell reached (touched) the lower part of the bench. Then the barbell was brought back to the starting position (resting on the ground). Conversely, during the BP the subject was in the supine position on the bench with their head supported. The barbell initially positioned at same level of the chest (resting on fixed supports) was pushed upward as fast as possible up to the maximum extension. The subjects were not allowed to bounce the barbell off the chest or lift the shoulders or trunk off the bench. During each of these tests, the athletes observed four minutes of rest for each load lift performance. The increasing loads lift was selected in function of 20-40-60-80-100% of 1RM for each athlete. The test of 1RM was carried out with an accuracy of 5 Kg.

Kayak sprint test (KST)

Each KST session was preceded by a standard warm-up phase where the kayaker performed ten minutes of continuous paddling at middle pace velocity followed by five trials on 50m at increasing velocity (near to maximum velocity) observing three minutes of rest between each sprint trial.

The KST consists of three trials of 100m each where the first 50m were covered increasing velocity gradually up to maximum and performing the last 50m at all-out pace velocity. Between the trials the athletes observed five minutes of rest. The velocity was measured by E-Kayak system (Bonaiuto et al., 2020), that was placed behind the seat of the paddler with the GPS antenna positioned over the

boat in order to obtain the best signal strength. The best sprint performance was selected for statistical analysis.

Statistical analysis

The statistical analysis was performed using SPSS software version 20.0 (SPSS, Chicago, I). The normality of each variable was initially tested with the Shapiro Wilk-test and all the variables have presented a normal distribution. Standard statistical methods were used in order to calculate the mean values, the standard deviations (SD) and the 95% confidence intervals for mean (95% CI). In order to verify the correlation between maximum power, 1 RM and kinematic parameters of sprint kayak (maximum velocity, stroke frequency), the Pearson product-moment correlation coefficient (r) was used. The repeated measure ANOVA (between-subjects factor) was used to evaluate the differences between BP and PBP exercises. Bonferroni corrected post-hoc analysis with paired measure was used. Statistical significance was accepted at the $p < 0.05$.

Results

The repeated measure (between-subjects factor) showed a significantly difference between the values of power and velocity in PBP and BP for loads ranging from 20% to 100% of 1 RM as reported in Table 1.

Table 1

Comparison between values of Power (W) and Velocity (m/s) expressed during BP and PBP. All values are mean \pm SD (95% confidence interval). Significant difference (between subject) as reported for $p < 0.05$ (*), for $p < 0.01$ (**) and for $p < 0.001$ (***)

Parameters	Bench Press	95% CI	Prone Bench Pull	95% CI	p
Power 20%	319.13 ± 129.40	226.56 - 411.71	484.44 ± 66.56	436.82 - 532.06	**
Power 40%	497.09 ± 202.62	352.15 - 642.04	720.99 ± 62.18	676.51 - 765.47	**
Power 60%	548.00 ± 218.65	391.58 - 704.42	805.16 ± 75.52	751.13 - 859.19	**
Power 80%	471.84 ± 177.83	344.63 - 599.06	736.95 ± 82.67	677.81 - 796.09	***
Power 100%	268.63 ± 93.93	201.43 - 335.82	516.36 ± 91.05	451.22 - 581.49	***
Velocity 20%	1.16 ± 0.35	0.91 - 1.42	1.80 ± 0.24	1.62 - 1.98	**
Velocity 40%	0.93 ± 0.27	0.73 - 1.12	1.45 ± 0.18	1.32 - 1.58	**
Velocity 60%	0.69 ± 0.19	0.55 - 0.83	1.09 ± 0.12	1.01 - 1.18	**
Velocity 80%	0.45 ± 0.12	0.36 - 0.53	0.75 ± 0.06	0.70 - 0.79	***
Velocity 100%	0.21 ± 0.06	0.17 - 0.25	0.39 ± 0.04	0.36 - 0.43	***

The linear regression between the muscle P_{max} expressed in the PBP and the average velocity during the all-out pace 50m KST has shown a close relationship with $r=0.80$ and $p<0.01$ (Figure 1; Table 2) while the correlation with stroke frequency shows a $r=0.61$ and $p<0.05$ (Table 2).

Table 2

Dynamic parameters (1 RM and P_{max} obtained for each athlete) expressed at PBP and BP in correlation with kinematic parameters observed on KTS. All values are mean ± SD. Correlation is reported $p<0.05$ (*) and $p<0.01$ (**)

Variables	Mean(±SD)	Correlation with KST _(50m) velocity (m/s)	Correlation with stroke frequency (stroke/min)
BP			
1RM (Kg)	135.50 ± 13.86	0.46	0.12
P _{max} (W)	549.50 ± 219.32	0.12	0.02
PBP			
1RM (Kg)	137.50 ± 12.52	0.33	0.08
P _{max} (W)	811.07 ± 70.89	0.80**	0.61*

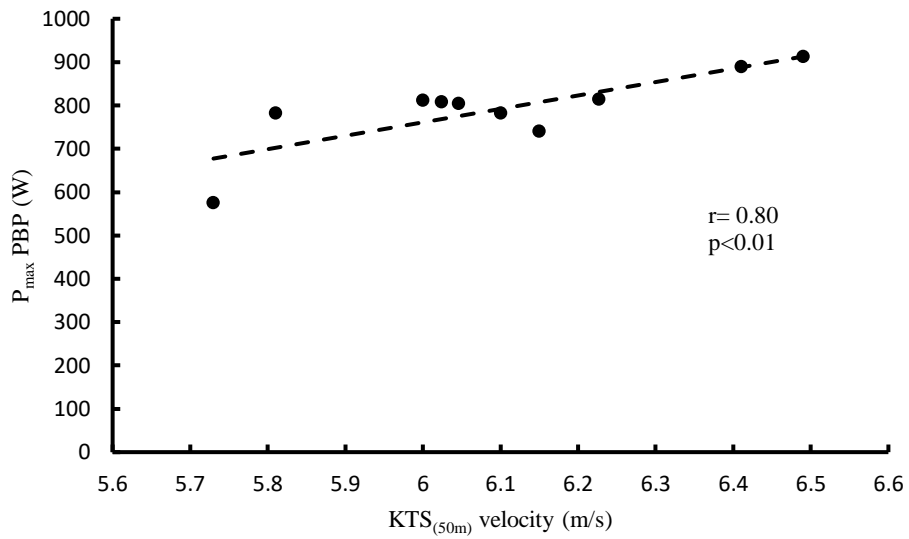


Figure 1. Correlation between P_{max} (W) expressed at PBP and kayak velocity (m/s) reached on KTS

Conversely, a poor correlation has been found between the Pmax in BP exercises and the velocity measured during KST with r=0.12 and p= 0.74 (Figure 2; Table 2).

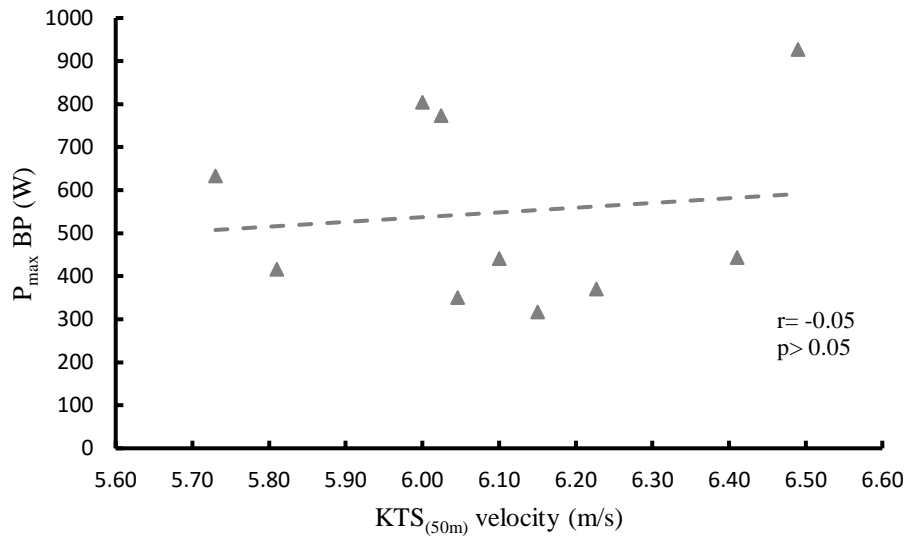


Figure 2. Correlation between P_{\max} (W) expressed at BP and kayak velocity (m/s) reached on KTS sprint.

Differently from the P_{\max} , the 1RM and the average velocity during the KST have been shown a poor and no significant correlation with all the kinematic parameters collected in both bench lift exercises (Table 2).

Discussion and conclusions

Both the power-load and velocity-load relationships, carried out by this study, respectively maintain the same quadratic and linear trend (Jaric, 2015; Sreckovic et al., 2015) such as those observed in leg or arm extensors muscles during the use of isotonic (Bosco et al., 1995) or isokinetic devices (Perrine & Edgerton, 1978) or ballistic movements (Bosco & Komi, 1979; Pearson et al., 2009; Sánchez-Medina et al., 2014). In accordance with previous studies, in BP exercise the load to perform maximum power was 60% of 1RM (Cronin et al., 2001; Izquierdo et al., 1999, 2002). Conversely, in

the PBP, our findings (60% of 1 RM) show values less than those reported in literature (70-80% of 1RM) (Pearson et al., 2009; Sánchez-Medina et al., 2014).

The resultant curves for PBP and BP exercises show a significant difference between the kinematic and dynamic parameters for each lifted up load considered in this study (Table 1). Probably, this finding could be correlated to the different muscle kinetic chains involved in both lifted up exercises (Costill et al., 1976). In fact, from an anatomical point of view, the muscles involved as prime movers in the PBP exercises (i.e. latissimus dorsi, biceps brachialis and brachialis) are composed by longer muscle fibers with a reduced angle relative to the force-generating axis (pennation angle) with a consequent faster muscle contraction than those involved as prime movers in the BP exercises (i.e. pectoralis major and triceps brachialis) which are characterized by shorter fibers and a greater pennation angles (Lieber & Fridén, 2000; Pearson et al., 2009). This allows generating a more strength as a consequence of slower muscle contraction velocity. Taking in account the movement of the paddle, Beverly et al (Trevithick et al., 2007) showed that the supraspinatus, the upper trapezius, the latissimus dorsi, serratus anterior and rhomboid major show a consistent activity pattern during kayak stroke. Moreover, it has been observed that the activity of the latissimus dorsi increases during the pull phase in water and reaches its peak during the following intermediate phase, confirming its role as prime mover muscle during the in water phase of the paddle stroke (Fleming et al., 2012; Trevithick et al., 2007; Yoshio et al., 1974). On the basis of these considerations, it seems that PBP exercises result to be more specific than BP ones relatively to the technical paddle gesture (Sánchez-Medina et al., 2014).

Several studies have verified a positive correlation between strength profile and the kayak performance, using isometric strength test performed in BP and PBP and kayak ergometer performance (Lum & Aziz, 2020; Petrović et al., 2021). Nevertheless, these studies have not

considered other relevant dynamic and kinematic parameters involved in both bench lift exercises and flatwater kayak performances. Differently from above mentioned studies, our findings shown a poor correlation, for each bench lift exercise, between the maximum dynamic strength (1RM) and the maximum kayak velocity (Table 2). Conversely, only the PBP maximum power are significantly correlated with the maximum kayak velocity performance ($r=0.80$; $p<0.01$) (Figure 1) and the related stroke frequency ($r=0.61$; $p<0.05$) (Table 2). On the contrary, the data obtained from the BP exercise show a poor correlation (Figure 2; Table 2) not only between 1RM but also with the Pmax and the kinematic parameters of the KST analyzed, showing the scant specificity with the biomechanical parameters and the muscular kinetic chains involved during paddle stroke.

Differently, in agreement with principle of specificity and training monitoring (Sale & MacDougall, 1981) only the Pmax developed in the PBP exercise results to be coherent with the technical paddle gesture (Gomes, Conceição, et al., 2015; P. Jackson et al., 1992; Tzabiras et al., 2010). Thus, in according with other factors as paddling techniques, athlete-canoe interactions and environmental conditions, the maximal muscle power output of the upper limbs seems to play an important role as limiting factor of the flatwater kayak performance.

In conclusion the PBP exercise should be used as primary dry-land exercise to improve specifically the upper limbs neuromuscular power, focusing on a power-based training. For opposite reasons, the use of the BP exercise could be advisable as a complement to conditioning the antagonist musculature only without uselessly overloading the paddler neuromuscular system.

Reference

- Aitken, D. A., & Neal, R. J. (1992). An On-Water Analysis System for Quantifying Stroke Force Characteristics during Kayak Events. *Journal of Applied Biomechanics*, 8(2), 165–173. <https://doi.org/10.1123/ijsb.8.2.165>
- Akca, F., & Muniroglu, S. (2008). Anthropometric – Somatotype and Strength Profiles and On – Water Performance in Turkish Elite Kayakers. *International Journal of Applied Sport Sciences*, 20, 22–34.
- Baker, J. (2012). BIOMECHANICS OF PADDLING. ISBS - Conference Proceedings Archive. <https://ojs.ub.uni-konstanz.de/cpa/article/view/5171>
- Begon, M., Colloud, F., & Sardain, P. (2010). Lower limb contribution in kayak performance: Modelling, simulation and analysis. *Multibody System Dynamics*, 23(4), 387–400. <https://doi.org/10.1007/s11044-010-9189-8>
- Bielik, V., Lendvorský, L., Lengvarský, L., Lopata, P., Petriska, R., & Pelikánová, J. (2017). Road to the Olympics: Physical fitness of medalists of the Canoe Sprint Junior European and World Championship events over the past 20 years. *The Journal of sports medicine and physical fitness*, 58(6), 768–777.
- Bjerkefors, A., Tarassova, O., Rosén, J. S., Zakaria, P., & Arndt, A. (2018). Three-dimensional kinematic analysis and power output of elite flat-water kayakers. *Sports Biomechanics*, 17(3), 414–427. <https://doi.org/10.1080/14763141.2017.1359330>
- Bonaiuto, V., Gatta, G., Romagnoli, C., Boatto, P., Lanotte, N., & Annino, G. (2020). A Pilot Study on the e-Kayak System: A Wireless DAQ Suited for Performance Analysis in Flatwater Sprint Kayaks. *Sensors (Basel, Switzerland)*, 20(2). <https://doi.org/10.3390/s20020542>

Bosco, C., Belli, A., Astrua, M., Tihanyi, J., Pozzo, R., Kellis, S., Tsarpela, O., Foti, C., Manno, R., & Tranquilli, C. (1995). A dynamometer for evaluation of dynamic muscle work. *European journal of applied physiology and occupational physiology*, 70(5), 379–386. <https://doi.org/10.1007/bf00618487>

Bosco, C., & Komi, P. V. (1979). Potentiation of the mechanical behavior of the human skeletal muscle through prestretching. *Acta Physiologica Scandinavica*, 106(4), 467–472. <https://doi.org/10.1111/j.1748-1716.1979.tb06427.x>

Costill, D. L., Daniels, J., Evans, W., Fink, W., Krahenbuhl, G., & Saltin, B. (1976). Skeletal muscle enzymes and fiber composition in male and female track athletes. *Journal of Applied Physiology*, 40(2), 149–154. <https://doi.org/10.1152/jappl.1976.40.2.149>

Cronin, J., McNair, P. J., & Marshall, R. N. (2001). Developing explosive power: A comparison of technique and training. *Journal of Science and Medicine in Sport*, 4(1), 59–70. [https://doi.org/10.1016/S1440-2440\(01\)80008-6](https://doi.org/10.1016/S1440-2440(01)80008-6)

Fleming, N., Donne, B., Fletcher, D., & Mahony, N. (2012). A Biomechanical Assessment of Ergometer Task Specificity in Elite Flatwater Kayakers. *Journal of Sports Science & Medicine*, 11(1), 16–25.

García-Pallarés, J., Sánchez-Medina, L., Carrasco, L., Díaz, A., & Izquierdo, M. (2009). Endurance and neuromuscular changes in world-class level kayakers during a periodized training cycle. *European Journal of Applied Physiology*, 106(4), 629–638. <https://doi.org/10.1007/s00421-009-1061-2>

Gomes, B. B., Conceição, F. A. V., Pendergast, D. R., Sanders, R. H., Vaz, M. A. P., & Vilas-Boas, J. P. (2015). Is passive drag dependent on the interaction of kayak design and paddler weight in flat-water kayaking? *Sports Biomechanics*, 14(4), 394–403. <https://doi.org/10.1080/14763141.2015.1090475>

Gomes, B. B., Ramos, N. V., Conceição, F. A., Sanders, R. H., Vaz, M. A., & Vilas-Boas, J. P. (2015). Paddling force profiles at different stroke rates in elite sprint kayaking. *Journal of Applied Biomechanics*, 31(4), 258–263. <https://doi.org/10.1123/jab.2014-0114>

Hamano, S., Ochi, E., Tsuchiya, Y., Muramatsu, E., Suzukawa, K., & Igawa, S. (2015). Relationship between performance test and body composition/physical strength characteristic in sprint canoe and kayak paddlers. *Open Access Journal of Sports Medicine*, 6, 191–199. <https://doi.org/10.2147/OAJSM.S82295>

Izquierdo, Ibañez, Gorostiaga, Garrues, Zúñiga, Antón, Larrión, & Häkkinen. (1999). Maximal strength and power characteristics in isometric and dynamic actions of the upper and lower extremities in middle-aged and older men: Strength and power and ageing. *Acta Physiologica Scandinavica*, 167(1), 57–68. <https://doi.org/10.1046/j.1365-201x.1999.00590.x>

Izquierdo, M., Häkkinen, K., Gonzalez-Badillo, J. J., Ibañez, J., & Gorostiaga, E. M. (2002). Effects of long-term training specificity on maximal strength and power of the upper and lower extremities in athletes from different sports. *European Journal of Applied Physiology*, 87(3), 264–271. <https://doi.org/10.1007/s00421-002-0628-y>

Jackson, P., Locke, N., & Brown, P. (1992). The hydrodynamics of paddle propulsion. 11th Australasian Fluid Mechanics Conference, 1197–1200.

- Jackson, P. S. (1995). Performance prediction for Olympic kayaks. *Journal of Sports Sciences*, 13(3), 239–245. <https://doi.org/10.1080/02640419508732233>
- Jaric, S. (2015). Force-velocity relationship of muscles performing multi-joint maximum performance tasks. *International journal of sports medicine*, 36(09), 699–704. <https://doi.org/10.1055/s-0035-1547283>
- Kendal, S. J., & Sanders, R. H. (1992). The technique of elite flatwater kayak paddlers using the wing paddle. *Journal of Applied Biomechanics*, 8(3), 233–250. <https://doi.org/10.1123/ijsb.8.3.233>
- Lieber, R. L., & Fridén, J. (2000). Functional and clinical significance of skeletal muscle architecture. *Muscle & Nerve*, 23(11), 1647–1666. [https://doi.org/10.1002/1097-4598\(200011\)23:11<1647::AID-MUS1>3.0.CO;2-M](https://doi.org/10.1002/1097-4598(200011)23:11<1647::AID-MUS1>3.0.CO;2-M)
- Liow, D. K., & Hopkins, W. G. (2003). Velocity specificity of weight training for kayak sprint performance. *Medicine and science in sports and exercise*, 35(7), 1232–1237.
- Lum, D., & Aziz, A. R. (2020). Relationship Between Isometric Force–Time Characteristics and Sprint Kayaking Performance. *International Journal of Sports Physiology and Performance*, 16(4), 474–479. <https://doi.org/10.1123/ijsp.2019-0607>
- Mann, R. V., & Kearney, J. T. (1980). A biomechanical analysis of the Olympic-style flatwater kayak stroke. *Medicine and Science in Sports and Exercise*, 12(3), 183–188.
- McKean, M. R., & Burkett, B. (2010). The relationship between joint range of motion, muscular strength, and race time for sub-elite flatwater kayakers. *Journal of Science and Medicine in Sport*, 13(5), 537–542. <https://doi.org/10.1016/j.jsams.2009.09.003>

- McKean, M. R., & Burkett, B. J. (2014). The Influence of Upper-Body Strength on Flat-Water Sprint Kayak Performance in Elite Athletes. *International Journal of Sports Physiology and Performance*, 9(4), 707–714. <https://doi.org/10.1123/ijsp.2013-0301>
- Michael, J. S., Rooney, K. B., & Smith, R. (2008). The Metabolic Demands of Kayaking: A Review. *Journal of Sports Science & Medicine*, 7(1), 1–7.
- Michael, J. S., Smith, R., & Rooney, K. B. (2009). Determinants of kayak paddling performance. *Sports Biomechanics*, 8(2), 167–179. <https://doi.org/10.1080/14763140902745019>
- Millward, A. (1987). A study of the forces exerted by an oarsman and the effect on boat speed. *Journal of Sports Sciences*, 5(2), 93–103. <https://doi.org/10.1080/02640418708729769>
- Pearson, S. N., Cronin, J. B., Hume, P. A., & Slyfield, D. (2009). Kinematics and kinetics of the bench-press and bench-pull exercises in a strength-trained sporting population. *Sports Biomechanics*, 8(3), 245–254. <https://doi.org/10.1080/14763140903229484>
- Pendergast, D., Mollendorf, J., Zamparo, P., Termin 2nd, A., Bushnell, D., & Paschke, D. (2005). The influence of drag on human locomotion in water. *Undersea Hyperb Med*, 32(1), 45–57.
- Perrine, J. J., & Edgerton, V. R. (1978). Muscle force-velocity and power-velocity relationships under isokinetic loading. *Medicine and science in sports*, 10(3), 159–166.
- Petrović, M., García Ramos, A., Janićijević, D., Pérez Castilla, A., Knezevic, O., & Mirkov, D. (2021). Force-Velocity Profile of Competitive Kayakers: Evaluation of a Novel Single Kayak Stroke Test. *Journal of Human Kinetics*, 80. <https://doi.org/10.2478/hukin-2021-0100>

Sale, D., & MacDougall, D. (1981). Specificity in strength training: A review for the coach and athlete. *Canadian journal of applied sport sciences. Journal canadien des sciences appliquées au sport*, 6(2), 87–92.

Sánchez-Medina, L., González-Badillo, J. J., Pérez, C. E., & Pallarés, J. G. (2014). Velocity- and Power-Load Relationships of the Bench Pull vs. Bench Press Exercises. *International Journal of Sports Medicine*, 35(3), 209–216. <https://doi.org/10.1055/s-0033-1351252>

Sreckovic, S., Cuk, I., Djuric, S., Nedeljkovic, A., Mirkov, D., & Jaric, S. (2015). Evaluation of force–velocity and power–velocity relationship of arm muscles. *European journal of applied physiology*, 115(8), 1779–1787. <https://doi.org/10.1007/s00421-015-3165-1>

Trevithick, B. A., Ginn, K. A., Halaki, M., & Balnave, R. (2007). Shoulder muscle recruitment patterns during a kayak stroke performed on a paddling ergometer. *Journal of Electromyography and Kinesiology*, 17(1), 74–79. <https://doi.org/10.1016/j.jelekin.2005.11.012>

Tzabiras, G. D., Polyzos, S. P., Sfakianaki, K., Diafas, V., Villiotis, A. D., Chrisikopoulos, K., & Kaloupsis, S. (2010). Experimental and numerical study of the flow past the Olympic class K-1 flat water racing kayak at steady speed. *The Sport Journal*, 13, 1–15.

Ualí, I., Herrero, A. J., Garatachea, N., Marín, P. J., Alvear-Ordenes, I., & García-López, D. (2012). Maximal Strength on Different Resistance Training Rowing Exercises Predicts Start Phase Performance in Elite Kayakers. *The Journal of Strength & Conditioning Research*, 26(4), 941–946. <https://doi.org/10.1519/JSC.0b013e31822e58f8>

Winchcombe, C. E., Binnie, M. J., Doyle, M. M., Hogan, C., & Peeling, P. (2019). Development of an On-Water Graded Exercise Test for Flat-Water Sprint Kayak Athletes. *International Journal of Sports Physiology and Performance*, 14(9), 1244–1249. <https://doi.org/10.1123/ijsp.2018-0717>

Yoshio, H., Takagi, K., Kumamoto, M., Ito, M., Ito, K., Yamashita, N., Okamoto, T., & Nakagawa, H. (1974). Electromyographic study of kayak paddling in the paddling tank. *Research Journal of Physical Education*, 18(4), 191–198.

Zumerchik, J. (1997). *Encyclopedia of sports science* (Vol. 1). Macmillan Reference USA.

Capitolo 6



Kinematic Analysis of Water Polo Player in the Vertical Thrust Performance to Determine the Force-Velocity and Power-Velocity Relationships in Water: A Preliminary Study

Giuseppe Annino ^{1,2}, **Cristian Romagnoli** ^{2,3}, **Andrea Zanela** ⁴, **Giovanni Melchiorri** ^{1,5}, **Valerio Viero** ⁵, **Elvira Padua** ^{6, *} and **Vincenzo Bonaiuto** ²

1 Department of Medicine Systems, “Tor Vergata” University of Rome, via Montpellier 1, 00133 Rome, Italy;

g_annino@hotmail.com (G.A.); gmelchiorri@libero.it (G.M.)

2 Sport Engineering Lab, Department of Industrial Engineering, “Tor Vergata” University of Rome, via del

Politecnico 1, 00133 Rome, Italy; cristian.romagnoli2@uniroma2.it (C.R.); vincenzo.bonaiuto@uniroma2.it (V.B.)

3 Department for Life Quality Studies, University of Bologna, 47900 Rimini, Italy

4 Robotics and Artificial Intelligence Lab, ENEA “Casaccia” Research Centre, via Anguillarese, 00301 Rome, Italy;

andrea.zanela@enea.it

5 Italian Swimming Federation, Stadio Olimpico Curva Nord, 00135 Rome, Italy; valerio.viero@gmail.com

6 Department of Human Science and Promotion of Quality of Life, San Raffaele Open University of Rome, via di

val Cannuta 247, 00166 Rome, Italy

* Correspondence: elvira.padua@uniroma5.it

Received: 7 February 2021

Accepted: 27 February 2021

Published: 5 March 2021

Abstract: Background: To date, studies on muscle force and power-velocity (F-v and P-v) relationships performed in water are absent. Aim: The goal of this study is to derive the F-v and P-v regression models of water polo players in water vertical thrust performance at increasing load. Methods: After use of a control object for direct linear transformation, displacement over the water and elapsed time was measured, by using a high-speed 2D-videoanalysis system, on 14 players involved in the study. Results: Intra-operator and player's performance interclass correlation coefficient (ICC) reliability showed an excellent level of reproducibility for all kinematic and dynamic measurements considered in this study with a coefficient of variation (CV) of less than 4.5%. Results of this study have shown that an exponential force-velocity relationship seems to explain better the propulsive force exerted in the water in lifting increasing loads compared to the linear one, while the power and velocity have been shown to follow a second-order polynomial regression model. Conclusion: Given the accuracy of the video analysis, the high reliability and the specificity of the results, it is pointed out that video analysis can be a valid method to determine force-velocity and power-velocity curves in a specific environment to evaluate the neuromuscular profile of each water polo player.

Keywords: water polo; biomechanics; video analysis; force-velocity relationship; power-velocity relationship

Introduction

Water polo is characterized by a complex number of movements: swim with speed changes, faster counterattack actions, frequent changes from horizontal to vertical positions, shots, blocks and fight to gain or maintain the position in water [1]. Most of these actions (handlings, shots, fight) performed at high intensity require a vertical position in water [2]. There are two actions in movement of lower limbs of the water polo player that can be identified: the eggbeater kick (cyclic movement) [3,4] and the breaststroke kick (ballistic movement) [5]. The latter skill, involving maximal lower limbs muscle power, is usually adopted in trunk vertical thrust over the water level to complete the pass, in overall shots and in goalkeeper save actions. Indeed, some studies have found in elite female water polo players a significant correlation between the shot speed and the vertical thrust over the water level performed with breaststroke kick [6,7]. Not of sex differences, it is plausible to consider the vertical thrust one of the main skills also for men's water polo.

From a biomechanical point of view, the maximal vertical thrust is obtained through the breaststroke kick techniques performed with quick movements on horizontal foot plan in extensive abduction, hip in flexion position and fast flexion-extension of knee [8]. Relative to muscular power and strength of lower limbs, it is common practice to test and condition the water polo players directly in the gravitational environment [1,9] without taking into account the specificity principle of neuromuscular and biomechanical performance that has to be transferred directly to the vertical thrust performed in water [10]. Relative to exercises performed on dry land, some authors showed a poor relationship between ground vertical jump and vertical thrust in water [11,12]. Recently, some authors, using different strength and power training methods performed on dry land or combined (dry-land and in-water) or in water only, showed a positive effect on some of the water polo skills performance with different results related to the method used [12–14]. Nevertheless, to date, studies

on muscle force and power-velocity (F-v and P-v) relationships performed in water are absent [15]. In fact, the relationship between force and muscular contraction velocity has been determined in athletes to evaluate the dynamic neuromuscular characteristics in isotonic or ballistic conditions [15–17]. For this reason, individual power load-based training is difficult to carry out in the water taking into account that this is not specific if performed in a gravitational field.

Usually, in a gravitational field, the most used devices for their practical applications in determining the mentioned above curves are linear encoders that, through a derivation process of measured space-time values, are able to calculate force and power parameters in relation to displaced mass [16,18]. Therefore, also taking into account the logistical difficulties in applying whatever isoinertial dynamometer in an aquatic environment, it remains mandatory to find a reliable and non-invasive assessment system. The practical goal of this study has been to verify an easy and reliable method, through a 2-D motion analysis approach, whose validity on kinematic measurements has already been shown [19], to assess the vertical displacement reached over the water level—net of the submerged breast-stroke kick technique—and the related derivative kinematic as well as dynamic parameters. Furthermore, this needs to determine the accuracy of the measurement system together with the intra-rater and neuromuscular performance reliability of the assessment method used. In order to obtain in the aquatic environment F-v and P-v relationships like those obtained in a gravitational field, a test protocol was used at increasing loads performing the vertical thrust with a breaststroke technique.

Materials and Methods

Subjects

Fourteen male sub-elite level water polo players, (age 22.7 ± 5 ; Body Weight, 72.9 ± 8.2 kg; height 178.9 ± 5.2 cm, Body Mass Index 22.8 ± 2.2 kg/m²) participating in the regional championships (Serie C level) organized by the Italian Swimming Federation participated in this study. The body mass and height of the subjects were measured to the nearest 0.5 kg and 0.5 cm, respectively (Seca Beam Balance-Stadiometer, Germany). The players with physical problems (pain or injuries) or with low compliance training were excluded from the study. Written informed consent was obtained from participants (n = 14) before being tested. The research was approved by the Internal Research Board of “Tor Vergata” University of Rome. All procedures were carried out in accordance with the Declaration of Helsinki.

Experimental Design

This study requires the subjects to perform in the water vertical thrust tests at increasing load. This has been applied to the subjects by using the Water polo Overload Test/Training (WOT) [1] equipment, shown in

Figure 1, that consists of a harness made of belts that are worn by the player and a load which can be fastened to its lower extremity, and does not interfere in any way with the legs' movements.

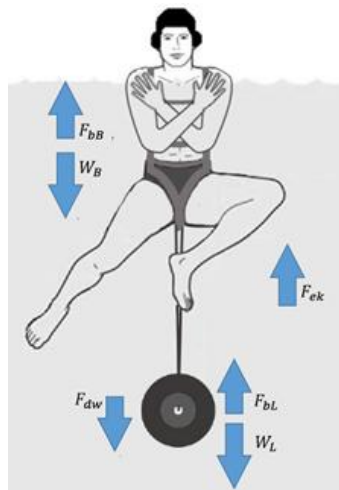


Figure 1. Frontal view of water polo overload test (WOT) conditions and acting forces. Buoyancy force of the subject (F_{bB}), Body weight of the subject (W_B), eggbeater kick force (F_{ek}), buoyancy force of the load (F_{bL}), weight of the load (W_L), force relative to power that is wasted to accelerate water downwards (F_{dw}).

The subjects, once they reached the position between the posts, spent a few seconds floating with the eggbeater kick technique to achieve and to maintain the optimal start position keeping the acromion at the same water level as before to perform, by using the breaststroke kick technique, an explosive boost to raise vertically the body as high as possible. In addition, to avoid any coordinative influence, the subjects held their upper limbs to their shoulders during the performance. Then, wearing the WOT system, they started to perform the increasing load test starting from free load condition which represents the reference trial for the test specificity. The player performed vertical thrusts increasing the load by 5 kg at each step (5, 10, 15, 20, 25 kg) where the 25 kg was the maximum load vertically raised at the limit of the buoyancy. The best trial of three measurements in terms of displacement and verticality at each increased load performance was selected for statistical analysis. Each subject completed raised load test with almost three-minute

rest time between the trials enough to recovery from single boost performance.

In order, to determine day-to-day reliability, the subjects underwent the same protocol after two rest days. The measurements were performed in the same swimming pool where the subjects usually train with the water temperature of 29 °C, pH of 7.2–7.6, and an environmental temperature that ranges between 24–26 °C at a humidity of 75%. These parameters remained unchanged in both the test days. One week before the test administration, the subjects performed some simulations for familiarization with the equipment. On the first test day, the anthropometric data were recorded and the subjects performed, after a warm-up, an incremental loads protocol test with the WOT. The warm-up exercises were completed in 15 min and consisted general to specific skills performed with a progressive increase intensity.

The subject, to maintain the assigned start position must produce, properly moving his limbs (eggbeater kick), an upward floating force (F_{ek}) equal to the difference between the sum of his body weight (W_B) plus the weight of the eventual additional load (W_L) and the sum of the respective buoyant forces (F_{bB} and F_{bL}) [20]. Equation (1) takes into account a further force (F_{dw}) related to the power that is wasted to accelerate the water downwards and that does not contribute to the thrust.

$$F_{ek} - F_{dw} = (W_B - F_{bB}) + (W_L - F_{bL}) \quad (1)$$

Considering that the body weight and the buoyant force, respectively (V_B [m³] is the volume of the body, ρ_S its density [kg/m³], ρ_w the water density (995.96 kg/m³ at 29°C), g [m/s²] the acceleration due to the gravity and f the fraction of the submerged body), are $W_B = gV_B\rho_B$ and $F_{bB} = g f V_B\rho_w$. The Equation (1) can be written as follow

$$F_{ek} = W_B \left(1 - f \frac{\rho_w}{\rho_B}\right) + (W_L - F_{bL}) + F_{dw} \quad (2)$$

where f_0 is the fraction of the submerged body at starting position (i.e., the volume of the whole body without the head and neck). Conversely, when the subject has to perform the vertical thrust, he has to provide, by moving his legs with a breaststroke kick, an upward force (F_{bk}) greater than the sum of the weight force of both load W_L and body W_B , the friction forces F_{fr} , the buoyant forces F_b and the losses F_{dw} as reported in the follow expression:

$$F_{bk} > (W_B - F_{bB} + F_{frB}) + (W_L - F_{bL} + F_{frL}) + F_{dw} \quad (3)$$

where F_{bB} and F_{bL} represent, respectively, the buoyant force of the subject and the load, while F_{frB} and F_{frL} are the respective friction forces [20]. The buoyant and friction forces of the load have been evaluated starting from manufacturing features (material, shape and dimensions). Moreover, because the load remains entirely immersed during the whole test, the relative buoyant force always presents the same value. Furthermore, since the friction depends on the displacement velocity, it will be possible, due to the features of the WOT, to use the same value of the vertical thrust velocity computed for the subject.

A different approach is required for the calculation of the same forces for the human body. Indeed, the buoyant force depends on the fraction of the volume of the immersed body that tends to vary during each test because the height of the vertical thrust changes at different loads. Therefore, the accuracy on the computation of such a term depends on a proper estimation of both the volumes of the different parts of the body and its density. In this study, this value of density ρ_B has been simply estimated, for each subject, starting from his weight and height by using the procedure suggested in [21,22]. Moreover, in order to identify the right fraction of the submerged body volume, we used the mean relative percentage values of the volumes of the different segments of the human body [23,24]. Finally, we chose to evaluate the upward force performed with the breaststroke kick considering the

buoyant force (F_{bB0}) at the start position only (i.e., when it presents its maximum level) and where the estimation of the immersed body volume shows the minimum error. Consequently, the calculation of the upward force will be underestimated, in the same way, for all the subjects.

In this context, to avoid the difficulties in evaluating the body volumes at different vertical thrust height, we consider this force minus the relative body weight (i.e., $F'_{bk} = F_{bk} - W_B$). Therefore, neglecting the skin friction drag of the body F_{frB} and the losses F_{dw} , the breaststroke force equation to lift the loads becomes

$$F'_{bk} = m_L(a + g) - F_{bB0} - F_{bL} + F_{frL} \quad (4)$$

where a is value of the acceleration in the thrust and m_L the mass of the load. Thus, the corresponding mechanical power P'_{bk} relative to the force exerted with the breaststroke kick during the vertical thrust can be computed as:

$$P'_{bk} = F'_{bk} \cdot v \quad (5)$$

Experimental Procedure

Each trial was recorded at 240 fps (time resolution ~ 4 ms) with a high-speed camera (Casio Exilim EX-ZR 3700—Japan) that was positioned at a distance of 2.30 m perpendicular at the sagittal plan of the subject in water. To verify the verticality of upper body displacement over the water level, a second camera was placed orthogonally (and at the same distance) to the first one so that the subject lay in the center of view angles of both cameras. No subject that performed a jump too far from his vertical was considered in this study.

The video analysis procedure allows, by processing the acquired videos, the value of the displacement Δd of the vertical jump to be obtained and the time Δt required by the subject to reach

the maximum elevation. In detail, the duration of the rising phase of each thrust was obtained by multiplying the frame time by the number of frames between the start of the movement (i.e., the frame where is observed the starting vertical movement) from the buoyance position and the point where the subject reaches the higher position. The starting position was identified where the subject stands stably with the acromion at the water level.

Moreover, the height of each thrust has been evaluated by measuring (in number of pixels) the distance between the position, in the two different frames of start and top position, of the marker placed on the center of the subject's headgear with respect to the level of the water (Figure 1). The values of mean velocity, force and power were calculated starting from these values while the muscular force and the relative power produced by the subject were computed starting from the maximum displacement reached in the jump by using Equations (4) and (5) respectively. A single operator provided the acquisition of these values, by using specific tools available inside the video analysis software BioMovie *ERGO*© (by Infolabmedia, Italy).

Video Analysis System Accuracy

The size of the images obtained by the camera was 432 x 320 pixels. The calibration factor K_C [pix/cm] has been evaluated by using a 2D-DLT (2D-direct linear transformation) [25] with vertical (post) and horizontal (crossbar) reference objects in the picture placed at the same distance of the subject (i.e., the subject and reference object are in the same calibration plane). Considering as negligible the horizontal displacement of the athletes during vertical jump performance, the post height (86 cm) only was considered for the calculation of the factor K_C that has been evaluated as 0.717 cm/pix.

Moreover, the relative errors (in percentages) of measured displacement ($\varepsilon_d\%$) and of measured time

($\varepsilon_t\%$) can be evaluated as:

$$\varepsilon_{d\%} = \frac{\varepsilon_u k_c}{d_{0kg}} \quad (6)$$

where d_{0kg} is the average of the height reached by the subjects during the trials at free load and ε_u is the uncertainty error, due to the motion blur [26] in the estimation of the maximum reference point in the vertical displacement. The time absolute error of the camera can be assumed as equal to a frame time ($\varepsilon_t = 4$ ms) with a negligible jitter considering that the inaccuracy of the internal clock oscillator of the camera can be estimated at less than $0.1 \mu\text{s}$. The percentage errors for the forces as well as the power were evaluated according to the usual methodologies for the error propagation [27]. The estimation of the error for the buoyancy force relative to the different subjects was computed to take into account a value equal to 3.5% for the percentage error in the measure of the body volumes ($\varepsilon_{VB\%}$) as reported by [22].

Statistical Analysis

Data in text, tables and figures are expressed as mean standard deviation (SD). The Kolmogorov-Smirnov test was used to validate the assumption of normality. Since no significant deviations from normality were detected, the coefficient of variation (CV), interclass correlation coefficients (ICC), standard error of measurement (SEM) and 95% confidence interval (95% CI) were calculated to determine the day-to-day reliability for displacement, time, velocity, acceleration, force and power. Moreover, the ICC was used as assessment test of consistency, repeatability of quantitative measurements made by same operator and to evaluate the athlete's performance in two different days.

Paired t-tests with Bonferroni adjustment and the Pearson correlation coefficient (r) were used for between-group comparisons, for test-re-test measurements repeatability and to determine the level of specificity among selected variables of the test. In addition, the effect sizes (ES) were also calculated using Cohen's d between the pre-test and post-test means [28], where small effect was 0.1, moderate 0.3 and large was 0.5 [29]. The level of statistical significance was set at $p < 0.05$. The IBM-SPSS 20.0 (SPSS, Inc., Chicago, IL, USA) was used for statistical analysis.

Results

System Accuracy

In order to evaluate the displacement relative error, we apply Equation (2) where $d(0\text{kg})$ is equal to 68 cm and the uncertainty error ϵ_u set to 3 pixels, the $\epsilon_d\%$ is equal to 3.11% while the percentage errors for the velocity, acceleration, force and power can be estimated as $\epsilon_v\% = 3.37\%$, $\epsilon_a\% = 4.25\%$, $\epsilon F_{bk}\% = 6.89\%$, $\epsilon P_{bk}\% = 7.58\%$ respectively.

Reliability

Test-retest values of Mean, SD, SEM, ICC, Pearson correlation coefficient (r) and the CV relative to the displacement, velocity, acceleration, force and power performed in the same day and day-to-day are reported in Table 1. The average displacement decreases from 0.69 m (without load) to 0.15 m (load 25 kg), with r ranging from 0.87 at 5 kg to 0.99 at 0, 10 and 25 kg respectively. The thrust performance time (s) decreases at increasing loads with r ranging from 0.86 at 15 kg to 0.99 at 25 kg. Also, the vertical velocity (m/s) decreases as the loads increase with r ranging from 0.95 at 5 kg to 0.99 at 25 kg. Also, the acceleration (m/s²) decreases at increase load with r ranging from 0.93 at 20 kg to 0.99 at 5 kg with high correlation values. By contrast with the kinematic parameters, the force

increases proportionally to the load ranging from 20.31 N at 5 kg to 304.35 N at 25 kg with high r values ranging from 0.95 at 20 kg to 0.99 at 5 kg. The power increases progressively from 5 kg ($r = 0.99$) to reach its maximal value at 20 kg (442.70 W with $r = 0.94$) and then decreases at 25 kg (313.80 W). The ICC of all parameters, expressed in detail in Table 1, showed an excellent level of reproducibility for all measurements. The CV, while remaining low in the kinematic parameters, tends to increase in the dynamic ones reaching its maximum value of 4.32 at the P_{bk} 10 kg. In addition, the SEM values observed in day-to-day trials are very low in all kinematic parameters considered for each load. The effect size (ES) calculated between pre-test and post-test means, showed a magnitude ranging from small to moderate in all kinematic and dynamic observed parameters (Table 1). The level of statistical significance was set at $p < 0.05$. An IBM-SPSS 20.0 (SPSS, Inc., Chicago, IL, USA) was used for statistical analysis.

Table 1. Day-to-day repeatability of average displacement (m), time (s), velocity (m/s) and acceleration (m/s^2), force and power \pm Standard Deviation (SD) of the vertical thrust exercise (in water) performed by 14 water polo players with increasing loads, r Pearson correlation coefficient; CV, Coefficient of Variation for repeated measurements; ICC, Interclass Correlation Coefficient; 95% Confidence Interval (CI); SEM, Standard Error of Measurement; and ES, Effect Size, for each load.

Different Day	Day1	Day 2	r	CV	ICC	95% CI	SEM	ES
Parameters	Mean \pm SD	Mean \pm SD						
Displacement (m)								
D0 kg	0.69 \pm 0.02	0.69 \pm 0.01	0.99	0.31	0.99	0.941 to 0.998	0.0013	0.004
D5 kg	0.55 \pm 0.04	0.57 \pm 0.05	0.87	1.61	0.85	0.315 to 0.978	0.0103	0.147
D10 kg	0.49 \pm 0.05	0.50 \pm 0.05	0.99	1.09	0.98	0.910 to 0.998	0.0031	-0.093
D15 kg	0.44 \pm 0.04	0.43 \pm 0.04	0.94	2.43	0.94	0.718 to 0.992	0.0061	0.091
D20 kg	0.35 \pm 0.03	0.34 \pm 0.04	0.97	1.72	0.95	0.595 to 0.993	0.0034	0.219
D25 kg	0.15 \pm 0.05	0.15 \pm 0.05	0.99	0.94	0.99	0.983 to 0.999	0.0013	0.004

Time (s)								
T0 kg	0.258 ± 0.009	0.257 ± 0.010	0.95	0.89	0.94	0.713 to 0.992	0.0013	0.134
T5 kg	0.244 ± 0.008	0.245 ± 0.010	0.91	1.28	0.94	0.648 to 0.991	0.0018	-0.173
T10 kg	0.235 ± 0.009	0.237 ± 0.013	0.90	1.82	0.93	0.561 to 0.990	0.0025	-0.191
T15 kg	0.225 ± 0.010	0.225 ± 0.011	0.86	1.78	0.93	0.494 to 0.991	0.0023	0.017
T20 kg	0.205 ± 0.008	0.206 ± 0.011	0.96	1.31	0.93	0.627 to 0.991	0.0015	-0.015
T25 kg	0.141 ± 0.023	0.143 ± 0.023	0.99	0.73	0.99	0.878 to 0.999	0.0008	-0.075
Velocity (m/s)								
V0 kg	2.68 ± 0.17	2.69 ± 0.17	0.98	0.90	0.98	0.891 to 0.997	0.0013	-0.062
V5 kg	2.30 ± 0.20	2.30 ± 0.23	0.95	2.13	0.95	0.733 to 0.994	0.0283	-0.023
V10 kg	2.11 ± 0.23	2.12 ± 0.25	0.98	1.41	0.98	0.916 to 0.998	0.0173	-0.022
V15 kg	1.95 ± 0.18	1.94 ± 0.21	0.97	1.98	0.96	0.808 to 0.995	0.0222	0.066
V20 kg	1.71 ± 0.14	1.65 ± 0.12	0.96	1.63	0.93	0.403 to 0.990	0.0159	0.279
V25 kg	1.03 ± 0.17	1.02 ± 0.17	0.99	1.38	0.98	0.903 to 0.999	0.0122	0.073
Acceleration (m/s ²)								
Acc0 kg	10.41 ± 1.04	10.51 ± 1.11	0.97	1.72	0.97	0.843 to 0.996	0.1041	-0.094
Acc5 kg	9.46 ± 1.09	9.43 ± 1.23	0.99	1.53	0.98	0.912 to 0.998	0.0839	0.025
Acc10 kg	8.99 ± 1.21	8.96 ± 1.40	0.96	3.11	0.96	0.752 to 0.994	0.1616	0.024
Acc15 kg	8.69 ± 0.95	8.66 ± 0.95	0.97	2.94	0.95	0.712 to 0.993	0.1472	0.031
Acc20 kg	8.34 ± 0.78	8.15 ± 0.79	0.93	2.37	0.92	0.552 to 0.988	0.1132	0.241
Acc25 kg	7.33 ± 0.46	7.15 ± 0.59	0.94	1.82	0.89	0.234 to 0.992	0.1061	0.323
Force F_k (N)								
F5 kg	20.31 ± 11.39	19.63 ± 11.74	0.99	2.37	0.99	0.976 to 0.999	0.3083	0.058
F10 kg	103.55 ± 17.01	103.39 ± 14.00	0.98	2.76	0.97	0.809 to 0.997	2.0393	0.009
F15 kg	183.20 ± 19.31	182.55 ± 18.17	0.98	2.16	0.97	0.750 to 0.996	2.8066	0.030
F20 kg	257.43 ± 18.51	253.36 ± 17.95	0.95	1.53	0.98	0.787 to 0.996	2.1082	0.223
F25 kg	304.35 ± 14.59	300.41 ± 17.15	0.96	1.02	0.93	0.431 to 0.995	2.5036	0.248
Power P_k (W)								
P5 kg	48.27 ± 29.35	47.01 ± 30.06	0.99	3.47	0.99	0.978 to 0.999	0.9558	0.042
P10 kg	221.99 ± 58.20	222.95 ± 64.92	0.98	4.32	0.97	0.862 to 0.997	5.5571	-0.015
P15 kg	361.15 ± 70.34	358.17 ± 84.30	0.97	4.30	0.96	0.784 to 0.995	8.9433	0.038
P20 kg	442.70 ± 62.11	421.90 ± 55.86	0.94	3.30	0.89	0.239 to 0.985	8.2565	0.353
P25 kg	313.80 ± 55.93	306.06 ± 55.89	0.97	2.47	0.97	0.733 to 0.998	6.5053	0.138

Specificity

For the specificity of the method analyzed in this study, the vertical thrust without overloads was considered as a specific water polo skill and, therefore, correlated with the same skill performed at

increasing loads. The analysis of correlation between displacement and the force, power and velocity at each load showed a strong correlation with low load (until 20 kg). As the loads increase, these correlations tend to decrease until it becomes not significant at 20 and 25 kg for velocity while for the force and power became non-significant at 25 kg only (Figure 2).

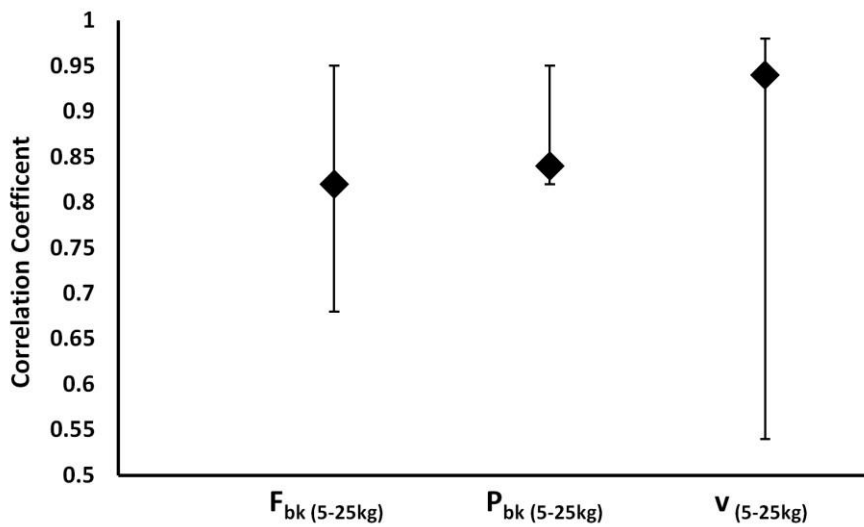


Figure 2. Median correlation coefficients and their ranges obtained comparing the vertical thrust's height free load with individual F_{bk} , P_{bk} and v at 5–25 kg.

Force-Velocity and Power-Velocity Relationships

Taking in account the means and SD values of force, power and velocity obtained by the measurements showed in Table 1, it was possible to determine a linear relationship between force and velocity and a quadratic curve between power and velocity (Figure 3).

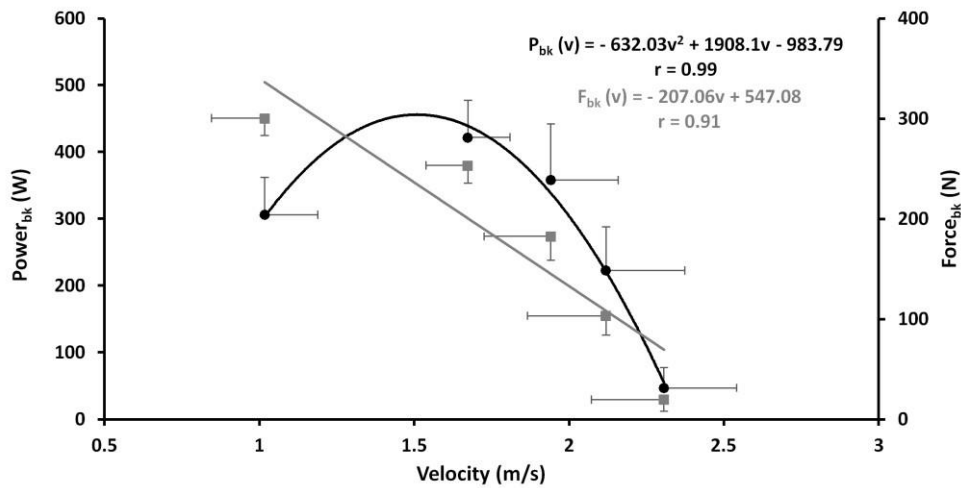


Figure 3. Linear F-v (grey line and squares) and second-order polynomial regression P-v (black line and dots) with the relative regression equations building on vertical thrust performed at incremental loads (from 5 to 25 kg). Both curves are depicted according the average and SD of velocity, force and power at different load as shown in Table 1.

It is worth noting that force and velocity values presented an inverse trend at increasing loads while the power reached the minimum value at 5 kg condition, reached a higher value at 20 kg, and then decreased again at 25 kg load. Both curves, depicted in Figure 2, show the linear and quadratic equation with a high correlation value ($r = 0.92$ and 0.99 for F-v and P-v curves respectively). Moreover, with a more accurate analysis of the F-v curve, it is interesting to highlight that the values recorded up to 20 kg maintain a linear relationship while at 25 kg the curve tends to assume an exponential like shape (Figure 4). Therefore, the following exponential equation (Equation (7)) seems to fit better the behavior of the F-v relationship of the incremental loads test ($r = 0.99$; $p < 0.001$) than the previous linear one ($r = 0.92$):

$$F_{bk}(v) = F_0 e^{-1/2 (v-a)b} \quad (7)$$

where F_0 is the maximum value of the force recorded at the lowest value of velocity (constant a) of the vertical thrust performed in the test, v is the velocity value recorded at each load while the constant b allows us to model the growth in the exponential rate.

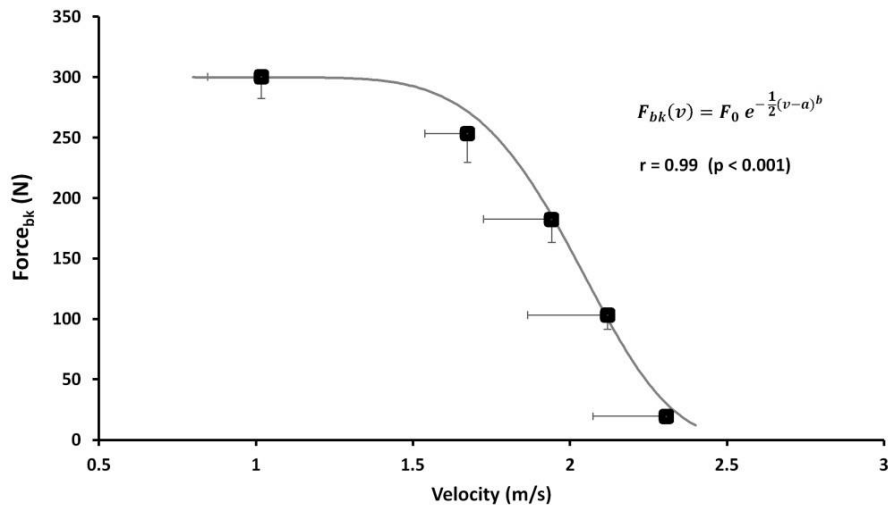


Figure 4. Exponential F-v with the relative regression equations building on vertical thrust performed at incremental loads (from 5 to 25 kg). The curve is depicted according to the average and SD of velocity and force with the different loads as shown in Table 1.

Discussion

The results of this study confirm the accuracy of the kinematic parameters measured with the video analysis system. Displacement, time and the calculated parameters as velocity and acceleration showed error values contained below 4.5% in any ballistic performance (breaststroke kick) load conditions, while the dynamic derivate as force and power showed the maximum error below 8%. It needs to be underlined that, for each parameter (measured or calculated), the relative error was less than the mean differences observed among athletes in each load condition performance. The level of reproducibility of all parameters assessed in this study was very high between the two trials performed

in two different days (Table 1) in terms of correlation (r from 0.86 to 0.99) and CV ($<4.5\%$). Thus, the intra-rater reliability on the video analysis system used in this study and the water polo player's performance provide a consistent result, with an excellent level of ICC, satisfying the basic requirement of any assessment method [16].

Usually, the methods used to determine the F-v and P-v curves of leg extensor muscles are the half-squat weightlifting or jumping test performed at increasing load in gravitational environment. Considering that the specificity represents the most important discriminant criterion of a test [30], it should be emphasized there is scant specificity from biomechanical and neuromuscular points of view between dry half squat, vertical jump and vertical thrust on the water performance [11]. The strong significant correlation showed in this study between the free load vertical displacement and the other kinematic and dynamic parameters obtained at increasing loads (Figure 2), gave to this method a high level of specificity from biomechanical and neuromuscular points of view. Biomechanically, lifting the upper body over the water level means apply a lift force able to counteract the drag force. Indeed, by using the breaststroke kick technique, Sanders [8] showed that the lift forces in the water polo boots are developed through the synergic action of feet where their velocity action is obtained using the anteroposterior and mediolateral directions, followed by the knee extension and trunk straightening from their start angle with respect to the horizontal plane. In this context, squat weightlifting or dry-land jump involves the neuromuscular system in a different biomechanics condition [31]. In addition, Platanou [11] observed no correlation between the vertical thrust on water and the vertical jump on dry land ($r = 0.25$). From a neuromuscular point of view, in this study the relationship between vertical thrust tends to decrease at increasing load just to become minimal in correspondence of the maximal strength (25 kg) (Figure 3). Furthermore, in the water the muscle contraction does not use the same strategies related to the stretching-shortening cycle and the

performance is not characterized neither by the use of elastic energy nor by stretch reflex, typical features of natural gravity movements on developing the ground reaction force. Currently, the methods used to assess the power and strength of the leg extensor and arm muscles are performed in a gravity environment [32]. This study represents the first tentative, in aquatic environment, able to determine the linear F-v and parabolic P-v relationship of lower limb muscles during a vertical thrust performance directly on the water. Both curves maintain the same characteristics of the F-v and P-v relationship observed on an athlete's performance made in a gravitational environment using a leg or arm extensors isotonic [16,18] or isokinetic devices [33] or ballistic movement [34]. According to Jaric [32], the linear relationship of F-v and consequent parabolic P-v relationship performed in a multi-joint performance showed a strong correlation revealing a high reliability of all the parameters considered in this study as reported in Table 1. Moreover, the second-order polynomial regression of P-v has shown a Pmax in correspondence with 20 kg that represents the optimal load averagely expressed by the analyzed subjects. In this context, also the high values of specificity observed with low loads tend to decrease becoming not significant after the Pmax load, probably due to a different neuromuscular pattern. In fact, according to the motor unit size recruitment principle of Henneman [35], by using an increasing loads protocol, the water polo players exhibited a decreasing heights and muscle contraction velocity on vertical thrust in relation to increasing muscular strength (increased loads) (Figure 3). Although the force and velocity values satisfy the linearity of the relationship, it is worth noting that, as shown in Figure 4, these values recorded at 25 kg tend to lose this linearity. Indeed, it can be presumed that the force exerted by the lower limbs in holding and lifting very heavy loads reached a saturation level (plateau) without ever reaching the maximum isometric force, which is impossible to obtain in a water environment, as instead it is observed in a gravitational field. In this condition, it seems conceivable to consider that the F-v curve

could switch its linearity in an exponential like relationship with heavy loads (i.e., when the vertical displacement will become negligible to the further increasing load without muscular force increase). In this case, the eggbeater and breaststroke kick are performed alternatively to maintain buoyancy, as happens in games during the hard attacks and blocks between centre forward and defender. Indeed, it is feasible to assume that the limiting factor of the maximal force exerted by a breaststroke kick is based upon the maximal buoyant force sustained with eggbeater kick performance [36]. In this context, the exponential model represented by Equation (7), with the strongest relationship ($r = 0.99$) compared with the previous linear curve ($r = 0.92$; $p < 0.001$), seems to better explain the development of the propulsive force exerted in the water-by-water polo players with the breaststroke kick technique [8,11]. Furthermore, the P-v curve (Figure 3) is not influenced by the linear or exponential F-v curve maintaining the same parabolic trend. The scant correlation observed between the maximal strength and boots performance shows that Pmax load could be considered as a reference load to plan strength or velocity conditioning training in water polo players.

Then, in accordance with the incremental load method for eggbeater kick used by Melchiorri [1] the method for breaststroke kick used in this study, seems to be able to overcome the specificity limits of all strength and power monitoring and training method performed on the land for water polo players.

As a limitation, the use of a more performing camera or a new sensor system able to detect the space-time variations of players on the water, should allow the improvement of such a measure with a consequent reduction of the error. In addition, the indirect assessment of the volumes of the different sections of the human body could lead to a less accurate estimation than the real buoyant force of the body players at the different heights reached during the vertical thrust.

Conclusions

Considering the accuracy and the reliability recorded between two consecutive trials and two days' video analysis measurements and the high specificity of the breaststroke kick performed at increasing loads, it is reasonable to consider the validity of this method. Thus, the kinematic assessment of the water polo player performing specific neuromuscular and biomechanical patterns in specific environments could reduce the bias in the assessment and training. In line with these considerations, this easy and practical method could provide coaches and trainers specific indications of the individual linear (especially at light loads) or exponential F-v and quadratic P-v relationships of each water polo player, useful for strength and power monitoring and conditioning to perform directly on the water without time spent in a non-specific regimen. Future studies should be required to verify these preliminary results calculating more accurately the human volumes and densities. Moreover, the same method should be also verified on female water polo players.

Author Contributions: G.A. and V.B. contributed to Conceptualization and Methodology. C.R. and V.V. did the data collection. A.Z., C.R. and G.M. analyzed the data; G.A. and E.P. helped in the literature review. V.B. and C.R. involved in manuscript revision. G.A., V.B., C.R. and E.P. wrote the manuscript. G.A. and V.B. supervised all the phases of the study. All authors have read and agreed to the published version of the manuscript.

Funding: This research received no external funding.

Institutional Review Board Statement: The study was conducted according to the guidelines of the Declaration of Helsinki, and approved by the internal Research Board of the “Tor Vergata” University of Rome.

Informed Consent Statement: Informed consent was obtained from all subjects involved in the study.

Data Availability Statement: All study data are included in the present manuscript.

Acknowledgments: We want to acknowledge the contribution of Cristiano Maria Verrelli, Niloofar Lamouchideli and Fabrizio Tufi.

Conflicts of Interest: The authors declare no conflict of interest.

References

1. Melchiorri, G.; Viero, V.; Triossi, T.; Tancredi, V.; Galvani, C.; Bonifazi, M. Testing and Training of the Eggbeater Kick Movement in Water Polo: Applicability of a New Method. *J. Strength Cond. Res.* 2015, 29, 2758–2764. [CrossRef] [PubMed]
2. Melchiorri, G.; Castagna, C.; Sorge, R.; Bonifazi, M. Game Activity and Blood Lactate in Men's Elite Water-Polo Players. *J. Strength Cond. Res.* 2010, 24, 2647–2651. [CrossRef]
3. Homma, M.; Homma, M. Swimming: Coaching Points for the Technique of the Eggbeater Kick in Synchronized Swimming Based on Three-Dimensional Motion Analysis. *Sports Biomech.* 2005, 4, 73–87. [CrossRef]
4. Sanders, R.H. Analysis of the Eggbeater Kick Used to Maintain Height in Water Polo. *J. Appl. Biomech.* 1999, 15, 284–291. [CrossRef]
5. Tsunokawa, T.; Nakashima, M.; Takagi, H. Use of Pressure Distribution Analysis to Estimate Fluid Forces around a Foot during Breaststroke Kicking. *Sports Eng.* 2015, 18, 149–156. [CrossRef]

6. McCluskey, L.; Lynskey, S.; Leung, C.K.; Woodhouse, D.; Briffa, K.; Hopper, D. Throwing Velocity and Jump Height in Female Water Polo Players: Performance Predictors. *J. Sci. Med. Sport* 2010, 13, 236–240. [CrossRef] [PubMed]
7. Platanou, T.; Varamenti, E. Relationships between Anthropometric and Physiological Characteristics with Throwing Velocity and on Water Jump of Female Water Polo Players. *J. Sports Med. Phys. Fit.* 2011, 51, 185.
8. Sanders, R.H. A Model of Kinematic Variables Determining Height Achieved in Water Polo Boosts. *J. Appl. Biomech.* 1999, 15, 270–283. [CrossRef]
9. Veliz, R.R.; Requena, B.; Suarez-Arrones, L.; Newton, R.U.; de Villarreal, E.S. Effects of 18-Week in-Season Heavy-Resistance and Power Training on Throwing Velocity, Strength, Jumping, and Maximal Sprint Swim Performance of Elite Male Water Polo Players. *J. Strength Cond. Res.* 2014, 28, 1007–1014. [CrossRef]
10. Gobbi, M.; D’ercole, C.; D’ercole, A.; Gobbi, F. The Components of the Jumps in Expert and Intermediate Water Polo Players. *J. Strength Cond. Res.* 2013, 27, 2685–2689. [CrossRef]
11. Platanou, T. On-Water and Dryland Vertical Jump in Water Polo Players. *J. Sports Med. Phys. Fit.* 2005, 45, 26–31.
12. Martin, M.S.; Blanco, F.P.; Villarreal, E.S.D. Effects of Different In-Season Strength Training Methods on Strength Gains and Water Polo Performance. *Int. J. Sports Physiol. Perform.* 2021, 1, 1–10. [CrossRef]

13. De Villarreal, E.S.; Suarez-Arrones, L.; Requena, B.; Haff, G.G.; Ramos-Veliz, R. Effects of Dry-Land Vs. In-Water Specific Strength Training on Professional Male Water Polo Players' Performance. *J. Strength Cond. Res.* 2014, 28, 3179–3187. [CrossRef]
14. Sáez de Villarreal, E.; Suarez-Arrones, L.; Requena, B.; Haff, G.G.; Ramos Veliz, R. Enhancing Performance in Professional Water Polo Players: Dryland Training, in-Water Training, and Combined Training. *J. Strength Cond. Res.* 2015, 29, 1089–1097. [CrossRef]
15. Kaneko, M. The Relation between Force, Velocity and Mechanical Power in Human Muscle. *Taiikugaku Kenkyu* 1970, 14, 143–147. [CrossRef]
16. Bosco, C.; Belli, A.; Astrua, M.; Tihanyi, J.; Pozzo, R.; Kellis, S.; Tsarpela, O.; Foti, C.; Manno, R.; Tranquilli, C. A Dynamometer for Evaluation of Dynamic Muscle Work. *Eur. J. Appl. Physiol. Occup. Physiol.* 1995, 70, 379–386. [CrossRef] [PubMed]
17. Cavagna, G.A.; Dusman, B.; Margaria, R. Positive Work Done by a Previously Stretched Muscle. *J. Appl. Physiol.* 1968, 24, 21–32. [CrossRef] [PubMed]
18. Sreckovic, S.; Cuk, I.; Djuric, S.; Nedeljkovic, A.; Mirkov, D.; Jaric, S. Evaluation of Force-Velocity and Power-Velocity Relationship of Arm Muscles. *Eur. J. Appl. Physiol.* 2015, 115, 1779–1787. [CrossRef] [PubMed]
19. Zult, T.; Allsop, J.; Taberner, J.; Pardhan, S. A Low-Cost 2-D Video System Can Accurately and Reliably Assess Adaptive Gait Kinematics in Healthy and Low Vision Subjects. *Sci. Rep.* 2019, 9, 1–11. [CrossRef]
20. Davidovits, P. *Physics in Biology and Medicine*; Academic Press: Cambridge, MA, USA, 2018.

21. Haycock, G.B.; Schwartz, G.J.; Wisotsky, D.H. Geometric Method for Measuring Body Surface Area: A Height-Weight Formula Validated in Infants, Children, and Adults. *J. Pediatrics* 1978, 93, 62–66. [CrossRef]
22. Sendroy Jr, J.; Collison, H.A. Determination of Human Body Volume from Height and Weight. *J. Appl. Physiol.* 1966, 21, 167–172. [CrossRef]
23. Daniell, N.; Olds, T.; Tomkinson, G. Volumetric Differences in Body Shape among Adults with Differing Body Mass Index Values: An Analysis Using Three-Dimensional Body Scans. *Am. J. Hum. Biol.* 2014, 26, 156–163. [CrossRef]
24. Var, S.M.; Marangoz, I. Leg Volume and Mass Scales of Elite Male and Female Athletes in Some Olympic Sports. *World J. Educ.* 2018, 8, 54–58.
25. Brewin, M.A.; Kerwin, D.G. Accuracy of Scaling and DLT Reconstruction Techniques for Planar Motion Analyses. *J. Appl. Biomech.* 2003, 19, 79–88. [CrossRef]
26. Tiwari, S.; Shukla, V.; Singh, A.; Biradar, S. Review of Motion Blur Estimation Techniques. *J. Image Graph.* 2013, 1, 176–184. [CrossRef]
27. Rabinovich, S.G. *Measurement Errors and Uncertainties: Theory and Practice*; Springer Science & Business Media: Berlin/Heidelberg, Germany, 2006; ISBN 978-0-387-29143-7.
28. Cohen, J. *Statistical Power Analysis for the Behavioral Sciences*; Academic Press: Cambridge, MA, USA, 2013; ISBN 978-1-4832-7648-9.
29. Cooper, H.; Hedges, L.V. *The Handbook of Research Synthesis*; Russell Sage Foundation: New York, NY, USA, 1993; ISBN 978-1-61044-137-7.

30. Sale, D.; MacDougall, D. Specificity in Strength Training: A Review for the Coach and Athlete. *Can. J. Appl. Sport Sci.* 1981, 6, 87–92. [PubMed]
31. Jacobs, R.; Bobbert, M.F.; van Ingen Schenau, G.J. Mechanical Output from Individual Muscles during Explosive Leg Extensions: The Role of Biarticular Muscles. *J. Biomech.* 1996, 29, 513–523. [CrossRef]
32. Jaric, S. Force-Velocity Relationship of Muscles Performing Multi-Joint Maximum Performance Tasks. *Int. J. Sports Med.* 2015, 36, 699–704. [CrossRef]
33. Perrine, J.J.; Edgerton, V.R. Muscle Force-Velocity and Power-Velocity Relationships under Isokinetic Loading. *Med. Sci. Sports* 1978, 10, 159–166. [CrossRef]
34. Bosco, C.; Mogroni, P.; Luhtanen, P. Relationship between Isokinetic Performance and Ballistic Movement. *Eur. J. Appl. Physiol. Occup. Physiol.* 1983, 51, 357–364. [CrossRef] [PubMed]
35. Henneman, E.; Somjen, G.; Carpenter, D.O. Functional Significance of Cell Size in Spinal Motoneurons. *J. Neurophysiol.* 1965, 28, 560–580. [CrossRef] [PubMed]
36. Kawai, E.; Tsunokawa, T.; Sakaue, H.; Takagi, H. Propulsive Forces on Water Polo Players' Feet from Eggbeater Kicking Estimated by Pressure Distribution Analysis. *Sports Biomech.* 2020, 1–15. [CrossRef]



Contents lists

Journal of Biomechanics

journal

www.elsevier.com/locate/ibio
www.JBiomech.com



Front crawl stroke in swimming: Phase durations and self-similarity

C.M. Verrelli ^a, C. Romagnoli ^{b,c}, R.R. Jackson ^d, I. Ferretti ^e, G. Annino ^{e,f}, V. Bonaiuto ^c

^a Electronic Engineering Department of the University of Rome Tor Vergata, Via del Politecnico 1, 00133 Rome, Italy ^b Department for Life Quality Studies, University of Bologna, 47900 Rimini, Italy ^c Sport Engineering Lab - Department of Industrial Engineering, University of Rome Tor Vergata, 00133 Rome, Italy ^d Institute of Automation Technology, Otto-von-Guericke University Magdeburg, 39106 Magdeburg, Germany ^e Biomechanical and Video-Analysis Area for the National Teams of “Federazione Italiana Nuoto (FIN)”, Italy ^f Department of Medicine Systems, University of Rome Tor Vergata, 00133 Rome, Italy

Article info

Article history:

Accepted

16

January

2021

Available

online

Keywords:

Front crawl swimming

Self-similarity

Golden ratio

Fibonacci sequence

Abstract

Human movements, such as walking and running, are able to generate rhythmic motor patterns, with the consequent appearance of hidden time-harmonic structures. Such harmonic structures are represented (at comfortable speed) by the occurrence of the golden ratio as ratio of durations of specific walking and running gait sub-phases. Preliminary experimental evidences suggest that front crawl swimming may behave, under this point of view, like walking and running. This paper aims to demonstrate that a mathematical connection between the golden ratio and the front crawl swimming stroke actually exists, at a pace that plays the role of the comfortable speed in walking and running. Generalized Fibonacci sequences are used to this purpose. They rely on the durations of aggregate phases of the front crawl swimming stroke with a clear physical meaning, while characterizing self-similarity of front crawl strokes in its simple nature and enhanced (stronger) variant. Experimental data on front crawl swimmers illustrate the theoretical derivations, suggesting that the pace playing the role of the comfortable speed in walking and running is the middle/long-distance one, while showing that the self-similarity level increases with the swimming technique and the enhanced self-similarity is associated with the performance of top-level swimmers.

Phi-Bonacci Butterfly Stroke Numbers to Assess Self-Similarity in Elite Swimmers

Cristiano Maria Verrelli^{1,*}, **Cristian Romagnoli**^{2,3}, **Roxanne Jackson**⁴, **Ivo Ferretti**⁵, **Giuseppe Annino**^{3,6,7}
and **Vincenzo Bonaiuto**³

¹ Department of the Electronic Engineering, University of Rome Tor Vergata, via del Politecnico 1, 00133 Rome, Italy

² Department for Life Quality Studies, University of Bologna, 47900 Rimini, Italy; cristian.romagnoli2@unibo.it

³ Sport Engineering Lab, Department of Industrial Engineering, University of Rome Tor Vergata, 00133 Rome, Italy; g-annino@hotmail.com (G.A.); vincenzo.bonaiuto@uniroma2.it (V.B.)

⁴ Institute of Automation Technology, Otto-von-Guericke University Magdeburg, 39106 Magdeburg, Germany; roxanne.jackson@ovgu.de

⁵ Biomechanical and Video-Analysis Area for the National Teams of “Federazione Italiana Nuoto (FIN)”, 00100 Rome, Italy ; ferrivo@libero.it

⁶ Department of Medicine Systems, University of Rome Tor Vergata, 00133 Rome, Italy

⁷ “Centro di Biomedicina Spaziale”, University of Rome Tor Vergata, 00133 Rome, Italy

* Correspondence: verrelli@ing.uniroma2.it; Tel.: +39-(0)6-72597410

Received: 21 May 2021

Accepted: 22 June 2021

Published: 1 July 2021

Abstract: A harmonically self-similar temporal partition, which turns out to be subtly exhibited by elite swimmers at middle distance pace, is formally defined for one of the most technically advanced swimming strokes—the butterfly. This partition relies on the generalized Fibonacci sequence and the golden ratio. Quantitative indices, named ϕ -bonacci butterfly stroke numbers, are proposed to assess such an aforementioned hidden time-harmonic and self-similar structure. An experimental validation on seven international-level swimmers and two national-level swimmers was included. The results of this paper accordingly extend the previous findings in the literature regarding human walking and running at a comfortable speed and front crawl swimming strokes at a middle/long distance pace.

Keywords: generalized Fibonacci sequence; self-similarity; golden ratio; butterfly swimming; elite swimmers

1. Introduction

Fibonacci numbers play crucial roles in combinatorial mathematics and elementary number theory. Although such numbers have been investigated for centuries, they continue to intrigue mathematicians and researchers in many areas of human endeavour (as can be seen in [1] and the references therein), while providing new tools for expanding the frontiers of mathematical study. In respect to this, the golden ratio $\varphi \approx 1.61803$, namely the positive solution to the equation $x^2 = 1 + x$, appears in some very fundamental relationships involving numbers, with one of the most basic occurrences of the golden ratio involving the use of two seed values and a simple Fibonacci-like additive recursion relationship.

Walking and running are human gait modes exhibiting different mechanics and energetics. A double support phase, i.e., both limbs are in ground contact, identifies the walking gait, whereas a double float phase, i.e., no limb is in ground contact, identifies the running gait. However, both physiological (symmetric and recursive) human walking and running are characterized, from a temporal point of view, by only four specific time intervals, associated with the durations of gait cycle, swing, stance and double support (double float) phases. More precisely, physiological symmetric walking (running) is classically recognized to exhibit:

- A stance (swing) duration, t_{ST} (t_{SW}), being close to 62% of gait cycle duration t_{GC} ;
- A swing (stance) duration being close to 38% of gait cycle duration;
- A double support (double float) duration, t_{DS} (t_{DF}), being consequently close to 24% of gait cycle duration.

As recently formally recognized in [2], the above sequence $\{0.24, 0.38, 0.62, 1\}$ can be viewed as a slight approximation of the special sequence in walking:

$$\Sigma : \{t_{DS}/t_{GC}, t_{SW}/t_{GC}, t_{ST}/t_{GC}, 1\} = n1/\varphi^3, 1/\varphi^2, 1/\varphi, 1 \quad (1)$$

and its conceptual counterpart in running:

$$\Sigma : \{t_{DF}/t_{GC}, t_{ST}/t_{GC}, t_{SW}/t_{GC}, 1\} = n1/\varphi^3, 1/\varphi^2, 1/\varphi, 1 \quad (2)$$

The above sequence Σ is nothing but a generalized four-length Fibonacci sequence [3] (with the real numbers $1/\phi^3$, $1/\phi^2$ as seeds), generally defined, for any values γ and δ , by (ψ is the negative solution to $x^2 = 1 + x$):

$$U_n = \gamma\phi^n + \delta\psi^n \quad (3)$$

satisfying the recurrence:

$$U_n = \gamma\phi^{n-1} + \delta\psi^{n-1} + \gamma\phi^{n-2} + \delta\psi^{n-2} = U_{n-1} + U_{n-2} \quad (4)$$

Regarding Σ : (i) the general Fibonacci sequence structure is rooted in the following duration constraints of symmetric walking (and running, respectively): $t_{DS} + t_{SW} = t_{ST}$ (respectively, $t_{DF} + t_{ST} = t_{SW}$), $t_{SW} + t_{ST} = t_{GC}$; (ii) the specific ϕ -dependent (temporally harmonic) self-similar structure relies on the special chain of ratios $t_{SW}/t_{DS} = t_{ST}/t_{SW} = t_{GC}/t_{ST}$ (respectively, $t_{ST}/t_{DF} = t_{SW}/t_{ST} = t_{GC}/t_{SW}$) all being equal to ϕ . Indeed, $1/\phi^3 \approx 0.23608$, $1/\phi^2 \approx 0.38198$, $1/\phi \approx 0.61804$. In other words, conditions in (i)–(ii) apparently induce a repeated self-proportional partition (namely self-similarity), in accordance with the fact that two quantities are in the golden ratio if their ratio is the same as the ratio of their sum to the larger of the two quantities. This way, walking and running implicitly involve a fractal nature, in which the structure of the larger scale resembles the structure of the sub-unit and in which one of the simplest ways of transformation, i.e., the new domain composed of two previous ones, is highlighted. Very recent experimental and theoretical analyses—inspired by the aforementioned cyclic human movements in walking and running (see also [4,5])—have found harmonic structures to even appear in front crawl swimming [6] at a middle/long distance pace, at which the presence of redundant movements is reduced via in-phase synchronization with the induced waves in the water. With respect to this, the recent paper [6] not only provides a mathematical framework and experimental consistency for recognizing preliminary evidence, for elite front-crawl swimmers swimming at a middle/long distance pace, a recovery phase duration that is very close to the fundamental unit $3u_f$ (where u_f is equal to the duration of the front crawl stroke divided by 12) but it also illustrates the existence of harmonic structures—in both their simple and enhanced

versions—that elite swimmers seek to reproduce in order to improve their performance. We also refer the reader to [7,8] for a different scenario involving the dimensionless Strouhal number.

A more technically advanced swimming stroke is the butterfly. Simultaneous strokes, such as breaststroke and butterfly, are in fact considered to be highly technical due to the complex coordination of the arm and leg actions [9]. In particular, in butterfly, the out of water arms recovery is facilitated by the leg undulation. To be effective, however, the kick must appear as a consequence of a body wave-like cefalo–caudal undulation motion [10]. Having a glide time with the arms extended forward at the top of the stroke is certainly a strategy used to reduce the energetic cost (metabolic power/velocity) for long-distance swims [11]. This way, the head, trunk and upper limbs are profiled in a streamlined position in order to glide, and consequently, provide some rest at each stroke during a long butterfly swim (some aquatic animals such as giant cormorants, penguins, and dolphins improve the metabolic efficiency of swimming by adopting locomotion patterns with alternating periods of propulsion and gliding [10]). However, this is not effective for achieving a higher stroke rate [10] and for avoiding great instantaneous velocity fluctuations. On the other hand, when velocity and stroke rate increase, coordination becomes closer to an in-phase mode [12,13], just like in human locomotion and in quadrupedal coordination. Indeed, the significant skill effect in [10] indicates that elite swimmers—whom are the object of analysis in this paper—have stronger arm/leg synchronization than the sub-elite swimmers: elite swimmers adopt a shorter glide to overcome great forward resistance and generate higher forces during the arm pull; sub-elite swimmers often compensate for coordination mistakes by applying greater force. With respect to this, we also refer the reader to [14]—for devices performing propulsion analysis in swimming; [15]—for a quantitative evaluation of phases of turns during competition; and [16]—for the role of the hip movement in the stroke mechanics.

The aim of this paper was to extend, for the first time in the literature—to the best of our knowledge—the aforementioned findings regarding human walking and running at comfortable speed and front

crawl swimming strokes at a middle/long distance pace: a harmonically self-similar temporal partition, which relies on the generalized Fibonacci sequence and the golden ratio, is formally defined for the highly complex and upper and lower-limbs-coordinated butterfly stroke. Quantitative indices, named ϕ -bonacci butterfly stroke numbers, are accordingly proposed to assess such a hidden time-harmonic and self-similar structure being subtly exhibited by elite swimmers at middle distance pace.

2. Generalized Fibonacci Sequences in Butterfly Stroke

This section presents the main result of the paper.

2.1. Butterfly Stroke Phases

Different arm and leg phases (see Figure 1) can be identified in a butterfly stroke S with duration t_S , here characterized by two leg undulations for one arm stroke [10,12,17]. They are in order, for the arms:

- (i) Entry and catch phase (between the entry of the hands into the water and the beginning of their backward movement), with duration t_{EC} ;
- (ii) Pull phase (between the beginning of the backward movement of the hands and their entry into the plane vertical to the shoulders), with duration t_{PL} ;
- (iii) Push phase (between the positioning of the hands below the shoulders and their exit from the water), with duration t_{PS} ;
- (iv) Recovery phase (between the arrival of the hands at the water level and their subsequent entry into the water), with duration t_{RE} ,

and for the legs:

- (i) Downward phase 1 (between the high and low break-even points– at first occurrence–of the feet during the first undulation), with duration t_{K1} ;

- (ii) Upward phase 1 (between the low and high break-even points—at first occurrence—of the feet during the first undulation), with duration t_{U1} ;
- (iii) Downward phase 2 (between the high and low break-even points—at first occurrence—of the feet during the second undulation), with duration t_{K2} ;
- (iv) Upward phase 2 (between the low and high break-even points—at first occurrence—of the feet during the second undulation), with duration t_{U2} .

The inter-limb coordination of such phases is governed by the time delays (with a positive or negative sign):

- T_1 , between the start of Entry and catch phase and the start of Downward phase 1;
- T_2 , between the start of Pull phase and the start of Upward phase 1;
- T_3 , between the start of Push phase, and the start of Downward phase 2;
- T_4 , between the start of Recovery phase, and the start of Upward phase 2.

As shown in [10], elite swimmers show a smaller total time gap, taken as the sum—expressed as the percentage of a complete stroke—of the absolute values of T_1 , T_2 , T_3 , T_4 and used to assess the effectiveness of the global arm–leg coordination.

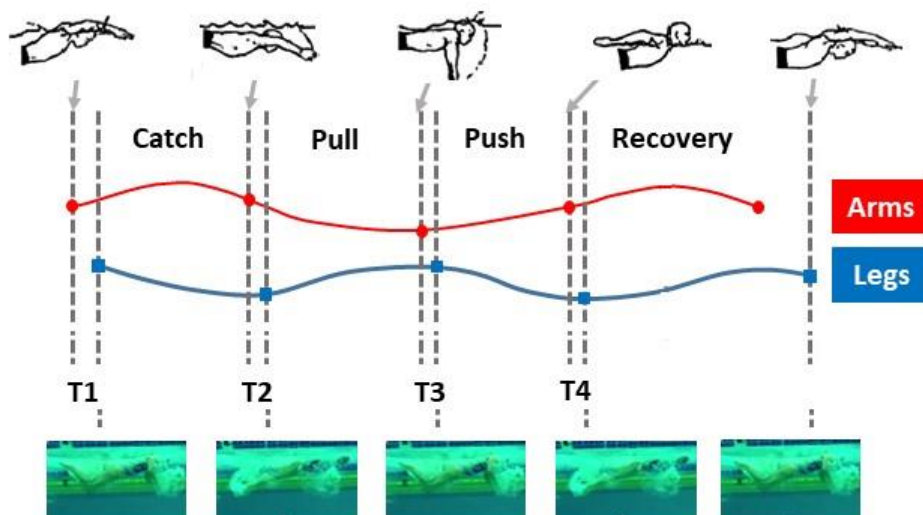


Figure 1. Butterfly stroke: arm and leg phases (case of $T_2, T_3, T_4 > 0$) according to [12].

2.2. Self-Similarity and Enhanced Self-Similarity in Butterfly Stroke

We first define the *repetitive butterfly stroke*, in which T_1 of the subsequent stroke equals T_1 of the stroke under investigation, so that the arm stroke (namely from the start of Entry and catch phase to the start of the subsequent Entry and catch phase) equals the leg stroke (namely, from the start of Downward phase 1 to the start of the subsequent

Downward phase 1). A repetitive butterfly stroke that is characterized by its values

$(T_1/t_S = a [\%], T_2/t_S = b [\%], T_3/t_S = c [\%], T_4/t_S = d [\%])$ is denoted hereafter by

(a, b, c, d) -repetitive butterfly stroke. We then define an (a, b, c, d) -repetitive butterfly stroke that is *kick-to-kick temporal symmetric* by imposing the equality of the Upward phase 1 and Upward phase 2 durations:

$$t_{U1} = t_{U2} + T_1 \quad (5)$$

Furthermore, a *highly coordinated (a, b, c, d) -kick-to-kick temporal symmetric repetitive butterfly stroke* is an (a, b, c, d) -kick-to-kick temporal symmetric repetitive butterfly stroke that exhibits a relatively small positive value for the normalized total delay:

$$NTD = \sqrt{a^2 + b^2 + c^2 + d^2} [\%] \quad (6)$$

In light of [6], a self-similar partition in highly coordinated (a, b, c, d) -kick-to-kick temporal symmetric repetitive butterfly strokes is presented hereafter.

Theorem 1. (F_4): In a highly coordinated (a, b, c, d) -kick-to-kick temporal symmetric repetitive butterfly stroke, the sequence:

$$F_4 : [t_{K1} + t_{K2}, t_{U1}, t_{K1} + t_{K2} + t_{U1}, t_S] \quad (7)$$

is a generalized Fibonacci sequence of length 4. If $t_{U1}/(t_{K1} + t_{K2}) = f$, then the chain of inequalities:

$$\frac{t_{K1} + t_{K2} + t_{U1}}{t_{U1}} = \frac{t_S}{t_{K1} + t_{K2} + t_{U1}} = \phi \quad (8)$$

holds and the sequence F_4 in (7) has a self-similar structure, with $t_{K1} + t_{K2} + t_{U1} \approx 61.804\%$ of t_S , $t_{U1} \approx 38.198\%$ of t_S and $t_{K1} + t_{K2} \approx 23.608\%$ of t_S .

Proof. As in [6], the sequence F_4 is represented through the discrete-time system:

$$y(k+2) = y(k+1) + y(k), k = 0, 1, \quad (9)$$

with $y(0) = t_{K1} + t_{K2}$, $y(1) = t_{U1}$ and $y(2) = t_S - t_{U2}$, $y(3) = t_S$. Then, it suffices to write the solution to its state-space description:

$$\zeta(k+1) = M_\zeta \zeta(k), k = 0, 1 \quad (10)$$

as

$$\zeta(1) = M_\zeta \zeta(0), \quad (11)$$

$$\zeta(2) = M^2 \zeta(0) \quad (12)$$

with $\zeta(l)$ being the vector $[y(l), y(l+1)]^T$, $l = 0, 1, 2$, and $M = [0, 1; 1, 1]$ with distinct eigenvalues φ , $1 - \varphi$ and orthogonal eigenvectors ($c_\varphi = (1 + \varphi^2)^{-1/2}$):

$$v_\varphi = c_\varphi [1, \varphi]^T, v_{1-\varphi} = c_\varphi [\varphi, -1]^T. \quad (13)$$

The following theorem characterizes a stronger self-similarity property, referred to as *enhanced self-similarity*. It relies on the following constraint (When $t_{K2} > t_{K1}$, it suffices to switch t_{K1} and t_{K2} in the C-constraint, in the sequence of Corollary 1 (including Remark (F7)), in the corresponding index (24), and in the fourth comment Section 4):

$$C : t_{U1} = t_{K1} + 2t_{K2} \quad (14)$$

Theorem 2. (F6): In a highly coordinated (a, b, c, d) -kick-to-kick temporal symmetric repetitive butterfly stroke under C, the sequence (7) enforced with $\{t_{K1}, t_{K2}\}$ to the left, meaning that:

$$F_6 : \{t_{K1}, t_{K2}, t_{K1} + t_{K2}, t_{U1}, t_{K1} + t_{K2} + t_{U1}, t_S\}, \quad (15)$$

is a generalized Fibonacci sequence of length 6. The equality $t_{U1}/(t_{K1} + t_{K2}) = \phi$ makes the sequence F_6 possess an enhanced self-similar structure, with $t_{K1} + t_{K2} + t_{U1} \approx 61.804\%$ of t_S , $t_{U1} \approx 38.198\%$ of t_S , $t_{K1} + t_{K2} \approx 23.608\%$ of t_S , $t_{K2} \approx 14.591\%$ of t_S , $t_{K1} \approx 9.0175\%$ of t_S .

Proof. Sequence F_6 can be represented by the discrete-time system:

$$y(k+2) = y(k+1) + y(k), \quad k = 0, 1, 2, 3, \quad (16)$$

with initial conditions $y(0) = t_{K1}$, $y(1) = t_{K2}$ and $y(2) = t_{K1} + t_{K2}$, $y(3) = t_{U1}$, $y(4) = t_{K1} + t_{K2} + t_{U1}$, $y(5) = t_S$. The previous analysis carried out in the proof of Theorem 1 can be extended to cover the generalized 6-length Fibonacci sequence case. In particular, the state-space representation of the system above reads:

$$\zeta(k+1) = M_\zeta \zeta(k), \quad k = 0, 1, 2, 3, \quad (17)$$

with $\zeta(l) = [y(l), y(l+1)]^T$, $l = 0, 1, 2, 3, 4$, and M as in the proof of Theorem 1. We now explicitly write:

$$\begin{bmatrix} y(2) \\ y(3) \end{bmatrix} = \phi^2 \beta v_\phi + (1-\phi)^2 \alpha v_{(1-\phi)} \quad (18)$$

$$\begin{bmatrix} y(3) \\ y(4) \end{bmatrix} = \phi^3 \beta v_\phi + (1-\phi)^3 \alpha v_{(1-\phi)} \quad (19)$$

$$\begin{bmatrix} y(4) \\ y(5) \end{bmatrix} = \phi^4 \beta v_\phi + (1-\phi)^4 \alpha v_{(1-\phi)} \quad (20)$$

in terms of

$$\alpha = \langle \zeta(0), v_{(1-\phi)} \rangle = (\phi y(0) - y(1)) c_\phi \quad (21)$$

$$\beta = \langle \zeta(0), v_\phi \rangle = (y(0) + \phi y(1)) c_\phi = (1 + \phi^2) c_\phi y(0) \quad (22)$$

When α is equal to zero, i.e., the initial vector $\zeta(0)$ has no components along the $v_{(1-\phi)}$ direction, $y(1)/y(0) = \phi$ holds and $y(2)/y(1) = \phi$, $y(3)/y(2) = \phi$, $y(4)/y(3) = \phi$, $y(5)/y(4) = \phi$ hold too.

Remark 1. (F₇): *In the very special case of $T_1 = t_{K2} - t_{K1}$ for the highly coordinated (a, b, c, d) kick-to-kick temporal symmetric repetitive butterfly stroke, the sequence (15), once enforced with T_1 to the left, becomes a generalized Fibonacci sequence of length 7, with the equality $t_{U1}/(t_{K1} + t_{K2}) = \varphi$ making the sequence F_7 possess a strongly enhanced self-similar structure; $T_1 \approx 5.5735\%$ of t_S is additionally obtained.*

2.3. Quantitative Measures of Self-Similarity and Enhanced Self-Similarities

Two indices $I_{f,4}, I_{f,6}$ —named *φ -bonacci butterfly stroke number* and *enhanced φ -bonacci butterfly stroke number*—can be naturally introduced, in order to quantitatively assess selfsimilarity or enhanced self-similarities of *highly coordinated (a, b, c, d) -kick-to-kick temporal symmetric repetitive butterfly strokes*. They are, in order:

$$I_{f,4} = 100 \left(\frac{t_{K1} + t_{K2} + t_{U1}}{t_S} - 0.62 \right)^2 + \left(\frac{t_{U1}}{t_S} - 0.38 \right)^2 + \left(\frac{t_{K1} + t_{K2}}{t_S} - 0.24 \right)^2 \quad (23)$$

$$I_{f,6} = 100 \left(\frac{t_{K1} + t_{K2} + t_{U1}}{t_S} - 0.62 \right)^2 + \left(\frac{t_{U1}}{t_S} - 0.38 \right)^2 + \left(\frac{t_{K1} + t_{K2}}{t_S} - 0.24 \right)^2 + \left(\frac{t_{K2}}{t_S} - 0.14 \right)^2 + \left(\frac{t_{K1}}{t_S} - 0.10 \right)^2 \quad (24)$$

where the values 0.62, 0.38, 0.24, 0.14, 0.10 are used to approximate 0.61804, 0.38198, 0.23608, 0.14591, 0.090175 of Theorem 1 and Theorem 2, respectively. The smaller such indices are, the stronger the self-similarity is. The just self-similarity of Theorem 1 may clearly lead to a non-zero value for $I_{f,6}$ that tends towards zero when the self-similarity tends to turn into the enhanced self-similarity.

3. Experimental Analysis

The feasibility of the preceding analysis is here illustrated by the dedicated analysis of butterfly stroke training sessions for: (i) seven international-level swimmers, namely IL1 (male, 31 y, 190 cm, 80 kg), IL2 (female, 31 y, 170 cm, 65 kg), IL3 (female, 27 y, 168 cm, 58 kg), IL4 (male, 20 y, 196 cm, 80 kg), IL5 (male, 19 y, 180 cm, 73 kg), IL6 (male, 19 y, 193 cm, 85 kg), IL7 (female, 27 y, 173 cm, 66 kg); (ii) two national-level swimmers, namely, NL1 (female, 19 y, 166 cm, 55 kg), NL2 (male, 25 y, 185 cm, 95 kg), all of them swimming at their own middle-distance pace. In particular, the above international-level swimmers and national level swimmers are reported, within the corresponding sets, in order of physical shape (measured as race performance capabilities) at the moment of data acquisition. While the international-level swimmers IL1–IL7 compete at major international events on a regular basis and hold national/international records, the national-level swimmers NL1–NL2 are national medallists who compete on a regular basis of major national events (with NL1 being close to becoming an international-level swimmer). The analysis was performed by using high frame rate videos (100 for IL1, NL2; 120 fps for IL2–IL7, NL1) of stable strokes via the 2D BioMovie ERGO system at <http://www.infolabmedia.eu/> (accessed on 7 June 2021).

3.1. Phase Durations and Interlimb Coordination

Phase and delay durations for all the swimmers IL1–IL7, NL1–NL2 are reported in Tables 1–4: (a, b, c, d) -(almost) kick-to-kick temporal symmetric repetitive butterfly strokes S (under constraints C) are exhibited (Kick-to-kick temporal symmetry appears to be almost verified for IL1–IL7, NL1–NL2, with the modulus of the difference between t_{U1} and $t_{U2} + T1$ belonging to the set [5, 67] ms. Constraint C even appears to be almost verified for IL1–IL7, NL1–NL2, with the modulus of the difference between t_{U1} and $t_{K1} + 2t_{K2}$ belonging to the set [1, 81] ms.), characterized by the (a, b, c, d)- and NTD-values reported in Tables 3 and 4. In accordance with the evidence of [10] on elite swimmers, all of such relatively small NTDs define highly coordinated strokes. All nine swimmers' strokes exhibit a negative delay T2 (leading to a lag time in glide position) and a positive delay T3. On the other hand, in contrast to the international-level swimmers IL1, IL3–IL6, the international-

level swimmers IL2, IL7 and the national-level swimmers NL1, NL2 are characterized by a small negative superposition of two contradictory actions ($T_1 < 0$). Furthermore, $T_4 = 0$ for NL1, whereas T_4 is negative for IL1–IL7 and NL2.

Table 1. Experimental data for swimmers IL1–IL7 and NL1–NL2: arm phase durations (in seconds).

	t_{EC}	t_{PL}	t_{PS}	t_{RE}	t_S
IL1	0.220	0.220	0.270	0.440	1.150
IL2	0.233	0.183	0.316	0.333	1.065
IL3	0.308	0.158	0.266	0.333	1.065
IL4	0.375	0.200	0.258	0.407	1.240
IL5	0.291	0.291	0.250	0.400	1.232
IL6	0.300	0.283	0.333	0.367	1.283
IL7	0.234	0.175	0.358	0.417	1.184
NL1	0.266	0.166	0.308	0.326	1.066
NL2	0.220	0.150	0.200	0.330	0.900

Table 2. Experimental data for swimmers IL1–IL7 and NL1–NL2: leg phase durations (in seconds).

	t_{K1}	t_{K2}	t_{U1}	t_{U2}	t_S
IL1	0.120	0.160	0.420	0.450	1.150
IL2	0.108	0.166	0.400	0.466	1.065
IL3	0.125	0.150	0.391	0.383	1.065
IL4	0.133	0.191	0.441	0.450	1.240
IL5	0.120	0.141	0.483	0.430	1.232
IL6	0.150	0.166	0.517	0.417	1.283
IL7	0.150	0.158	0.467	0.475	1.184
NL1	0.108	0.183	0.417	0.408	1.066
NL2	0.120	0.140	0.330	0.330	0.900

Table 3. Delays and related values for swimmers IL1–IL7 and NL1–NL2: delay durations (in seconds) and NTD.

	T_1	T_2	T_3	T_4	NTD
IL1	0.000	-0.100	0.100	-0.010	12.320%
IL2	-0.075	-0.200	0.017	-0.133	23.680%
IL3	0.016	-0.167	0.066	-0.050	17.570%
IL4	0.025	-0.217	0.024	-0.043	18.060%
IL5	0.058	-0.113	0.079	-0.030	12.380%
IL6	0.033	-0.117	0.117	-0.050	13.720%
IL7	-0.066	-0.150	0.142	-0.058	18.960%
NL1	-0.050	-0.208	0.043	-0.082	21.860%
NL2	-0.020	-0.120	0.060	0.000	15.070%

Table 4. Delays and related values for swimmers IL1–IL7 and NL1–NL2: (a, b, c, d)-values.

	<i>a</i>	<i>b</i>	<i>c</i>	<i>d</i>
IL1	0.00%	−8.69%	8.69%	−0.87%
IL2	−7.04%	−18.78%	1.60%	−12.49%
IL3	1.50%	−15.68%	6.20%	−4.69%
IL4	2.02%	−17.50%	1.94%	−3.47%
IL5	4.71%	−9.17%	6.41%	−2.44%
IL6	2.57%	−9.12%	9.12%	−3.90%
IL7	−5.57%	−12.67%	11.99%	−4.90%
NL1	−4.69%	−19.51%	4.03%	−7.69%
NL2	−2.22%	−13.33%	6.67%	0.00%

3.2. Self-Similarity Analysis

The aggregate phase percentage values for the international-level swimmers IL1–IL7 and the national-level swimmers NL1–NL2 are reported in Tables 5 and 6, along with the values for the indices $I_{f,4}$ and $I_{f,6}$ in (23) and (24). Comments are in order:

- Rather small values are obtained for IL1–IL7, with IL1’s one being the smallest, owing to the strict closeness of the corresponding phase percentage values to 62%, 38%, 24%, 14%, and 10%;
- Relatively large reductions in the self-similarity and enhanced self-similarity magnitudes (especially of the latter) appear for the national-level swimmers NL1–NL2 when compared to the international-level swimmers IL1–IL7;
- The $I_{f,4}$ - and $I_{f,6}$ - values turn out to reproduce the order of physical shape within the two swimmers’ set;
- IL5 even presents an $a = T_1/t_S$ -value (4.71%) that is close to the one (5.57%) characterizing the strongly enhanced self-similar structure of Remark (F7);
- The slight differences in the phase durations of Tables 1 and 2 (compare, for instance, IL2 to NL1, or IL4 to IL5, or IL2 to IL3), which lead to the differences in self-similarity magnitudes of

Tables 5 and 6, have been successfully identified via the high frame rate analysis used in this paper, with the self-similarity information complementing the delay partition values of Tables 3 and 4;

- Larger percentage reductions in enhanced self-similarity (with respect to self-similarity) are exhibited by IL2, IL3, IL5—when compared to IL1, IL4, IL5, IL6, NL1, NL2—so that the $I_{f,6}$ - values for IL2–IL3 and IL5 tend to thicken (more than the $I_{f,4}$ -ones) towards the $I_{f,6}$ - values for IL4 and IL6, respectively.

Table 5. Data analysis for swimmers IL1–IL7 and NL1–NL2: aggregate phases (percentage values).

	$(tk_1 + tk_2 + tu_1)/ts$	tu_1/ts	$(tk_1 + tk_2)/ts$	tk_2/ts	tk_1/ts
IL1	60.87	36.52	24.35	13.91	10.43
IL2	63.29	37.56	25.73	15.59	10.14
IL3	62.54	36.71	25.82	14.08	11.74
IL4	61.69	35.56	26.13	15.40	10.73
IL5	60.39	39.20	21.19	11.44	9.74
IL6	64.93	40.30	24.63	12.94	11.69
IL7	65.46	39.44	26.01	13.34	12.67
NL1	66.42	39.12	27.30	17.17	10.13
NL2	65.56	36.67	28.89	15.56	13.33

Table 6. Data analysis for swimmers IL1–IL7 and NL1–NL2: values of indices (23) and (24).

	$I_{f,4}$	$I_{f,6}$
IL1	1.89	1.94
IL2	2.20	2.72
IL3	2.30	2.88
IL4	3.25	3.61
IL5	3.45	4.31
IL6	3.78	4.27
IL7	4.25	5.06
NL1	5.63	6.46
NL2	6.19	7.20

4. Discussion

By following up the direction highlighting the connections of human walking and running gaits and front crawl swimming strokes with the generalized Fibonacci sequences and golden ratio, this paper aimed to provide an answer to the question regarding the existence of subtle and unveiled self-similar structures at the root of the butterfly stroke of elite swimmers, for whom—as in dolphins and fish

[18]—energy accrued by raising the upper body is transmitted along the body through wave-like movements [19]. Harmonically characterizing butterfly strokes through self-similarity—in both its simple and enhanced versions—and the φ -bonacci butterfly stroke numbers constitutes the original contribution of this paper, as a relevant application of computational number theory involving generalized Fibonacci sequences.

When compared to the front crawl scenario of [6] (concerning the arm stroke):

- Theorem 1 and Theorem 2 provide partition constraints that regard the leg stroke, with the inter-delay composition linking the arm phase partition with the leg phase partition;
- The four-length generalized Fibonacci sequence F_4 of Theorem 1 is generated by $t_{K1} + t_{K2}$, which plays the role of the recovery phase duration in the front crawl of [6] and of the double support (double float) duration in walking (running) of [2];
- The durations t_{U1} and $t_{U2} + T_1$ play the role of t_{Fa} and t_{Fb} in the front crawl stroke in [6] and of the right and left swing (right and left stance) durations in the asymmetric walking (running) of [2,5], with the involved equality between the durations of such phases simply transposing the swing (stance)-symmetry constraint of symmetric walking (running);
- In light of the twelve-tone equal temperament-based interpretation, constraint C imposes that the stroke duration t_S of an (a, b, c, d) -kick-to-kick temporal symmetric repetitive butterfly stroke equals the sum of the durations of eight disjoint sub-phases, three among them with duration t_{K1} and five among them with duration t_{K2} : according to [6], notes D4, E4, G4, C5 correspond, in the (suspended and restored) C-variant Cadd2-chord, to the frequencies: $f_{3(D4)} = f_0 2^{\frac{3}{12}} = 293.7 \text{ Hz}$, $f_{5(E4)} = f_0 2^{\frac{5}{12}} = 329.6 \text{ Hz}$, $f_{8(G4)} = f_0 2^{\frac{8}{12}} = 391.96 \text{ Hz}$, $f_{13(C5)} = f_0 2^{\frac{13}{12}} = 2f_1(C4) = 523.2 \text{ Hz}$ ($f_0 = 246.9175 \text{ Hz}$), with $n = 3, 5, 8, 13$ corresponding to elements of a Fibonacci sequence and with the ratios $5/3 \approx 1.667$, $8/5 = 1.6$, $13/8 = 1.625$ of consecutive elements of such sequence quickly getting close to φ ;

- The above results—again occurring in elite swimmers—confirm that, in contrast to walking, a precise swimming technique (coming from a considerable amount of practice and instruction repeating specifically precise movements for a long enough time, while producing rhythmic motor patterns through the interrelationship between cortical input, central pattern generator (CPG), and sensory feedback) is relevantly involved (the intra-cyclic variation of the horizontal velocity of the hip is larger in non-expert swimmers than their expert counterparts [20]) as recalled by [6], the fractal dimension is 1.8–1.9 for highly qualified expert swimmers [20], whereas it is 1.1–1.4 for on-land walking [21].

5. Practical Implications

Self-similarity, as defined in this paper, may become a reference point in the formulation of advanced training programs (on the basis of (23), (24)) for elite swimmers, while: (i) going beyond the evaluation of the inter-limb synchronicity level, classically used to assess the performance of high-level butterfly stroke swimmers; and (ii) not affecting the peculiar stroke duration of the swimmer. It is clear that improvements of the muscle strength remain valid as well, but at a different level of analysis. The findings of this paper might also provide comparative (quantitative) information about: (i) the physical recovery level of the swimmer after a hard and intense workout; (ii) the conditioning of the rhythmic neural patterns of the swimmer during the contingent-moment-based swimming actions; and (iii) the swimmers' improvements over time and the necessary correction actions to improve the performance. Indeed, at a high-level, at which inter-individual coordination variability reduces to a narrow range of movement variants [20], each small change that a practitioner may perform might lead to a relevant change in the dynamic interaction of the systems components [22].

6. Strengths and Limits

The derivations of this paper seem to provide meaningful information about both the swimmer's level and physical shape, which complement the analysis of the normalized total delay. The results of this

paper also seek to open new research directions aiming to connect computational number theory (involving generalized Fibonacci sequence) to human neural system modulating principles at the root of highly effective cyclic rhythmic patterns of swimming. Anyway, the results of the present study should be interpreted with caution, owing to its specific limits, such as: (i) the small size of the samples enrolled in the experiments; and (ii) the dependence on high-frame rate analyses. Many aspects should be further investigated in future studies. One of them relies on the fact that the present analysis is focused on the proportions among the stroke phases, limiting this type of analysis to temporal features. Furthermore, it could be certainly interesting to put self-similarity in relationship with the role played by different sensory information in constructing and maintaining the aforementioned stroke harmony.

7. Forecast

It is worth noticing how Figure 3 of [23] (200 m-pace, high-level male swimmer) seems to respect such a self-similar partition in breaststroke, with the arm recovery and the out-sweep phases in place of t_{Fa} , t_{Fb} and the arm in-sweep phase in place of the front crawl stroke recovery phase. On the other hand, we recognized the same self-similar partition in the fourth stroke of the start phase (which accounts for a greater percentage of the race success [24]) in elite sprint kayaking contests, once the sequence generated by $\min \{t_{Ext}, t_{Pull}\}$, $t_{Imm} + \max \{t_{Ext}, t_{Pull}\}$ is considered under the experimentally verified constraint $t_{Rec} - (2t_{Imm} + t_{Pull} + t_{Ext} + \max \{t_{Ext}, t_{Pull}\})$, in terms of the paddle immersion, pull, paddle extraction and recovery phases of the stroke. Analogously, the reader can appreciate in Table 2 and Figure 2 of [25] how, in the forward swing of the forehand tennis stroke (cross court and down the line situations) of elite tennis players, the same self-similar partition can be found owing to: (i) a temporal distance between the instants of maximum racquet rotation angle and maximum hip linear velocity that is almost equal to the temporal distance between the instants of maximum trunk angular velocity and ball impact; (ii) instants of maximum wrist linear velocity and maximum trunk angular velocity that occur at about 24% and 38% of the temporal distance duration between the ball impact and the maximum racquet rotation angle, with these proportions not being exhibited by high-level

tennis players. All of these scenarios seem to suggest that harmonic properties in top-level athletes—possessing talent, natural aptitudes or skills— are an expression of a harmonic rhythm generated by CPG, in which the repetitive proportions of phases act as an attractor for a smooth, efficient, graceful and melodic flow of movements in which different limbs, joints and muscles are controlled at the same time and with a high level of coordination.

8. Conclusions

A temporal partition for the butterfly stroke that is harmonically characterized by Fibonacci sequence-based self-similarity—in both its simple and enhanced versions—was presented and discussed. High frame rate video-based experiments on nine elite swimmers (seven of international level and two of national level) were included. The practical implications, strengths and limits of the analysis were discussed.

Author Contributions: Conceptualization: C.M.V., I.F., V.B., G.A.; Methodology: C.M.V., V.B., G.A., R.J.; Software and Resources: C.M.V., V.B., C.R., I.F.; Formal Analysis: C.M.V.; Validation, Investigation: C.M.V., I.F., V.B., C.R., G.A.; Writing—Original Draft: C.M.V.; Writing—Review and Editing:

C.M.V., V.B., R.J., G.A. All authors have read and agreed to the published version of the manuscript.

Funding: This research received no external funding.

Institutional Review Board Statement: The Internal Research Board (University of Rome Tor Vergata) examined the documentation about this paper and recognized that: it is in accordance with ethical principles for medical research involving human subjects of Declaration of Helsinki; it just assesses motor skills during standard practice routines, while involving no invasive technique.

Informed Consent Statement: Informed consent was obtained from all subjects involved in the study.

Data Availability Statement: No publicly archived datasets were analyzed or generated during the study.

Acknowledgments: The first author is indebted to Marcello Molinari, Technical Director of “New Country Club Frascati” and “Federazione Italiana Tennis (FIT)”– National Master, for drawing attention to the phase partitions of the forehand tennis stroke.

Conflicts of Interest: The authors declare no conflict of interest.

References

1. Chen, L.; Wang, X. The power sums involving fibonacci polynomials and their applications. *Symmetry* **2019**, *11*, 635. [CrossRef]
2. Verrelli, C.M.; Iosa, M.; Roselli, P.; Pisani, A.; Giannini, F.; Saggio, G. Generalized finite-length Fibonacci sequences in healthy and pathological human walking: Gait recursivity, asymmetry, consistency, self-similarity, and variability. In *Frontiers in Human Neuroscience*; Special Issue: Rhythmic Patterns in Neuroscience and Human Physiology; to be published.
3. Horadam, A.F. A generalized Fibonacci sequence. *Am. Math. Mon.* **1961**, *68*, 455–459. [CrossRef]
4. Iosa, M.; Fusco, A.; Marchetti, F.; Morone, G.; Caltagirone, C.; Paolucci, S.; Peppe, A. The golden ratio of gait harmony: Repetitive proportions of repetitive gait phases. *Biomed Res. Int.* **2013**, *2013*, 918642. [CrossRef]
5. Marino, R.; Verrelli, C.M.; Gnucci, M. Synchronicity rectangle for temporal gait analysis: Application to Parkinson’s Disease. *Biomed. Signal Process. Control* **2020**, *62*, 102156. [CrossRef]
6. Verrelli, C.M.; Romagnoli, C.; Jackson, R.R.; Ferretti, I.; Annino, G.; Bonaiuto, V. Front crawl stroke in swimming: Ratios of phase durations and self-similarity. *J. Biomech.* **2021**, *118*, 110267. [CrossRef] [PubMed]
7. Taylor, G.K.; Nudds, R.L.; Thomas, A.L.R. Flying and swimming animals cruise at a Strouhal number tuned for high power efficiency. *Lett. Nat.* **2003**, *425*, 707–711. [CrossRef] [PubMed]

8. Eloy, C. Optimal Strouhal number for swimming animals. *J. Fluids Struct.* **2012**, *30*, 215–218. [CrossRef]
9. Barbosa, T.M.; Keskinen, K.L.; Fernandes, R.; Colaço, P.; Lima, A.B.; Vilas-Boas, J.P. Energy cost and intracyclic variation of the velocity of the centre of mass in butterfly stroke. *Eur. J. Appl. Physiol.* **2005**, *93*, 519–523. [CrossRef]
10. Seifert, L.; Boulesteix, L.; Chollet, D.; Vilas-Boas, J.P. Differences in spatial-temporal parameters and arm–leg coordination in butterfly stroke as a function of race pace, skill and gender. *Hum. Mov. Sci.* **2008**, *27*, 96–111. [CrossRef]
11. Di Prampero, P.E.; Pendergast, D.R.; Wilson, D.W.; Rennie, D.W. Blood Lactic Acid Concentrations in High Velocity Swimming. In *Swimming Medicine IV, Proceedings of the Fourth International Congress on Swimming Medicine, Stockholm, Sweden*; Eriksson, B., Furberg, B., Eds.; University Park Press: Baltimore, MD, USA, 1978; pp. 249–261.
12. Chollet, D.; Seifert, L.; Boulesteix, L.; Carter, M. Arm–leg coordination in elite butterfly swimmers. *Int. J. Sport Med.* **2006**, *27*, 322–329. [CrossRef]
13. Seifert, L.; Delignieres, D.; Chollet, D. Effect of expertise on butterfly stroke coordination. *J. Sport. Sci.* **2007**, *25*, 131–141. [CrossRef] [PubMed]
14. Lanotte, N.; Annino, G.; Bifaretti, S.; Gatta, G.; Romagnoli, C.; Salvucci, A.; Bonaiuto, V. A new device for propulsion analysis in swimming. *Proceedings* **2018**, *2*, 285. [CrossRef]
15. Tourny-Chollet, C.; Chollet, D.; Hogie, S.; Pappardopoulos, C. Kinematic analysis of butterfly turns of international and national swimmers. *J. Sport. Sci.* **2002**, *20*, 383–390. [CrossRef]
16. Mason, B.R.; Tong, Z.; Richards, R.J. A biomechanical analysis of the butterfly stroke. *Excel* **1991**, *7*, 6–11.
17. Chollet, D.; Chalies, S.; Chatard, J.C. A new index of coordination for the crawl: Description and usefulness. *Int. J. Sport. Med.* **1999**, *21*, 54–59. [CrossRef] [PubMed]

18. Ungerechts, B.E. A comparison of the movements of the rear parts of dolphins and butterfly swimmers. In *Biomechanics and Medicine in Swimming*; Hollander, A.P., Huijing, P.A., de Groot, G. , Eds.; Human Kinetics: Champaign, IL, USA, 1983; pp. 215–221.
19. Sanders, R.H.; Cappaert, J.M.; Devlin, R.K. Wave Characteristics of butterfly swimming. *J. Biomech.* **1995**, *28*, 9–16. [CrossRef]
20. Barbosa, T.M.; Goh, W.X.; Morais, J.E.; Costa, M.J. Variation of linear and nonlinear parameters in the swim strokes according to the level of expertise. *Mot. Control* **2017**, *21*, 312–326. [CrossRef]
21. Schiffman, J.M.; Chelidze, D.; Adams, A.; Segala, D.B.; Hasselquist, L. Nonlinear analysis of gait kinematics to track changes in oxygen consumption in prolonged load carriage walking: A pilot study. *J. Biomech.* **2009**, *42*, 2196–2199. [CrossRef] [PubMed]
22. Barbosa, T.M.; Goh, W.X.; Morais, J.E.; Costa, M.J. Comparison of classical kinematics, entropy, and fractal properties as measures of complexity of the motor system in swimming. *Front. Psychol.* **2016**, *7*, 1–7. [CrossRef]
23. Takagi, H.; Sugimoto, S.; Nishijima, N.; Wilson, B. Differences in stroke phases, arm-leg coordination and velocity fluctuation due to event, gender and performance level in breaststroke. *Sport. Biomech.* **2004**, *3*, 15–27. [CrossRef] [PubMed]
24. Ualí, I.; Herrero, A.J.; Garatachea, N.; Marín, P.J.; Alvear-Ordenes, I.; García-López, D. Maximal strength on different resistance training rowing exercises predicts start phase performance in elite kayakers. *J. Strength Cond. Res.* **2012**, *26*, 941–946. [CrossRef] [PubMed]
25. Landlinger, J.; Lindinger, S.; Stöggel, T.; Wagner, H.; Müller, E. Key factors and timing patterns in the tennis forehand of different skill levels. *J. Sport. Sci. Med.* **2010**, *9*, 643–651.

Discussione

La performance sportiva può essere migliorata in diversi modi. Il movimento coinvolge fattori anatomici, abilità neuromuscolari, capacità fisiologiche e abilità psicologiche/cognitive. Per questo motivo lo studio e la valutazione della performance sportiva risultano essere utili al miglioramento e controllo della tecnica, della struttura fisica e delle capacità fisiologiche che rappresentano i fattori limitanti la prestazione. Attraverso l'innovazione tecnologica e l'utilizzo di sempre più frequente di strumentazioni nelle varie discipline sportive, la valutazione funzionale ricopre un ruolo di primaria importanza all'interno della programmazione annuale dell'allenamento e rappresenta lo strumento utile a quantificare, con dati accurati e precisi, i miglioramenti o peggioramenti della prestazione permettendo un'attenta analisi quantitativa e qualitativa del movimento umano [45].

Kayak

Lo sprint flatwater kayak (Kayaking di velocità in acqua piatta) è uno sport in cui l'atleta attraverso l'utilizzo degli arti superiori e la stabilità fornita dagli arti inferiori, durante ogni pagaiata, cerca di coprire la distanza gara (200-500-1000m) assegnata nel più breve tempo possibile. Il canoista per far avanzare il kayak deve generare e applicare sufficiente forza propulsiva per superare le forze di drag che agiscono sul kayak (drag d'onda, frizione e pressione) [64,65]. Per uno studio del movimento risulta quindi fondamentale conoscere sia i parametri cinematici (frequenza di pagaiata, velocità lineare, accelerazione e velocità angolare) che quelli dinamici (forza media, forza propulsiva e potenza) che caratterizzano la prestazione dell'atleta. Sulla base delle richieste di allenatori e atleti, negli ultimi anni, sono emersi diversi sistemi in grado di monitorare e valutare la performance del canoista [66–68], tra cui il sistema E-kayak [7] sviluppato da Aplab di Roma.

Il primo studio proposto (Capitolo 1) presenta l'architettura dell'E-kayak, un nuovo sistema di rete di sensori wireless (WSN) per il flatwater kayak. La rete è composta da un nodo master che può collegare fino a otto nodi periferici (nodi slave), ciascuno è in grado di alloggiare uno o più sensori

diversi. Il numero di nodi può essere aumentato con nodi slave di secondo livello e la natura dei sensori può variare in funzione della specifica applicazione sportiva (piattaforme inerziali, GPS, estensimetro, encoder, potenziometro). L'E-kayak è quindi un sistema di acquisizione digitale multicanale, composto da GPS ad alta frequenza, IMU a 9 assi e una coppia di sensori di forza applicati su puntapiedi e pagaia di ciascuno degli atleti che compone l'equipaggio. Il nodo master sincronizza e gestisce il flusso di dati dai sensori dinamici e l'acquisizione dei dati cinematici dall'IMU e dal GPS.

La comunicazione tra i nodi avviene tramite un ricetrasmittitore da 2,4 GHz ad alte prestazioni e la rete ha una portata superiore qualche metro rendendo possibile l'utilizzo in applicazioni dove la distanza tra i nodi è elevata, ad esempio in sport come il kayak, la vela o il canottaggio. La comunicazione con l'utente (Pc, tablet, smartphone) e il download dei dati avvengono tramite collegamento Wi-Fi. L'interfaccia di comunicazione tra sistema e utente è quindi rappresentata da una pagina web rendendo il sistema completamente indipendente dalla piattaforma utilizzata (computer, tablet, smartphone) e dal suo sistema operativo (Windows, iOS, Android,).

Questo nuovo sistema ha trovato principalmente applicazione nel kayak e il secondo e terzo capitolo ne indagano l'applicabilità e la funzionalità.

Dopo una descrizione dettagliata dei vari sistemi di valutazione, esistenti, per il monitoraggio della performance del paddler (dal 1974 al 2019), sono state indagate la capacità dell'E-kayak. I dati forniti dal sistema (prove effettuate su 50-100 e 150m) sono risultati attendibili (Tabelle 3-4-5, Capitolo 2) (Figura 2, Capitolo 3) dopo aver effettuato il confronto con i parametri disponibili in letteratura ottenuti da strumentazioni con caratteristiche simili [68,69]. Inoltre, dalle singole curve Forza-tempo (F-t), generate dal sistema, è stato possibile analizzare le fasi di applicazione della forza e la relativa morfologia delle curve F-t andando a studiare in dettaglio le curve unimodali o bimodali (Figura 6, Capitolo 2). Questa differenza, in accordo con quanto riportato in letteratura [69], spiega come una curva unimodale a singolo picco di forza consente un'applicazione uniforme ed efficiente della forza

nell'unità di tempo. Infatti, un'applicazione uniforme della forza si traduce teoricamente in un'accelerazione regolare del kayak diversamente dalle curve bimodali che sono accostate ad errori tecnici durante la pagaiata in acqua [69]. Pertanto, il sistema potrà consentire all'allenatore di effettuare un ampio studio sull'applicazione della forza del paddler evidenziando, allo stesso tempo, l'insorgere di specifici difetti tecnici durante la pagaiata.

Verificata l'attendibilità dei dati forniti dal sistema E-Kayak si è potuto individuare e studiare per la prima volta la forza propulsiva (F_p) applicata dal paddler e di verificare la teoria "dell'equilibrio dinamico" (Capitolo 4) durante prove svolte in piscina, su una distanza di 50m, a tre diversi range di velocità mantenuta costante. Comunemente la pagaiata in acqua è suddivisa in 4 fasi: presa (fase di entrata)-immersione (fase di trazione)-estrazione (fase di uscita)-rilascio (fase aerea), e la forza applicata in ciascuna fase non è costante [70–74]. Visto che la fase subacquea della pagaiata non contribuisce pienamente alla propulsione diversi studi hanno cercato di identificare le fasi di applicazione di F_p [70,71,75,76], la maggior parte di questi hanno riportato che la F_p si genera principalmente durante le fasi di immersione ed estrazione, con differenze nella durata della fase e nello spostamento della pala in acqua. Ad oggi gli unici risultati pubblicati riguardano esclusivamente i valori di forza media, forza di picco e impulso di forza espressi durante la pagaiata.

Per equilibrio dinamico si intende quel sistema in cui la velocità istantanea coincide con la velocità media, quindi, ci si trova in una situazione di moto rettilineo uniforme. All'equilibrio dinamico tutta la forza propulsiva prodotta dall'atleta viene impiegata per vincere le resistenze dell'acqua (se presente) e dell'aria: $F = D$. L'elemento che si intende indagare prevede che: la relazione tra il sistema propulsivo e quello frenante (drag) del paddler sia determinato da un equilibrio non dalle forze presenti nel sistema pagaia-canoa-acqua (sistema di leve instabile), ma delle potenze che si vengono a produrre ossia che la potenza propulsiva dell'atleta (P_p) è uguale alla potenza di drag (P_d) che incontra il kayak durante l'avanzamento ($P_p = P_d$).

Dalla sincronizzazione tra E-Kayak e video analisi 2D è stato possibile misurare il valore della F_p , la durata di F_p , lo spostamento orizzontale e la velocità della pala (V_{pa}) mentre i valori di P_p e P_d sono stati rispettivamente calcolati e stimati. I risultati emersi dalle prove svolte a differenti range di velocità mostrano che la durata (s) della fase di applicazione di F_p diminuisce dal 44% al 36%, lo spostamento orizzontale che compie la pala diminuisce da 0.15 a 0.13 cm mentre il valore di F_p aumenta da 139 a 213N. Questo perché all'aumentare della velocità del kayak corrisponde un incremento, da parte del canoista, dei livelli di forza con tempi di applicazioni brevi (Tabella 1, Capitolo 4). Misurata la F_p è stato calcolato il valore di P_p ($P_p = F_p * V_{pa}$) dell'atleta e confrontato con il valore stimato teoricamente di P_d ($P_d = k_d * V^3$) della barca verificando il concetto di equilibrio dinamico. I dati di potenza sono in accordo tra loro come mostrato dal Bland Altman inoltre nessuna differenza statistica è stata riscontrata tra i valori di P_p e P_d (Figura 1-Tabella 2, Capitolo 4). Questo risultato conferma la validità del valore di F_p misurato.

Lo studio fornisce un nuovo approccio per misurare e monitorare le prestazioni del kayak attraverso l'introduzione di un nuovo parametro dinamico come la F_p . Infatti, l'identificazione spazio-temporale della F_p del paddler consentirà agli allenatori di intervenire sui parametri reali necessari per migliorare la propulsione del colpo, evitando dispersioni nel generare la P_p .

Nel quinto capitolo si presenta uno studio finalizzato alla valutazione delle prestazioni del paddler in risposta agli esercizi di trazione su panca retroversa (PBP) e panca piana (BP), svolti in ambiente gravitazionale. È noto che per aumentare la velocità del kayak, il canoista, immergendo e tirando indietro la pala (fase di trazione), deve produrre una forza propulsiva maggiore della forza di drag [64,77]. Al contrario, durante la fase di recupero, dove non vengono applicate forze sull'imbarcazione, intervengono solo le forze di drag che decelerano (attrito, forma, onda) [7]. Pertanto, è possibile dedurre che la velocità media del kayak è la conseguenza degli effetti combinati della propulsione e delle forze di drag [48,49]. Quindi, al fine di migliorare la fase di propulsione per ridurre le prestazioni del tempo di gara, il canoista deve condizionare la forza e la potenza dei muscoli degli arti superiori

attraverso esercizi specifici svolti in ambiente gravitazionale. Lo scopo di questo studio è di identificare quale esercizio tra PBP e BP sia più efficace al miglioramento delle prestazioni di sprint nel kayak.

Lo studio ha previsto il confronto dei parametri cinematici misurati su 50m sprint e i parametri neuromuscolari espressi negli esercizi PBP e BP. I test effettuati hanno previsto la determinazione dell'1RM (forza dinamica massima), delle curve forza-velocità e potenza velocità per entrambe gli esercizi su panca utilizzando un encoder lineare. Invece, per quanto riguarda i test in acqua sono state svolte 3 prove da 50m (per ciascun atleta) sprint misurando con l'E-kayak la massima velocità e la frequenza di pagaiata. Dai risultati di questo studio emerge che la potenza massima sviluppata sulla PBP è fortemente correlata alla velocità di sprint ($r=0.80$ $p<0.01$) e alla frequenza di pagaiata ($r=0.60$; $p<0.05$) rispetto alla BP (Table2, Capitolo 5). Inoltre, non sono state trovate correlazione tra i parametri di forza dinamica massima (1RM), espressi sia su BP che su PBP, e i parametri cinematici della prestazione di sprint (Tabella 2, Capitolo 5). Pertanto, l'interpretazione dei dati suggerisce che l'esercizio su PBP sembra essere più adatto per la valutazione e l'allenamento del paddler rispetto alla BP. Sulla base di quanto emerso, gli allenatori potrebbero quindi concentrarsi sullo sviluppo di un carico di allenamento basato sulla potenza muscolare eseguito sul PBP durante la stagione sportiva. Per ragioni opposte, l'uso della BP potrebbe essere consigliabile come complemento al condizionamento della sola muscolatura antagonista senza sovraccaricare inutilmente il sistema neuromuscolare del canoista.

Pallanuoto

La pallanuoto è uno sport complesso, nel quale bisogna muovere il proprio corpo dentro un fluido (l'acqua) e spesso in opposizione con l'avversario. La partita prevede spostamenti a bassa velocità (0,8 m/s), alternati da sprint di pochi metri eseguiti alla massima velocità (circa 2 m/s). È uno sport caratterizzato da un numero complesso di movimenti: azioni di attacco e difesa, passaggi,

mantenimento della posizione orizzontale e verticale, tiri, blocchi e fasi di lotta per guadagnare o mantenere la posizione in acqua. La maggior parte delle azioni (passaggio, tiro, lotta) richiedono una posizione in acqua quasi verticale [78]. Si possono individuare due azioni nel movimento degli arti inferiori del pallanuotista l'“*eggbeater kick*” (movimento ciclico) e il “*breaststroke kick*” (movimento balistico). Durante la gara questi movimenti vengono eseguiti alternativamente o simultaneamente a seconda della situazione di gara, il movimento di *breaststroke kick* viene impiegato durante la fase di alzo e tiro, nel cambio di direzione e nello “svincolo” dell'avversario mentre il movimento di *eggbeater kick* viene utilizzato nella lotta (presa di posizione) e nei passaggi. Per questi motivi l'allenamento e valutazione degli arti inferiori sono essenziali per lo svolgimento di azioni tecniche, di lotta, di blocco e anche per ottimizzare compiti di attacco e di difesa [79]. Inoltre è noto che la capacità e l'abilità del *breaststroke kick* e la componente di velocità con cui si lancia la palla sono essenziali per il tiro e il passaggio nella pallanuoto [63,80].

Attualmente gli studi presenti in letteratura sull'allenamento della forza e della potenza muscolare in acqua sono assenti o meglio vengono svolti in ambiente gravitazionale [81] oppure svolti in acqua senza uno specifico indirizzo sulla percentuale di carico sollevato e sull'intensità della prestazione [82,83]. Pertanto la questione pratica dello studio è quella di individuare un metodo essenziale semplice per migliorare e valutare la forza e in particolar modo la potenza espressa durante il *breaststroke kick*.

Il sesto capitolo rappresenta il primo tentativo, in ambiente acquatico, in grado di determinare la relazione Forza-velocità (F-v) e Potenza-velocità (P-v) dei muscoli degli arti inferiori durante la prestazione di spinta verticale (*vertical thrust*) a carico crescente utilizzando il *breaststroke kick*. Per l'analisi del *vertical thrust* è stata adottata l'analisi video 2D che ha permesso il calcolo dei parametri cinematici (tempo, spostamento, velocità e accelerazione) e ha permesso la derivazione dei parametri dinamici utili a identificare la potenza e la forza espressa dal pallanuotista ad ogni carico sollevato.

I risultati di questo studio confermano l'accuratezza dei parametri cinematici misurati con il sistema di video analisi. Spostamento, tempo e i parametri calcolati come velocità e accelerazione hanno mostrato valori di errore contenuti al di sotto del 4.5% in qualsiasi condizione di carico, mentre la derivata dinamica come forza e potenza hanno mostrato un errore massimo inferiore all'8%. Va sottolineato che, per ogni parametro (misurato o calcolato), l'errore relativo era inferiore alle differenze medie osservate tra gli atleti in ciascuna prestazione delle condizioni di carico. Il livello di riproducibilità di tutti i parametri valutati in questo studio è stato molto elevato tra le due prove eseguite in due giorni diversi (Tabella 1, Capitolo 6) in termini di correlazione (r da 0.86 a 0.99) e coefficiente di variazione -CV- (<4.5%). Inoltre, i risultati di questo studio mostrano che la relazione esponenziale F-v (Figura 4) sembra spiegare meglio la forza propulsiva esercitata nell'acqua nel sollevare carichi crescenti rispetto a quella lineare mentre la curva P-v mantiene lo stesso andamento quadratico come osservato in letteratura (Figura 3, Capitolo 6).

Si può infatti presumere che la forza esercitata dagli arti inferiori nel mantenere e sollevare carichi molto pesanti raggiunga un livello di saturazione (plateau) senza mai arrivare alla massima forza isometrica, impossibile da ottenere in ambiente acquatico, rispetto a quello osservato in campo gravitazionale. Quindi in questa condizione, sembra concepibile considerare che la curva F-v possa commutare la sua linearità in una relazione di tipo esponenziale con carichi pesanti (cioè, quando lo spostamento verticale diventerà trascurabile all'ulteriore aumento del carico senza aumento della forza muscolare).

Dunque, la valutazione cinematica del giocatore di pallanuoto che esegue specifici pattern neuromuscolari e biomeccanici in ambienti specifici potrebbe ridurre il bias nella valutazione e nell'allenamento che di solito viene svolto in ambiente gravitazionale. In linea con queste considerazioni, questo metodo potrebbe fornire ad allenatori e preparatori indicazioni specifiche sul profilo neuromuscolare di ciascun giocatore di pallanuoto, utili per il monitoraggio e il condizionamento di forza e potenza eseguite direttamente in acqua e non in un ambiente aspecifico.

In conclusione, si può dedurre che sono necessari ulteriori studi per verificare i risultati preliminari. Lo stesso metodo dovrebbe essere verificato anche sulle giocatrici di pallanuoto.

Nuoto

Il nuoto agonistico è uno degli sport più impegnativi per eseguire le ricerche scientifiche. Infatti, valutare gli esseri umani nell'ambiente acquatico risulta difficoltoso poiché non è il loro ambiente naturale e devono essere presi in considerazione altri principi fisici rispetto all'ambiente gravitazionale. Di solito, per l'analisi del movimento umano, compresi quelli effettuati in ambienti acquatico, vengono utilizzati metodi sperimentali e numerici. I metodi sperimentali sono caratterizzati dall'uso di sensori/mezzi per l'analisi dei soggetti (IMU, video analisi, palette strumentate), dall'acquisizione dei parametri e successivamente dall'elaborazione dei dati. Invece, i metodi numerici sono caratterizzati dall'introduzione di dati di input selezionati, dall'elaborazione dei dati secondo determinate equazioni meccaniche e quindi dalla raccolta dei dati di output. Entrambi i gruppi di metodi mirano a eseguire l'analisi cinematica, l'analisi dinamica e l'analisi neuromuscolare del nuotatore [84]. Nei capitoli 7 e 8 è stato impiegato il metodo sperimentale con l'impiego della video analisi 2D e il metodo numerico per individuare il "golden ratio" (rapporto aureo) nello stile libero e nello stile farfalla. È noto, che i movimenti umani come camminare e correre, sono in grado di generare schemi motori ritmici, con la conseguente comparsa di strutture tempo-armoniche nascoste. Tali strutture armoniche sono rappresentate (a velocità *confortevole*) dal verificarsi del rapporto aureo come rapporto tra le durate di specifiche sottofasi del cammino e della corsa. Pensando alla sezione aurea ci si può ricollegare ai concetti di bellezza, di equilibrio, di proporzione e di efficienza del gesto motorio. Indicata con la lettera greca ϕ (phi), la sezione aurea è, come π , un numero la cui espansione decimale prosegue all'infinito senza mai ripetersi in uno schema generale.

L'espansione decimale di π inizia con 3,14159 quella di ϕ con 1,61803. La connessione fra i numeri di Fibonacci (i.e. 1, 2, 3, 5, 8, 13, 21, 34, 55...) e la sezione aurea venne verificata nel XIX secolo: se ogni numero di Fibonacci viene diviso per quello precedente, man mano che avanziamo nella sequenza il risultato ottenuto tende a ϕ cioè si avvicina progressivamente alla sezione aurea (i.e. $2/1 = 2$; $3/2 = 1.5$; $5/3 = 1.666$; $8/5 = 1.6$; $13/8 = 1.625$; $21/13 = 1.615$; $34/21 = 1.619$; $55/34 = 1.618$). La sezione aurea gode di moltissime proprietà algebriche uniche e sorprendenti da cui deriva legittimamente il suo appellativo di “quantità divina”. Ci si renderà conto che queste proprietà non sono semplici coincidenze, ma precise leggi dimostrate che derivano tutte dalla stessa definizione della sezione aurea, e, in particolare, dalla “parabola d’oro” definita come: $x^2 = 1+x$.

La predilezione della natura per l’efficienza fa sì che la disposizione dei petali dei fiori, dei loro semi e delle foglie sugli steli dipenda dalla sezione aurea che porta all’ottimizzazione della struttura.

In molti esseri viventi o in parti anatomiche, certe proporzioni rispettano la successione matematica di Fibonacci ϕ . Evidenze sperimentali preliminari suggeriscono che il golden ratio è presente nel nuoto a stile libero (crawl) e può comportarsi, da questo punto di vista, come il cammino e la corsa. L’obiettivo di questo studio (Capitolo 7) è stato di dimostrare che esiste effettivamente una connessione matematica tra il rapporto aureo e la nuotata a stile libero. A questo scopo vengono utilizzate le sequenze di Fibonacci generalizzate. Le sequenze si basano sulle durate delle fasi “aggregate” della bracciata a crawl con un chiaro significato fisico, mentre caratterizzano l’auto-similarità delle bracciate a crawl nella sua natura semplice e nella variante potenziata (più forte). La bracciata a crawl è stata suddivisa mediante l’uso della video analisi 2D nei seguenti intervalli di tempo che rappresentano ogni singola fase:

- 1- Entry-and-stretch (ES): inizia quando la mano entra in acqua e raggiunge la massima posizione frontale della sua traiettoria (massimo allungamento);
- 2- Downsweep-and-catch (DC): quando la mano scende verticalmente dopo la fase di allungamento nel piano sagittale;

- 3- Insweep (IN): in cui la mano, al termine della fase di downsweep, si sposta internamente da sinistra a destra sul piano frontale;
- 4- Upsweep (UP): identificabile come fase di ascesa sul piano sagittale;
- 5- Exit (EX): la mano arriva nella posizione finale prima di uscire fuori dall'acqua
- 6- Recovery (RE): inizia quando il braccio esce dall'acqua e termina quando il lo stesso braccio rientra in acqua.

I dati sperimentali sui nuotatori crawl illustrano le derivazioni teoriche, suggerendo che: i) la connessione matematica tra il rapporto aureo e la nuotata a crawl esiste effettivamente al ritmo su media/lunga distanza (svolgendo il ruolo della velocità confortevole nel camminare e in esecuzione); il livello di auto similarità aumenta con la tecnica del nuoto, risultando cruciale nell'ottenere risparmio energetico tramite canoni fondamentali di perfezione memorizzati all'interno di loop ricorsivi; l'aumentata autosimilarità, caratterizzata da schemi motori altamente ripetitivi e ritmici, è associata alle prestazioni dei nuotatori di alto livello. I risultati possono fornire informazioni comparative (quantitative) sia sul livello di recupero fisico (dopo un allenamento intenso) sia sul condizionamento dei modelli neurali ritmici del nuotatore durante una specifica prestazione di nuoto (basata sul momento contingente): nei nuotatori di alto livello, in cui la variabilità della coordinazione interindividuale è limitata a una gamma ristretta di soluzioni di movimento [85], ogni cambiamento che un professionista può evidenziare/percepire potrebbe effettivamente essere un cambiamento nell'interazione dinamica dei componenti del sistema [86].

Nel successivo capitolo (Capitolo 8) è stata proposta una partizione temporale armonicamente auto-simile, che risulta essere esibita dai nuotatori d'élite ad un passo gara adatto per la media distanza (200m), è stata formalmente definita per uno degli stili di nuoto tecnicamente più avanzato: il delfino (farfalla). Anche questa partizione come nel precedente capitolo, si basa sulla sequenza di Fibonacci

generalizzata e sul rapporto aureo. Lo studio ha previsto l'analisi cinematica 2D delle fasi della bracciata e della gambata nello stile a farfalla.

La bracciata è stata suddivisa in:

- 1- Entry and catch: tra l'ingresso delle mani in acqua e l'inizio del loro movimento all'indietro
- 2- Pull: l'inizio dell'arretramento delle mani fino a raggiungere la perpendicolarità con le spalle
- 3- Push: tra il posizionamento delle mani sotto le spalle e la loro uscita dall'acqua
- 4- Recovery: tra l'arrivo delle mani a livello dell'acqua e il loro successivo ingresso in acqua

Invece la gambata è stata suddivisa in:

- 1- Downward phase 1: movimento dall'alto verso il basso della prima gambata
- 2- Upward phase 1: movimento dal basso verso l'alto della prima gambata
- 3- Downward phase 2: movimento dall'alto verso il basso della seconda gambata
- 4- Upward phase 2: movimento dal basso verso l'alto della seconda gambata

I risultati di questo studio (Tabella 6 - Capitolo 8) potrebbero fornire informazioni comparative (quantitative) su:

- il livello di recupero fisico del nuotatore dopo un allenamento duro e intenso;
- il condizionamento dei pattern neurali ritmici del nuotatore durante le azioni di nuoto basate sul momento contingente;
- i miglioramenti dei nuotatori nel tempo e le azioni correttive necessarie per migliorare le prestazioni.

Infatti, nell'alto livello, la variabilità della coordinazione interindividuale si riduce a una gamma ristretta di varianti di movimento, ogni piccolo cambiamento che un professionista può eseguire potrebbe portare a un cambiamento rilevante nell'interazione dinamica dei componenti del

sistema[85]. Quindi, l'auto similarità, come è stata definita in questo lavoro, può diventare un punto di riferimento nella formulazione di programmi di allenamento avanzato e nella valutazione per nuotatori d'élite.

Conclusioni

Dall'analisi fornita da questi studi emerge chiaramente l'importanza che ha assunto oggi la valutazione funzionale nel mondo sportivo sia come mezzo di verifica delle capacità fisiche e monitoraggio della prestazione. L' E-kayak (Tecnologia MEMS + strain guage+ GPS) risulta essere un valido sistema per il monitoraggio dei parametri dinamici e cinematici della prestazione del paddler e il suo impiego ha permesso di misurare per la prima volta la forza propulsiva e di verificare la condizione di equilibrio dinamico quando il kayak si muove a velocità mediamente costante. Per quanto riguarda gli altri sport acquatici (nuoto e pallanuoto) la video analisi ad oggi risulta l'unico mezzo valido e affidabile per determinare, sia i parametri cinematici e dinamici della prestazione. Le relazioni Forza-velocità e Potenza-velocità individuate nel pallanuotista saranno utili agli allenatori per condizionare in maniera specifica gli arti inferiori indirizzando l'allenamento allo sviluppo della forza e della potenza direttamente in acqua. Inoltre, la sequenza di Fibonacci riscontrata nel nuoto a stile libero e a farfalla sarà utile a fornire informazioni quantitative sia sul livello di recupero fisico che sul condizionamento dei modelli neurali ritmici del nuotatore.

Chiaramente tutti i mezzi e metodi indagati consentiranno agli allenatori di poter attuare una corretta valutazione della prestazione e uno studio della biomeccanica del gesto, focalizzandosi principalmente sui fattori limitanti delle discipline sportive.

Ringraziamenti

Altro obiettivo raggiunto, sono stati tre anni ricchi di emozioni!

Partiamo da noi il gruppo del XXXIV ciclo: Luca, Aurelio, Michela, Lara e la nostra seconda “mamma” Monica. Che dire, siamo stati fantastici in questo periodo, siete persone meravigliose e sono fiero di aver instaurato con voi un rapporto che va ben oltre l’aspetto professionale e che ci ha permesso, grazie alla nostra unione, di condividere e superare anche i momenti più critici che ci ha riservato il nostro percorso di studio.

Non dimenticherò mai i ragazzi del XXXIII ciclo, un gruppo altrettanto forte che ha rappresentato per noi una guida fondamentale!

Un ringraziamento speciale va al mio caro compagno di “MANDRAKATE” l’Avv. Luca Zambelli, non dimenticherò il Festival della Scienza Medica.

Se questo percorso è iniziato e terminato lo devo ad una serie di persone fondamentali, ringraziarle non sarà mai abbastanza.

Inizio ringraziando il Prof Giorgio Gatta, Guglielmo Guerrini e Matteo Cortesi che mi hanno permesso di poter intraprendere questo percorso di ricerca indirizzando i miei studi sul kayak e sul nuoto trasmettendomi conoscenze e nuovi metodi di valutazione del gesto sportivo.

Un ringraziamento va poi a Nunzio e Paolo sempre disponibili e di gran supporto per le mie ricerche con le loro tecnologie.

Un ringraziamento speciale lo dedico al Prof Giuseppe Annino e al Prof Vincenzo Bonaiuto, per avermi trasmesso, nei cinque anni di Università a Roma, le conoscenze utili a poter intraprendere il dottorato di ricerca.

Sento di dover ringraziare il Prof. Carmelo Bosco anche se non ho avuto modo di conoscerlo, i suoi insegnamenti trasmessi tramite il Prof. Giuseppe Annino mi hanno portato a cambiare il modo di vedere le cose!

Ringrazio anche Stefano Loddo, Antonio Cannone, Misha Vartolomei, Davide Aliprandi e Antonio Gianfelici perché sono stati punti di riferimento per il periodo trascorso con la nazionale di canoa/kayak. Non dimenticherò mai quel bronzo mondiale in Portogallo.

Grazie anche a Luca Ghelardini, Claudio Ghelardini, Lucia Lissoni e il Presidente Claudio Schermi persone semplici e speciali. Se non fosse stato per voi non avrei mai potuto indagare la forza propulsiva nel kayak.

Bene, ora passiamo a coloro che hanno permesso tutto questo con enormi sacrifici.

Parto dalla mia famiglia, grazie per aver sempre creduto in me! Un pensiero va alle mie nonne e ai miei nonni che mi hanno sempre sostenuto e incoraggiato da lassù, spero di avervi riempito il cuore di orgoglio.

Cara Alessandra, grazie per la tua presenza costante, sei sempre stata e lo sarai una fedele compagna di vita! So di essere stato molto concentrato sui miei obiettivi in questi anni ma sappi che ne varrà la pena, sei la mia vita!

Caro Yuri è stata un'estate difficile spero che tu abbia trovato la pace che tanto desideravi. Avrai sempre un posto speciale nel mio cuore ed io non dimenticherò mai la tua colazione preferita che sicuramente starai gustando anche da lassù, il tuo danese e cappuccino. Ciao cugino saluta nonno.

Un grazie va anche al gruppo politico comunale che rappresento insieme a Fabio e Alessandro e che ci vede sempre in prima linea a difesa della nostra piccola comunità. Grazie anche al neo gruppo intercomunale (Franco, Federico, Giovanni, Antonio, Alessandro, Angelo, Marco B., Marco, Fabio e Alessandro G) continueremo a portare in risalto la voce del cittadino!!!

Grazie anche a Ireneo Rogulski per la fiducia e il supporto fornito in questo ultimo periodo

Un grazie alla mia seconda famiglia... la mia squadra di pallanuoto.

Un grazie anche ai miei amici Carlo, Valerio, Simone, Ottavio, Ezio e Lorenzo che mi hanno accompagnato durante questi 3 anni con grasse risate e anche incazzature!

Infine un grazie a me stesso e alla mia perseveranza.... VOLERE È POTERE!!!

Lista delle figure

Accelerometro e Giroscopio

Figura 1: Schema riassuntivo accelerometro capacitivo.

Figura 2: Schema di funzionamento del giroscopio

Strain Gauge

Figura 3: Estensimetri disposti a ponte di Wheatstone

Catene di misura e reti di sensori

Figura 4: IMU a 9 DOF (accelerometro, giroscopio e magnetometro)

Video analisi

Figura 5: Suddivisione della nuotata crawl nelle fasi: Entry-Stretch (ES), Downsweep-and-catch phase (DC), Insweep phase (IN), Upsweep phase (UP), Exit phase (EX)

Encoder Lineare

Figura 6: Raffigurazione interna dell'encoder.

Figura 7: Encoder lineare

Cenni di meccanica dei fluidi (galleggiabilità, drag, forza propulsiva)

Figura 8: Forze agenti sul nuotatore

Modelli di prestazioni di alcuni sport acquatici

Figura 9: Rappresentazione delle azioni tipiche delle bracciate a stile libero, dorso, rana e delfino

Capitolo 1

Figure 1. Wireless sensor network (WSN) architecture.

Figure 2. A K4 racing kayak.

Figure 3. The nRF24L01P+PA+LNA module.

Figure 4. The webpage acts a communication interface.

Figure 5. Block scheme of the master node (**a**) and slave node (**b**). IMU = Inertial measurement unit, MCU = Microcontroller unit, GPS = Global positioning system, SPI = Serial peripheral interface, PPS = Pulse per second.

Figure 6. (**a**) Master node in a waterproof case; (**b**) slave node placed in the paddle shaft.

Figure 7. Example of screenshot of the application for e-kayak session analysis.

Figure 8. Force on the paddles measured on K2.

Figure 9. Examples of screenshot of the application for karting session analysis. (**a**) Analysis app; (**b**) kart's speed.

Figure 10. Screenshot of the application for karting session analysis.

Figure 11. (**a**) System equipped for swimming; (**b**) screenshot of the app analysis.

Capitolo 2

Figure 1. Block scheme of the *e-Kayak* system. Legend: GPS, Global Positioning System; IMU, inertial measurement unit; S1, paddle; S2, footrest.

Figure 2. *E-Kayak* system: (a) paddle node, (b) footrest node, and (c) master node installed on the boat.

Figure 3. Block scheme of the paddle slave node (where d is the distance of the strain gauge sensor from the tip blade).

Figure 4. Screenshot of the *e-Kayak* data visualization software.

Figure 5. Kayak paddling stroke phases: (a) entry, (b) catch, (c) pull, (d) exit, (e) recovery.

Figure 6. Kayak paddling stroke phases. Legend: T_{catch} [s] = length of the catch phase, T_{pull} [s] = length of the pull phase, T_{air} [s] = length of the air (recovery) phase, T_{wet} [s] = length of the wet phase ($T_{\text{catch}} + T_{\text{pull}}$), T_{stroke} [s] = length of the stroke phase ($T_{\text{air}} + T_{\text{wet}}$), $I_{\text{stroke_R}}$ = right stroke pulse, $I_{\text{stroke_L}}$ = left stroke pulse.

Figure 7. Bimodal (highlighted by arrows) and unimodal paddle force curves.

Figure 8. Measure of force on the paddle (F_{paddle} —dashed), roll (light blue), and the boat's acceleration (A_{fwd} —red).

Figure 9. Measure of force on the paddle (F_{paddle} —blue) and the boat's velocity (v_{boat} —red).

Figure 10. Measure of force on the paddle (F_{pad} —orange) and the footrest (F_{fr} —blue).

Figure 11. Detail of the force on the paddle (orange) and footrest (blue). Legend: F_{pad} [N] = force impressed on the paddle, F_{fr} [N] = force impressed on the footrest, T_{Dpf1} = leg-arm anticipation time [s], T_{Dpf2} = leg-arm delay time.

Capitolo 3

Figure 1. DAQuino configuration for K2 kayaking.

Figure 2. DAQuino: Example of report.

Figure 3. Boat's forward acceleration (orange) vs. force on the paddle (blue).

Figure 4. Boat's velocity (orange) vs. force on the paddle (blue).

Capitolo 4

Figure 1. Horizontal reference object: the reference distance between the markers M1-M2 (212 cm). M3 is the marker used to measure the paddle displacement.

Figure 2. The underwater paddle phase ($A+B+C+D = T_w$) is divided in *entry* ($A+B = T_{en}$), *dynamic propulsive* ($B+C = T_p$) and *exit* ($C+D = T_{ex}$) time. The corresponding positions are: *catch* (A), *end immersion* (B), *start extraction* (C) and *release* (D).

Figure 3. Bland–Altman plot of drag power (P_d) and propulsive power (P_p). Bias and random error lines (95% limits of agreement, LOA) are included.

Figure 4. Bland–Altman plot of average paddle velocity developed by the athlete (V_{pa}) and average paddle velocity calculated theoretically (V_{pt}). Bias and random error lines (95% limits of agreement, LOA) are included.

Capitolo 5

Figure 1. Correlation between P_{max} (W) expressed at PBP and kayak velocity (m/s) reached on KTS

Figure 2. Correlation between P_{max} (W) expressed at BP and kayak velocity (m/s) reached on KTS sprint.

Capitolo 6

Figure 1. Frontal view of water polo overload test (WOT) conditions and acting forces. Buoyancy force of the subject (F_{bB}), Body weight of the subject (W_B), eggbeater kick force (F_{ek}), buoyancy force of the load (F_{bL}), weight of the load (W_L), force relative to power that is wasted to accelerate water downwards (F_{dw}).

Figure 2. Median correlation coefficients and their ranges obtained comparing the vertical thrust's height free load with individual Fbk, Pbk and v at 5–25 kg.

Figure 3. Linear F-v (grey line and squares) and second-order polynomial regression P-v (black line and dots) with the relative regression equations building on vertical thrust performed at incremental loads (from 5 to 25 kg). Both curves are depicted according the average and SD of velocity, force and power at different load as shown in Table 1.

Figure 4. Exponential F-v with the relative regression equations building on vertical thrust performed at incremental loads (from 5 to 25 kg). The curve is depicted according to the average and SD of velocity and force with the different loads as shown in Table 1.

Capitolo 8

Figure 1. Butterfly stroke: arm and leg phases (case of $T_2, T_3, T_4 > 0$)

Lista delle Tabelle

Capitolo 1

Table 1. Comparison of different wireless communication protocol.

Capitolo 2

Table 1. State of the art on DAQ systems developed for kayaking Legend: Dyn, dynamic; Kin, kinematic.

Table 2. Female 100 m—slow pace (stroke rate (SR) = 62 str/min; velocity = 3.67 ± 0.26 m/s).

Table 3. Female 50 m—fast pace (SR = 82 str/min; velocity = 3.76 ± 0.10 m/s).

Table 4. Male 150 m—low pace (SR = 63 str/min; velocity = 3.24 ± 0.08 m/s).

Table 5. Male 40 m—fast pace (SR = 90 str/min; velocity = 4.14 ± 0.25 m/s).

Capitolo 4

Table 1. Summary of kinematic and dynamic variables (Mean \pm SD).

T_{en} =Entry time (catch+ immersion); T_p =dynamic propulsive time; T_{ex} =extraction time; T_w = wet time; S_p =propulsive displacement of paddle; V_{pa} =paddle velocity; F_p =propulsive force; F_m =mean force; F_{pk} =peak force; SR=stroke rate. T_{en} , T_p and T_{ex} are also expressed in percentage of T_w and F_p in percentage of F_{pk} .

Table 2. Mean values (\pm SD) of propulsion power (P_p) and drag power (P_d); and paddle velocity determined with the 2D video analysis (V_{pa}) and paddle velocity calculated theoretically (V_{pt}). P values from the paired t-test are also reported.

Capitolo 5

Table 1. Comparison between values of Power (W) and Velocity (m/s) expressed during BP and PBP. All values are mean \pm SD (95% confidence interval). Significant difference (between subject) as reported for $p < 0.05$ (*), for $p < 0.01$ (**) and for $p < 0.001$ (***)

Table 2. Dynamic parameters (1 RM and P_{max} obtained for each athlete) expressed at PBP and BP in correlation with kinematic parameters observed on KTS. All values are mean \pm SD. Correlation is reported $p < 0.05$ (*) and $p < 0.01$ (**)

Capitolo 6

Table 1. Day-to-day repeatability of average displacement (m), time (s), velocity (m/s) and acceleration (m/s^2), force and power \pm Standard Deviation (SD) of the vertical thrust exercise (in water) performed by 14 water polo players with increasing loads, r Pearson correlation coefficient; CV, Coefficient of Variation for repeated measurements; ICC, Interclass Correlation Coefficient; 95% Confidence Interval (CI); SEM, Standard Error of Measurement; and ES, Effect Size, for each load.

Capitolo 8

Table 1. Experimental data for swimmers IL1–IL7 and NL1–NL2: arm phase durations (in seconds).

Table 2. Experimental data for swimmers IL1–IL7 and NL1–NL2: leg phase durations (in seconds).

Table 3. Delays and related values for swimmers IL1–IL7 and NL1–NL2: delay durations (in seconds) and NTD.

Table 4. Delays and related values for swimmers IL1–IL7 and NL1–NL2: (a, b, c, d)-values.

Table 5. Data analysis for swimmers IL1–IL7 and NL1–NL2: aggregate phases (percentage values).

Table 6. Data analysis for swimmers IL1–IL7 and NL1–NL2: values of indices (23) and (24).

Bibliografia

1. Baumgartner, T.A.; Jackson, A.S. Measurement for Evaluation in Physical Education and Exercise Science. *Measurement for evaluation in physical education and exercise science*. **1998**.
2. R, M., Jr., James; Dale, M.; James, D.; Minsoo, K. *Measurement and Evaluation in Human Performance, 5E*; Human Kinetics, 2015; ISBN 978-1-4504-7043-8.
3. Wong, T.C.; Webster, J.G.; Montoye, H.J.; Washburn, R. Portable Accelerometer Device for Measuring Human Energy Expenditure. *IEEE Transactions on Biomedical Engineering* **1981**, *BME-28*, 467–471, doi:10.1109/TBME.1981.324820.
4. Chen, K.; Bassett, D. The Technology of Accelerometry-Based Activity Monitors: Current and Future. *Medicine and science in sports and exercise* **2005**, doi:10.1249/01.MSS.0000185571.49104.82.
5. Troiano, R.P.; McClain, J.J.; Brychta, R.J.; Chen, K.Y. Evolution of Accelerometer Methods for Physical Activity Research. *Br J Sports Med* **2014**, *48*, 1019–1023, doi:10.1136/bjsports-2014-093546.

6. Bächlin, M.; Tröster, G. Swimming Performance and Technique Evaluation with Wearable Acceleration Sensors. *Pervasive and Mobile Computing* **2012**, *8*, 68–81, doi:10.1016/j.pmcj.2011.05.003.
7. Bonaiuto, V.; Gatta, G.; Romagnoli, C.; Boatto, P.; Lanotte, N.; Annino, G. A Pilot Study on the E-Kayak System: A Wireless DAQ Suited for Performance Analysis in Flatwater Sprint Kayaks. *Sensors (Basel)* **2020**, *20*, doi:10.3390/s20020542.
8. Chambers, R.; Gabbett, T.J.; Cole, M.H.; Beard, A. The Use of Wearable Microsensors to Quantify Sport-Specific Movements. *Sports Med* **2015**, *45*, 1065–1081, doi:10.1007/s40279-015-0332-9.
9. McGregor, S.J.; Busa, M.A.; Yaggie, J.A.; Bollt, E.M. High Resolution MEMS Accelerometers to Estimate VO₂ and Compare Running Mechanics between Highly Trained Inter-Collegiate and Untrained Runners. *PLOS ONE* **2009**, *4*, e7355, doi:10.1371/journal.pone.0007355.
10. *Intuizione e Scienza Nella Tecnologia Giroscopica Dal 1750 al 1930*;
11. Wagner, J.F. About Motion Measurement in Sports Based on Gyroscopes and Accelerometers—an Engineering Point of View. *Gyroscopy Navig.* **2018**, *9*, 1–18, doi:10.1134/S2075108718010091.
12. Bonaiuto, V.; Gatta, G.; Romagnoli, C.; Boatto, P.; Lanotte, N.; Annino, G. A Pilot Study on the E-Kayak System: A Wireless DAQ Suited for Performance Analysis in Flatwater Sprint Kayaks. *Sensors* **2020**, *20*, 542, doi:10.3390/s20020542.
13. Mooney, R.; Corley, G.; Godfrey, A.; Quinlan, L.R.; ÓLaighin, G. Inertial Sensor Technology for Elite Swimming Performance Analysis: A Systematic Review. *Sensors* **2016**, *16*, 18, doi:10.3390/s16010018.
14. Yuji, O. Mems Sensor Application for the Motion Analysis in Sports Science. *Memory* **2005**, *32*, 128Mbit.

15. Connaghan, D.; Kelly, P.; O'Connor, N.E.; Gaffney, M.; Walsh, M.; O'Mathuna, C. Multi-Sensor Classification of Tennis Strokes. In Proceedings of the 2011 IEEE SENSORS; October 2011; pp. 1437–1440.
16. Silva, A.L.; Varanis, M.; Mereles, A.G.; Oliveira, C.; Balthazar, J.M. A Study of Strain and Deformation Measurement Using the Arduino Microcontroller and Strain Gauges Devices. *Rev. Bras. Ensino Fís.* **2018**, *41*, doi:10.1590/1806-9126-RBEF-2018-0206.
17. Kos, A.; Wei, Y.; Tomažič, S.; Umek, A. The Role of Science and Technology in Sport. *Procedia Computer Science* **2018**, *129*, 489–495, doi:10.1016/j.procs.2018.03.029.
18. Bonaiuto, V.; Boatto, P.; Lanotte, N.; Romagnoli, C.; Annino, G. A Multiprotocol Wireless Sensor Network for High Performance Sport Applications. *Applied System Innovation* **2018**, *1*, 52, doi:doi.org/10.3390/asi1040052.
19. Ballestra, A.; Somà, A.; Pavanello, R. Experimental-Numerical Comparison of the Cantilever MEMS Frequency Shift in Presence of a Residual Stress Gradient. *Sensors* **2008**, *8*, 767–783, doi:10.3390/s8020767.
20. Brusa, E.; De Bona, F.; Gugliotta, A.; Somà, A. Modeling and Prediction of the Dynamic Behaviour of Microbeams Under Electrostatic Load. *Analog Integrated Circuits and Signal Processing* **2004**, *40*, 155–164, doi:10.1023/B:ALOG.0000032596.58984.0c.
21. Somà, A.; Pasquale, G.D.; Brusa, E.; Ballestra, A. Effect of Residual Stress on the Mechanical Behaviour of Microswitches at Pull-In. *Strain* **2010**, *46*, 358–373, doi:https://doi.org/10.1111/j.1475-1305.2009.00651.x.
22. Zhao, H.; Wang, Z. Motion Measurement Using Inertial Sensors, Ultrasonic Sensors, and Magnetometers With Extended Kalman Filter for Data Fusion. *IEEE Sensors Journal* **2012**, *12*, 943–953, doi:10.1109/JSEN.2011.2166066.
23. Zhu, R.; Zhou, Z. A Real-Time Articulated Human Motion Tracking Using Tri-Axis Inertial/Magnetic Sensors Package. *IEEE Transactions on Neural Systems and Rehabilitation Engineering* **2004**, *12*, 295–302, doi:10.1109/TNSRE.2004.827825.

24. Ahmad, N.; Ghazilla, R.A.R.; Khairi, N.M.; Kasi, V. Reviews on Various Inertial Measurement Unit (IMU) Sensor Applications. *International Journal of Signal Processing Systems* **2013**, *1*, 256–262.
25. Wisbey, B.; Rattray, B.; Pyne, D. Quantifying Changes in AFL Player Game Demands Using GPS Tracking: 2008 AFL Season. *Florey (ACT): FitSense Australia* **2008**.
26. Cunniffe, B.; Proctor, W.; Baker, J.S.; Davies, B. An Evaluation of the Physiological Demands of Elite Rugby Union Using Global Positioning System Tracking Software. *The Journal of Strength & Conditioning Research* **2009**, *23*, 1195–1203, doi:10.1519/JSC.0b013e3181a3928b.
27. Cummins, C.; Orr, R.; O'Connor, H.; West, C. Global Positioning Systems (GPS) and Microtechnology Sensors in Team Sports: A Systematic Review. *Sports Med* **2013**, *43*, 1025–1042, doi:10.1007/s40279-013-0069-2.
28. Gabbett, T.J. Quantifying the Physical Demands of Collision Sports: Does Microsensor Technology Measure What It Claims to Measure? *The Journal of Strength & Conditioning Research* **2013**, *27*, 2319–2322, doi:10.1519/JSC.0b013e318277fd21.
29. Picerno, P.; Camomilla, V.; Capranica, L. Countermovement Jump Performance Assessment Using a Wearable 3D Inertial Measurement Unit. *Journal of Sports Sciences* **2011**, *29*, 139–146, doi:10.1080/02640414.2010.523089.
30. Woodman, O.J. *An Introduction to Inertial Navigation*; University of Cambridge, Computer Laboratory, 2007;
31. Liu, T.; Inoue, Y.; Shibata, K. Measurement of Soft Tissue Deformation to Improve the Accuracy of a Body-Mounted Motion Sensor. *Journal of Medical Devices* **2009**, *3*, doi:10.1115/1.3212558.
32. Lafortune, M.A. Three-Dimensional Acceleration of the Tibia during Walking and Running. *Journal of Biomechanics* **1991**, *24*, 877–886, doi:10.1016/0021-9290(91)90166-K.

33. Hamill, J.; Caldwell, G.E.; Derrick, T.R. Reconstructing Digital Signals Using Shannon's Sampling Theorem. *Journal of Applied Biomechanics* **1997**, *13*, 226–238, doi:10.1123/jab.13.2.226.
34. McMaster, D.T.; Gill, N.; Cronin, J.; McGuigan, M. A Brief Review of Strength and Ballistic Assessment Methodologies in Sport. *Sports Med* **2014**, *44*, 603–623, doi:10.1007/s40279-014-0145-2.
35. Düking, P.; Fuss, F.K.; Holmberg, H.-C.; Sperlich, B. Recommendations for Assessment of the Reliability, Sensitivity, and Validity of Data Provided by Wearable Sensors Designed for Monitoring Physical Activity. *JMIR mHealth and uHealth* **2018**, *6*, e9341, doi:10.2196/mhealth.9341.
36. van der Kruk, E.; Reijne, M.M. Accuracy of Human Motion Capture Systems for Sport Applications; State-of-the-Art Review. *Eur J Sport Sci* **2018**, *18*, 806–819, doi:10.1080/17461391.2018.1463397.
37. Barris, S.; Button, C. A Review of Vision-Based Motion Analysis in Sport. *Sports Medicine* **2008**, *38*, 1025–1043.
38. Duthie, G.; Pyne, D.; Hooper, S. The Reliability of Video Based Time Motion Analysis. *Journal of Human Movement Studies* **2003**, *44*, 259–272.
39. Verrelli, C.M.; Romagnoli, C.; Jackson, R.R.; Ferretti, I.; Annino, G.; Bonaiuto, V. Front Crawl Stroke in Swimming: Phase Durations and Self-Similarity. *Journal of Biomechanics* **2021**, *118*, 110267, doi:10.1016/j.jbiomech.2021.110267.
40. Brewin, M.A.; Kerwin, D.G. Accuracy of Scaling and DLT Reconstruction Techniques for Planar Motion Analyses. *Journal of Applied Biomechanics* **2003**, *19*, 79–88.
41. Annino, G.; Romagnoli, C.; Zanela, A.; Melchiorri, G.; Viero, V.; Padua, E.; Bonaiuto, V. Kinematic Analysis of Water Polo Player in the Vertical Thrust Performance to Determine the Force-Velocity and Power-Velocity Relationships in Water: A Preliminary Study.

International Journal of Environmental Research and Public Health **2021**, *18*, 2587,
doi:10.3390/ijerph18052587.

42. Zult, T.; Allsop, J.; Taberner, J.; Pardhan, S. A Low-Cost 2-D Video System Can Accurately and Reliably Assess Adaptive Gait Kinematics in Healthy and Low Vision Subjects. *Scientific reports* **2019**, *9*, 1–11.
43. Lanotte, N.; Lem, S. Sportivi Ad Alta Tecnologia. *Bologna: Zanichelli* **2013**.
44. Hatze, H. The Meaning of the Term" Biomechanics". *Journal of biomechanics* **1974**, *7*, 189–190.
45. Knudson, D.V.; others *Fundamentals of Biomechanics*; Springer, 2007; Vol. 183;.
46. Romagnoli, C.; Bonaiuto, V.; Gatta, G.; Romagnoli, N.; Alashram, A.; Padua, E.; Annino, G. 2D Video Analysis System to Analyze the Performance Model of Figure Roller Skating: A Pilot Study. *Proceedings* **2020**, *49*, 155, doi:10.3390/proceedings2020049155.
47. McLean, S.P.; Hinrichs, R.N. Influence of Arm Position and Lung Volume on the Center of Buoyancy of Competitive Swimmers. *Research Quarterly for Exercise and Sport* **2000**, *71*, 182–189, doi:10.1080/02701367.2000.10608896.
48. Michael, J.S.; Smith, R.; Rooney, K.B. Determinants of Kayak Paddling Performance. *Sports Biomechanics* **2009**, *8*, 167–179, doi:10.1080/14763140902745019.
49. Pendergast, D.; Mollendorf, J.; Zamparo, P.; Termin 2nd, A.; Bushnell, D.; Paschke, D. The Influence of Drag on Human Locomotion in Water. *Undersea Hyperb Med* **2005**, *32*, 45–57.
50. Truijens, M.; Toussaint, H. Biomechanical Aspects of Peak Performance in Human Swimming. *Animal Biology* **2005**, *55*, 17–40, doi:10.1163/1570756053276907.
51. Blazeovich, A.; Blazeovich, A.J. *Sports Biomechanics: The Basics: Optimising Human Performance*; Bloomsbury Publishing, 2017;
52. Gomes, B.B.; Machado, L.; Ramos, N.V.; Conceição, F.A.V.; Sanders, R.H.; Vaz, M.A.P.; Vilas-Boas, J.P.; Pendergast, D.R. Effect of Wetted Surface Area on Friction, Pressure, Wave

- and Total Drag of a Kayak. *Sports Biomechanics* **2018**, *17*, 453–461, doi:10.1080/14763141.2017.1357748.
53. Sumner, D.; Springings, E.J.; Bugg, J.D.; Heseltine, J.L. Fluid Forces on Kayak Paddle Blades of Different Design. *Sports Eng* **2003**, *6*, 11–19, doi:10.1007/BF02844156.
54. Maglischo, E.W. *Swimming Fastest*; Human Kinetics, 2003; ISBN 978-0-7360-3180-6.
55. Voloshin, A. Impact Propagation and Its Effects on the Human Body. In *Biomechanics in sport: performance enhancement and injury prevention*; 2008; pp. 577–587 ISBN 978-0-470-69379-7.
56. Smith, H.K. Applied Physiology of Water Polo. *Sports medicine* **1998**, *26*, 317–334.
57. Hohmann, A.; Frase, R. Analysis of Swimming Speed and Energy Metabolism in Competition Water Polo Games. *Swimming science VI: Biomechanics and medicine in swimming* **1992**, 313–319.
58. Melchiorri, G.; Padua, E.; Sardella, F.; Manzi, V.; Tancredi, V.; Bonifazi, M. Physiological Profile of Water Polo Players in Different Competitive Levels. *J Sports Med Phys Fitness* **2010**, *50*, 19–24.
59. D’Auria, S.; Gabbett, T. A Time-Motion Analysis of International Women’s Water Polo Match Play. *International Journal of Sports Physiology and Performance* **2008**, *3*, 305–319, doi:10.1123/ijsp.3.3.305.
60. Ramos Veliz, R.; Requena, B.; Suarez-Arrones, L.; Newton, R.U.; Sáez de Villarreal, E. Effects of 18-Week In-Season Heavy-Resistance and Power Training on Throwing Velocity, Strength, Jumping, and Maximal Sprint Swim Performance of Elite Male Water Polo Players. *The Journal of Strength & Conditioning Research* **2014**, *28*, 1007–1014, doi:10.1519/JSC.0000000000000240.
61. Hollander, A.P.; Dupont, S.H.J.; Volkerijk, S.M. Physiological Strain during Competitive Water Polo Games and Training. *Medicine and Science in Aquatic Sports* **1994**, *39*, 178–185, doi:10.1159/000423725.

62. Rodríguez, F. Physiological Testing of Swimmers and Water Polo Players in Spain. *Medicine and Sport Science* **1994**, *39*, 172–172.
63. McCluskey, L.; Lynskey, S.; Leung, C.K.; Woodhouse, D.; Briffa, K.; Hopper, D. Throwing Velocity and Jump Height in Female Water Polo Players: Performance Predictors. *Journal of Science and Medicine in Sport* **2010**, *13*, 236–240, doi:10.1016/j.jsams.2009.02.008.
64. Millward, A. A Study of the Forces Exerted by an Oarsman and the Effect on Boat Speed. *null* **1987**, *5*, 93–103, doi:10.1080/02640418708729769.
65. Baudouin, A.; Hawkins, D. A Biomechanical Review of Factors Affecting Rowing Performance. *British Journal of Sports Medicine* **2002**, *36*, 396–402, doi:10.1136/bjism.36.6.396.
66. Sturm, D. Wireless Multi-Sensor Feedback Systems for SportsPerformance Monitoring : Design and Development. **2012**.
67. Sturm, D.; Yousaf, K.; Eriksson, M. A Wireless, Unobtrusive Kayak Sensor Network Enabling Feedback Solutions. In Proceedings of the 2010 International Conference on Body Sensor Networks; IEEE, 2010; pp. 159–163.
68. Gomes, B.B.; Ramos, N.V.; Conceição, F.A.; Sanders, R.H.; Vaz, M.A.; Vilas-Boas, J.P. Paddling Force Profiles at Different Stroke Rates in Elite Sprint Kayaking. *Journal of Applied Biomechanics* **2015**, *31*, 258–263, doi:10.1123/jab.2014-0114.
69. Baker, J. Evaluation of Biomechanic Performance Related Factors with On-Water Tests. In Proceedings of the International seminar on kayak-canoe coaching and science; University of Gent Press: Gent, Belgium, 1998; pp. 50–66.
70. McDonnell, L.K.; Hume, P.A.; Nolte, V. An Observational Model for Biomechanical Assessment of Sprint Kayaking Technique. *Sports Biomechanics* **2012**, *11*, 507–523, doi:10.1080/14763141.2012.724701.

71. Plagenhoef, S. Biomechanical Analysis of Olympic Flatwater Kayaking and Canoeing. *Research Quarterly. American Alliance for Health, Physical Education, Recreation and Dance* **1979**, *50*, 443–459, doi:10.1080/00345377.1979.10615632.
72. Mann, R.V.; Kearney, J.T. A Biomechanical Analysis of the Olympic-Style Flatwater Kayak Stroke. *Medicine and Science in Sports and Exercise* **1980**, *12*, 183–188.
73. Logan, S.M.; Holt, L.E. Sports Performance Series: The Flatwater Kayak Stroke. *Strength & Conditioning Journal* **1985**, *7*, 4–11.
74. Cox, R.W. *The Science of Canoeing: A Guide for Competitors and Coaches to Understanding and Improving Performance in Sprint and Marathon Kayaking*; Coxburn Press, 1992;
75. Kendal, S.J.; Sanders, R.H. The Technique of Elite Flatwater Kayak Paddlers Using the Wing Paddle. *Journal of Applied Biomechanics* **1992**, *8*, 233–250, doi:10.1123/ijsb.8.3.233.
76. Qiu, Y.; Wei, W.; Liu, A.; Cao, J. COMPARATIVE RESEARCH ON THE STROKE RHYTHM OF MEN AND WOMEN KAYAKERS IN THE INTERNATIONAL COMPETITION. *ISBS - Conference Proceedings Archive* **2005**.
77. Jackson, P.S. Performance Prediction for Olympic Kayaks. *Journal of Sports Sciences* **1995**, *13*, 239–245, doi:10.1080/02640419508732233.
78. Platanou, T. On-Water and Dryland Vertical Jump in Water Polo Players. *J Sports Med Phys Fitness* **2005**, *45*, 26–31.
79. Melchiorri, G.; Viero, V.; Triossi, T.; Tancredi, V.; Galvani, C.; Bonifazi, M. Testing and Training of the Eggbeater Kick Movement in Water Polo: Applicability of a New Method. *The Journal of Strength & Conditioning Research* **2015**, *29*, 2758–2764, doi:10.1519/JSC.0000000000000946.
80. Platanou, T.; Varamenti, E. Relationships between Anthropometric and Physiological Characteristics with Throwing Velocity and on Water Jump of Female Water Polo Players. *Journal of Sports Medicine and Physical Fitness* **2011**, *51*, 185.

81. Gobbi, M.; D'ercole, C.; D'ercole, A.; Gobbi, F. The Components of the Jumps in Expert and Intermediate Water Polo Players. *The Journal of Strength & Conditioning Research* **2013**, *27*, 2685–2689, doi:10.1519/JSC.0b013e318240ebf1.
82. de Villarreal, E.S.; Suarez-Arrones, L.; Requena, B.; Haff, G.G.; Ramos-Veliz, R. Effects of Dry-Land vs. in-Water Specific Strength Training on Professional Male Water Polo Players' Performance. *The Journal of Strength & Conditioning Research* **2014**, *28*, 3179–3187.
83. Martin, M.S.; Blanco, F.P.; Villarreal, E.S.D. Effects of Different In-Season Strength Training Methods on Strength Gains and Water Polo Performance. *International Journal of Sports Physiology and Performance* **2021**, *1*, 1–10, doi:10.1123/ijsp.2020-0046.
84. Klika, V. *Biomechanics in Applications*; BoD – Books on Demand, 2011; ISBN 978-953-307-969-1.
85. Barbosa, T.M.; Goh, W.X.; Morais, J.E.; Costa, M.J. Variation of Linear and Nonlinear Parameters in the Swim Strokes According to the Level of Expertise. *Motor Control* **2017**, *21*, 312–326, doi:10.1123/mc.2015-0097.
86. Barbosa, T.M.; Goh, W.X.; Morais, J.E.; Costa, M.J.; Pendergast, D. Comparison of Classical Kinematics, Entropy, and Fractal Properties As Measures of Complexity of the Motor System in Swimming. *Frontiers in Psychology* **2016**, *7*, 1566, doi:10.3389/fpsyg.2016.01566.